Development of Recycled Polypropylene Composite Materials for Applications in 3D Printing

A thesis
submitted in fulfilment
of the requirements for the degree
of
Master of Engineering (Mechanical)
at
The University of Waikato
by

David Stoof

THE UNIVERSITY OF
WAIKATO
Te Whare Wānanga o Waikato

2016

Abstract

The adverse effects that waste plastics are having on the environment is becoming increasingly apparent. However, the plastics recycling industry in New Zealand is entirely market driven, necessitating the development of new markets to account for increasing quantities of waste. Innovations in additive manufacturing (AM) have presented opportunities to recycle thermoplastics for use as AM feedstock material. Using waste thermoplastic materials to fabricate composites in this way, adds value to the polymer by enhancing mechanical and aesthetic properties.

The main objective of this research was to produce strong, stiff and dimensionally consistent composite AM feedstock material using recycled polypropylene. Alkali treated natural hemp and harakeke fibres were chosen as composite constituents based on the advantages gained in terms of mechanical performance as well as low environmental impact compared to synthetic fibres. In addition, recycled gypsum powder (which is a currently underutilised waste product), was selected as a composite constituent primarily to investigate the influence it has on polymer shrinkage.

Initial screening tests using 20 wt% harakeke fibre were conducted to determine effective AM feedstock filament fabrication parameters, which were then used to fabricate all subsequent composite filaments. The parameters that provided the most significant improvements in tensile properties were: 105^{o}C constituent drying temperature for approximately 24 hours (as opposed to 80^{o}C), Maleated polypropylene (MAPP) coupling agent in powdered form (as opposed to granulated form) and initial compounding carried out on a 16mm twin screw extruder (as opposed to a larger more intensive, 20mm extruder).

A range of composite filaments with differing fibre and gypsum weight contents were then produced using pre and post-consumer polypropylene (PP). The most successful filaments in terms of tensile properties consisted of 30 wt% harakeke in a post-consumer PP matrix which had a tensile strength and Young's modulus of 41MPa and 3.8 GPa respectively. Comparing these results to those of plain PP filament, showed improvements in tensile strength and Young's modulus of 77% and 275% respectively.

To investigate the effects of 3d printing on tensile properties, feedstock filaments were 3d printed into tensile test samples. Compared to the filaments, 3d printed samples showed a reduction in tensile strength and Young's modulus as large as 40% and 60% respectively. An investigation was conducted to determine the cause of this reduction which was considered possibly due to moisture absorption and/or reduction of printing pressure relative to extrusion pressure. Pre-drying materials prior to printing resulted in strength and stiffness improvements, relative to undried filament of up to 26% and 44% respectively supporting moisture absorption to be an issue. However, densities were also found to be reduced, predominantly in the fibre reinforced materials supporting reduced pressure to also be a contributing factor. Specific strength and stiffness values of filament and printed materials were found to be closer than strength and stiffness, further supporting the relationship between a decrease in density and mechanical properties. Unlike fibre reinforced samples, the difference in specific strength and stiffness for plain PP filament and printed materials was equal to the difference in strength and stiffness. This could also suggest loss of polymer orientation to be a factor.

Finally, a novel method of measuring shrinkage in 3d printed components was developed and used to compare relative shrinkage of different composites. Natural fibre composites showed less shrinkage than gypsum composites with 10 wt% natural fibre showing a similar shrinkage value (1.17 %). as 50wt% gypsum. The composite that showed the least shrinkage consisted of 30 wt% harakeke with a shrinkage value of 0.34% corresponding to a net reduction of 84% relative to plain PP.

Acknowledgments

Of all the people that I have to thank for assisting me through my studies nobody has helped me more than my mother Sandy Wotton. Selflessly offering advice and assistance whenever possible she has played a pivotal role in my studies.

I would also like to thank my Father for all the conversations that have maintained excitement in my field of research and my studies.

The combination of enthusiasm, ceaseless curiosity and academic intuition make Professor Kim Pickering an exciting person to learn from and develop ideas with. This work could not have been carried out without her encouragement for which I am most grateful.

To Cheryl Ward I would like to say that I have really appreciated the selfless help you have offered throughout my studies. Your calm and collected attitude has preserved my sanity more than once.

I would like to thank my partner Felicia, who has sacrificed a lot to help me with my studies. I also appreciate her politely enduring conversations about the future of 3d printing.

I would also like to thank the Waikato district and Hamilton city councils for their financial support during this project. I hope that this research aligns well with their respective plans for the future.

I would also like to thank all of the technical staff, especially Chris Wang, Yuanji Zhang and Helen Turner who have always been there to offer wisdom and assistance.

Table of Contents

List of Figures

List of Tables

Chapter 1:
Introduction

Chapter 1

Introduction

1.1 Overview of Polymers and Polymer Recycling in New Zealand

Polymers are an incredibly diverse (and commonly) durable group of materials that have been utilised in an increasing quantity particularly over the past 100 years. There are many different types of naturally occurring polymers such as wool, cellulose, proteins and DNA, some of which have been used in an engineering context for many years. In addition to natural polymers; there are also many types of synthetic polymers; some of which are known as plastics.

Predominantly derived from petrochemicals, plastics can be readily formed into any solid shape with a wide range of modifiable properties. Due to the low cost and diversity of plastics, many products previously made from more traditional materials such as ceramics or wood are now being made with plastic. However, the durability of plastic makes it difficult to decompose and considerable amounts of waste plastic is accumulating in the environment.

Plastics can be classified into two groups known as thermosets and thermoplastics. Thermosets rely on an irreversible chemical reaction to solidify polymer resin into a desirable form. Thermoplastics consist of long linear chains of monomers that are bonded with one another by weak chemical bonds. When the plastic is heated, these weak bonds are broken and the chains are free to flow allowing the polymer to assume different shapes. Once the molten polymer cools, the bonds reform causing solidification and potential shrinkage.

Thermoplastic materials can be further categorised as either amorphous or semi-crystalline based on the degree of order (crystallinity) within the monomer chains after the polymer has solidified. The monomer chains within an amorphous polymer will solidify into a random pattern displaying no evidence of crystallinity.

The monomer chains in a semi-crystalline polymer however, will contain both crystalline and amorphous regions. The crystalline regions within semi-crystalline polymers are the primary cause of shrinkage or warping within these polymers on solidification. Thermoplastics can be heated and reformed (recycled) multiple times, however, every time thermoplastics are recycled the linear chains can become shorter having an adverse effect on the properties of the finished material [1; 2]. When heat is applied to a thermoset however, the polymer simply burns making it difficult to recycle.

It is estimated that plastics can take between 450 – 1000 years to decompose, meaning that apart from burnt and plastics, virtually every piece ever made is still in existence. Increased public awareness of the strain that waste plastics are having on the environment has made it a marketing advantage for companies to use recycled plastics [3]. This has led to an increase in collection and processing systems throughout New Zealand. The current plastic recycling method can be broken down into the following five steps:

- Collection of bulk recycled plastics.
- Sorting of plastics into individual plastic types.
- Cleaning and removal of contaminants.
- Chipping or resizing into small pieces.
- Extrusion into manufacturing pellets for resale.

Of the five steps above each has associated costs that affect the viability of different waste plastic streams. Attempts to standardise the sorting process have led to the numbers system shown in Figure 1. The system assigns a number and an abbreviated title for each type of plastic. This information is displayed on most plastic products making it much easier to distinguish the different types. The first six numbers are the most commonly used and make up the majority of house hold consumable plastics. The number seven is used when the plastic does not fit into any of these categories and could be any one of the hundreds of types.

Figure 1.1, Plastic numbering system

The recycled plastics industry is entirely market driven; therefore if no market has been identified or if the market value is too low, the collected plastics are sent to landfill. This is currently happening in most parts of New Zealand with plastics 3,4,6 and 7, mainly because the supply is insufficient to warrant further processing and compete with virgin plastic prices. Manufacturers of plastic products generally prefer using virgin plastics to reduce the risk of defects and contamination. This causes the sales of recycled plastic granules to fluctuate in accordance with the price of virgin plastics, which reflects the current price of crude oil.

Polypropylene (PP) which is represented by the number 5 in the recycling system, is a thermoplastic polymer derived from propene, a relatively inexpensive by-product of the oil refining process. As propene is inexpensive, virgin PP is relatively cheap when compared to other virgin materials which leads to a low market price for recycled PP (varies between$100-$200 per tonne). Given the market dependence on recycled polymer viability and the manufacturers preference for virgin material, the market price for recycled polypropylene varies between $100 - $200 per tonne. Despite the high quantity of PP being used in consumer products, the low market value often does not warrant the cost of collection and sorting resulting in the polymer going to landfill.

Properties of recycled plastics can be modified and improved in a number of ways. The most common of which is to add a certain percentage of virgin material to the recycled mix. This method increases the average linear chain length, therefore increasing the properties of the material as a whole. Another method of improving the mechanical properties is to blend in other additives such as fibre to form composite materials.

1.2 Overview of Composite Materials

A composite is a combination of two or more materials where the properties of each complement one another to form a superior result. This allows the properties of the composite material to be tailored specifically to suit the application. Composite materials have been in use for thousands of years. Ancient Egyptians used a combination of wood, water buffalo horn, sinew and glue to construct archery bows superior to wooden bows; concrete that was extensively used to build roman structures which still stand today, is a combination of volcanic ash, water, aggregate, and mortar. The significant benefits of modern composites have allowed them to steadily replace traditional materials in many different industries.

Broadly speaking composites can be categorised into five main groups namely: ceramic matrix composites, metal matrix composites, intermetallic composites, carbon – carbon composites and polymer matrix composites [4]. Polymer matrix composites offer advantages such as lightweight, ability to fabricate complex shapes and good mechanical properties along the direction of reinforcement.

Fibres of various types are often used for reinforcement in composite materials because they are strong, light weight and readily available. Fibre reinforced composites (FRC) can be manufactured with either short or continuous fibres each with associated advantages and disadvantages. Continuous fibre reinforced composites are often more difficult and time consuming to accurately manufacture than short fibre composites, but yield superior mechanical properties. These composites are often used in high performance applications; for example, in the aerospace industry various metals are being replaced with carbon fibre composites which, because of the strength of carbon, can occupy a smaller space with higher mechanical properties.

The mechanical properties of a FRC are largely controlled by the selection of fibre and matrix constituents but are also influenced by the interfacial bond strength between the fibre and the matrix. A weak bond between the fibre and the matrix will mean poor stress transfer to the fibres which could potentially result in lower mechanical properties than that of the unreinforced polymer.

This research focuses on the development of short fibre reinforced thermoplastic composites. Thermoplastic composites combine the enhanced mechanical properties of composite with the versatility and ease of moulding of thermoplastics. The choice of which thermoplastic to use as a matrix material will largely affect the end use capabilities for the material. For example, using poly vinyl chloride (PVC) as a matrix material would mean the composite would have improved ultra violet stability whereas using PLA would mean the composite could biodegrade more readily. Some key factors that influence the choice of fibre reinforcement could be cost, performance, weight or recyclability. Synthetic fibres tend to be difficult to recycle due to their brittle nature. If minimal effects on the environment are of high priority then it could be better to choose a non-mineral natural fibre.

1.3 Natural Fibre Reinforced Composites

Natural fibre composites offer a more sustainable alternative to synthetic counterparts and an area of growing interest in composites engineering. Synthetic fibres such as carbon and aramid have numerous benefits which make them an attractive option if remarkable properties are necessary. However, synthetic fibres can be costly to fabricate as well as hard wearing on moulds and production machinery.

Glass fibre is the most widely used of synthetic fibre for composite manufacturing owing to its relatively low cost, versatility and high strength. However, when glass fibre composites fracture in service, there will often be an ‘unfriendly’ or abrasive fracture surface, which can be pose significant health risks. In addition to health risks, the brittle nature of the fibre can cause fibre length reductions during processing which leads to significant reductions in mechanical properties. The incineration of these composites is impractical, as the mineral content is often upwards of 50 wt% which can cause blockages in furnaces and they generally go to landfill.

Many different types of natural fibre have been investigated for the purpose of finding a more sustainable alternative to glass fibre. Natural fibres not only have the potential to reduce adverse effects on the environment, but they can potentially do so at a lower cost than glass.

The properties of various natural fibres compared with various synthetic fibre are shown in Table 1.1. Although the tensile strength and stiffness of synthetic fibres is certainly higher, the low density of natural fibre allows compensation by means of higher fibre loading to produce a composite of the comparable weight.

Table 1.1, Comparison of natural fibre properties with those of synthetic fibres [5-8]

Natural Fibre	**Fibre density (kg/m3)**	**Tensile strength (MPa)**	**Young's Modulus (GPa)**	**Elongation at break (%)**
Flax	1500	345-1000	27.6	2.7 - 3.2
Hemp	1250	550-1110	30 - 60	1.6
Jute	1300 - 1400	393 - 773	13.0 - 26.5	1.2 - 1.5
Kenaf	1500	930	53	1.6
Ramie	1500	400 - 938	61.4 - 128	1.2 - 3.8
Abaca	1500	400	12	3.0 - 10
Curaua	1400	500 - 1150	11.8	3.7 - 4.3
Pineapple	1440	413 - 1627	34.5 - 82.5	1.6
Sisal	1400	468 - 640	9.4 - 22.0	3.0 - 7.0
Coir	1100	131 - 175	4.0 - 6.0	15.0 - 40
Cotton	1500 - 1600	287 - 800	5.5 - 12.6	7.0 - 8.0
Oil palm	700 - 1550	248	3.2	25
Bagasse	1250	290	17	
Bamboo	600 - 1100	140 - 230	11.0 - 17.0	
Harakeke	1270 - 1520	440-990	32.09	4.58
Synthetic				
Aramid	1400	3000 - 3150	63.0 - 67.0	3.3 - 3.7
Carbon	1700	4000	230 - 240	1.4 - 1.8
E-glass	2500	2000 - 3500	70	2.5
S-glass	2500	4570	86	2.8

The recyclability of natural fibre composites after service is yet another compelling reason for the replacement of glass fibre. Recycling involves the mechanical and thermal degradation of both the matrix and reinforcing fibres. Cellulose based natural fibres such as hemp or harakeke are durable enough to largely withstand the shear forces involved in reprocessing. This means they can be recycled several times without significant reductions in strength or stiffness [9; 10].

Cellulose based fibres occur naturally as a result of photosynthesis and require very little additional energy to assist in their growth. Synthetic fibres on the other hand, often need to be processed from raw materials requiring significant amounts of additional energy. A study conducted by Joshi *et al* compared the energy required in the production of glass and flax fibre composites shown in Table 1.2 below.

Table 1.2, Non-renewable energy resources for glass and flax fibre mat (MJ/kg) [11]

Glass fibre mat		**Flax fibre mat**	
Raw materials	1.7	Seed production	0.05
Mixture	1	Fertilizers	1
Transport	1.6	Transport	0.9
Melting	21.5	Cultivation	2.0
Spinning	5.9	Fibre separation	2.7
Mat production	23.0	Mat production	2.9
Total	54.7	**Total**	9.55

One of the main factors that restrict the wide spread application of natural fibre composites is the variability in both their physical and mechanical properties. The wide range of strength, stiffness and fibre dimensions found from plant to plant make it challenging to accurately predict the performance of the resulting composites. Without additional modification (chemical or otherwise), natural fibres are inherently hydrophilic and will absorb much more water than their synthetic counterparts. Water absorption can result in dimensional instability and a reduction in mechanical properties.

Mineral based synthetic have a high resistance to heat before degradation. Natural fibres, however, begin to thermally degrade at around 190 ^{o}C. This can restrict the potential matrix materials for composite fabrication depending on the melting temperature. For example polyethylene terephthalate (PET) has a melting temperature of approximately 250^{o} C which could lead to significant natural fibre degradation in processing if it were used as a matrix material.

1.4 The 3d Printing Industry and The Opportunities For Enhanced Materials

Almost 30 years since its conception, additive manufacturing also called 3D printing, has gradually overcome its niche applications and is revolutionising all manner of practices within the manufacturing industry [12]. To produce a component utilising this technology, an accurate model must be generated using computer aided design software. The virtual model is then incrementally divided into layers within the x-y plane before sending to the printer. The printer then proceeds to either deposit or solidify material in the exact shape of each layer until the sum of layers adds to make the entire part. The efficiency of this process minimises consumption of raw material by almost 75%, leading to a reduction in carbon footprint, whilst attaining a high level of geometric accuracy [12; 13].

Corresponding to the increased interest in 3d printing technologies, there has been a substantial increase in the total market value of the additive manufacturing industry. Incorporating machine sales, materials and associated services, the market valuation was estimated to be $7.8 billion USD in 2014. This sector is forecasted to expand at an annual rate of around 35%, with an expected market valuation in excess of $21.2 billion USD in 2020. Household consumers constituted 91.6% of machine sales in 2014, whilst industrial consumers accounted for the remaining 8.4% [14]. Growth in the industry has been largely attributed to the further development of stronger and cheaper materials with polymeric materials occupying over 80% of the market [15].

There are several different types of 3d printing techniques and more are being developed as the technology progresses. Modern 3d printers are capable of printing a wide range of materials from plastics to ceramics, however, for the purposes of this work we are primarily concerned with thermoplastic 3d printers which are the most economical and most often used. Currently, the two most common methods that print with thermoplastic materials are selective laser sintering and fused deposition modelling Table .1.3

Table 1.3, Processes, materials, advantages and disadvantages of different 3d printing technologies

Technology	Process	Typical materials	Advantages	Disadvantages
Fused deposition modelling	Material extrusion	Thermoplastics, composites	Complex geometries, low cost printers and materials	Poor surface finish compared to other methods, relatively slow build time.
Selective laser sintering	Powder bed fusion	Thermoplastics, Paper, metal, glass, ceramic, composites	High speed, no support material required, high heat and temperature resistance	Accuracy limited to powder particle size, rough surface finish

Fused deposition modelling (FDM) is one of the cheapest and most widely adapted methods of 3d printing to date. In this process, a thermoplastic filament is melted and extruded through a circular nozzle. The movement of the nozzle is controlled by using a 3-axis system allowing the molten plastic to be deposited onto a print bed. FDM allows parts of any geometry to be constructed in layers, through the successive deposition of molten material. Thermoplastics are the preferred filament material, although a wide range of materials, including cement and composites, are compatible with the FDM process [16; 17]. The success of FDM has largely been accredited to its simplicity, accuracy and affordability, which has enabled the general public to become acquainted with additive manufacturing.

The most popular thermoplastic materials used in FDM are acrylonitrile butadiene styrene (ABS) and polylactic acid (PLA). One quality that these materials have in common is that they are amorphous polymers. Amorphous polymers are used in FDM primarily because of the low degree of shrinkage relative to the semi-crystalline alternatives. Any shrinkage or warping of the polymer layers produced through FDM will greatly affect the quality of the printed component. Therefore, when using semi-crystalline polymers such as polypropylene, it is of paramount importance to limit shrinkage.

Introducing fibres or particles into polymers not only reduces shrinkage [18-20], but also improves the aesthetics and mechanical performance. Laywood is a brand of wood fibre reinforced composite FDM filament that contains up to 40 wt% recycled wood fibre in a PLA matrix. Since it was released in 2013 laywood has seen significant popularity amongst 3d printing communities and it has distributers in 11 countries. Laywood filament has been marketed more for its aesthetics, producing a textured finish of which the shade can be darkened by increasing the temperature and burning the fibres slightly.

When strength and performance are important, composite filaments have been developed which incorporate a range of different synthetic fibres. Tekinelp *et al* [21] found that the addition of short carbon fibres to ABS polymer increased the tensile strength and Young's modulus by 115 and 700% respectively. There is no clear evidence that this study has been commercialised into marketable filament; however, there are filaments available on the market such as Proto Pasta [22] and 3dxtech [23] that commercially produce carbon fibre composite filaments.

1.5 Research Objectives

The aim of this research was to fabricate a composite 3d printing filament from recycled polypropylene with enhanced mechanical properties and increased dimensional stability.

To these ends, the following were investigated:

- Creating dimensionally consistent filament by controlling extrusion parameters and spooling techniques;
- Investigating the effect on polymer shrinkage with varying fibre and gypsum powder content;
- Optimising fibre reinforcement by altering coupling agent particle size, fibre drying temperature and compounding cycles;
- The influence of fibre and gypsum content on tensile properties.

Chapter 2:
Literature Review

Chapter 2

Literature Review

2.1 Natural Fibres

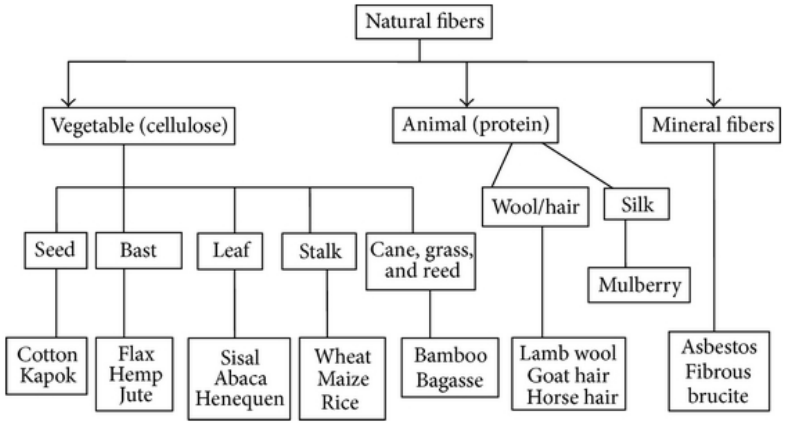

Figure 2.1, Types of natural fibres

Natural fibres are defined as hair like solids that can be directly obtained from an animal, vegetable or mineral source as shown in Figure 2.1. Renewable natural fibres are those that can be replenished in a predictable time period and exclude mineral natural fibres. Renewable natural fibres are used as a low cost alternative to synthetic fibres due to their reasonable mechanical properties, biodegradability, low density and the fact that they can be readily reproduced requiring little energy [5].

In plants generally, the bast and leaf fibres are used as mechanical support (holding up the stem and leaves respectively). Bast fibres surround the core of the plant stem and are found on the inner surface of the bark (phloem) [8]. Leaf fibres come from the structural component of the leaf such as the middle support in abaca or the leaf itself in the case of Harakeke [7], [6]. The disadvantages associated with using organic as opposed to synthetic fibres are high moisture absorption, low level of geometrical consistency, poor adhesion with matrices and low thermal stability [24].

2.2 Plant Based Natural Fibre Constituents

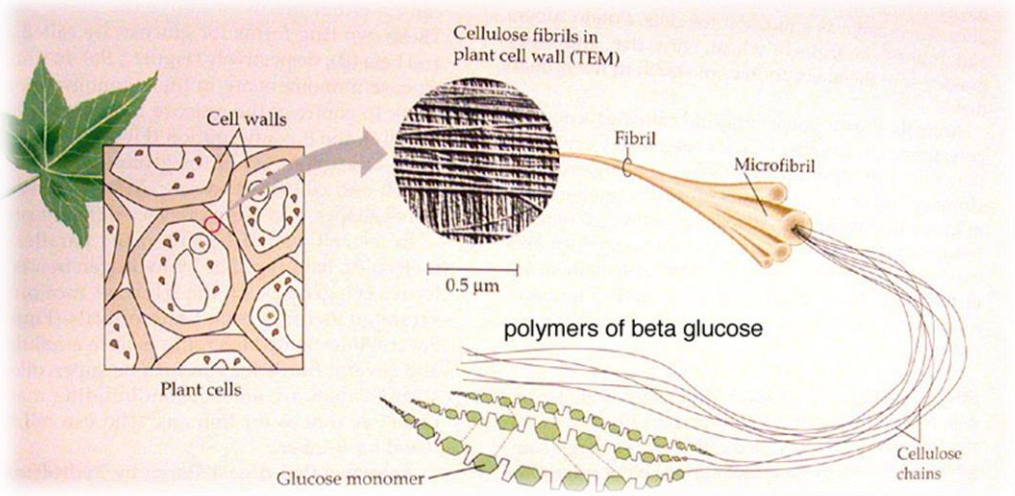

Figure 2.2, Composition of natural fibres

Plants can be considered to be excellent examples of naturally occurring composite materials. They consist of multiple layers of different constituents collectively determining the properties of the plant as a whole Figure 2.2 [5]. The majority of the stiffness and strength come from the earth's most abundant natural polymer known as cellulose. The cell walls of a plant consist of reinforcing oriented semi-crystalline cellulose micro fibrils which are embedded in a mainly two phase (lignin-hemicellulose) amorphous matrix [8]. Contained within these micro fibrils is where the cellulose chains can be found.

2.2.1 Cellulose

Generally most natural cellulosic fibres contain 60–70% cellulose which is primarily composed of C, H, and O_2. The general formula for cellulose is $(C_6H_{10}O_5)_n$ and the structure of the glucose monomer is shown in brackets in Figure 2.3. Molecular chains of cellulose, composed of thousands of covalently bonded glucose monomers are oriented in the fibre direction. There are three hydroxyl groups contained within each repeating glucose unit. These enable the cellulose to form strong hydrogen bonds with its own chains to form micro fibrils [25].

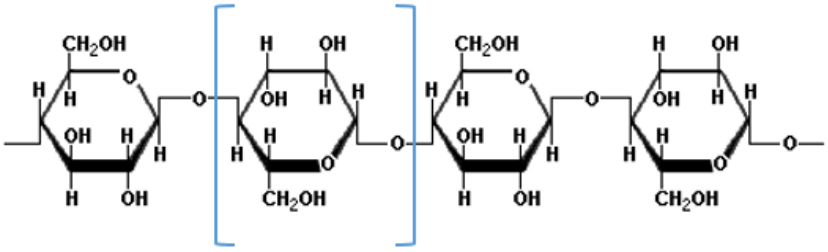

Figure 2.3, Chemical structure of cellulose [26]

Cellulose micro fibrils are wound around the cell wall, at an angle with respect to the fibre axis (Figure 2.4).This angle largely dictates the transmission of the force to the cellulose reinforcement. This explains for example, the higher stiffness and strength of hemp (~4^0 angle) as opposed to cotton (~25-35^o angle) regardless of the fact that cotton has approximately 30% more cellulose than hemp [8] and [27]. This has a lot to do with the function of the fibre in its natural setting. Hemp fibres from the stalk are required to be strong in order to support the 2-4.5m plant, while cotton fibres come from the flower and are not there to serve as mechanical reinforcement.

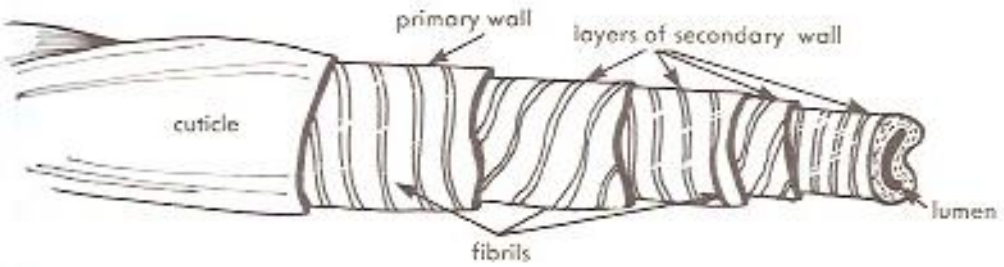

Figure 2.4, Microstructure of the cotton fibre showing the angle of fibrils with respect to the fibre axis [27] .

Cellulose comprises of both crystalline and amorphous regions, depending on whether the cellulose chains are held in a highly ordered (crystalline) structure due to intermolecular hydrogen bonding. Crystalline and amorphous cellulose have significantly different mechanical properties. The tensile stiffness of crystalline cellulose can be up to 15 times more than that of amorphous cellulose [28].

In addition to cellulose there are three other main constituents contained within plants (hemicellulose, lignin and pectin). The relative amounts of these are known to vary between different types of plant fibre [29]. Individually these constituents have poor tensile properties when compared to cellulose. These constituents do contribute to the rigidity and compressive strength of the plant however, their primary function is to serve more as a matrix material.

2.2.2 Hemicellulose

The second most abundant constituent within natural cellulosic fibres is generally hemicellulose. Despite the misleading name, hemicellulose is not a form of cellulose but belongs to a group of polysaccharides that are linked together in short branching chains [8]. Hemicellulose has very poor mechanical properties and functions more as a coupling agent between cellulose and lignin. The moisture absorption and biodegradability inherent in natural fibre is attributed predominantly to hemicellulose [30].

2.2.3 Lignin

Lignin is a totally amorphous three dimensional polymer which provides compressive strength to the very small micro fibrils. Lignin also serves as a moisture barrier to the absorbent hemicellulose. Although it makes reasonable contributions to the rigidity of a plant, lignin is undesirable for use in composites and is therefore one of the constituents commonly removed [29].

2.2.4 Pectin

Pectin is a carbohydrate polymer found within bast fibres and is useful for providing flexibility in plants. Although present in most natural fibres, pectin is a minor constituent accounting for 0.9% in both flax and hemp fibres [31]. Separation of fibre bundles from surrounding cells of the stem can be achieved with effective removal of pectin material [32]

2.3 Hemp Fibre

Hemp is a lignocellulosic bast fibre, which comes from the *Cannabis Sativa* plant species. Depending on the climate, hemp grows quickly with little difficulty producing a crop with the high yield of 0.25-1.4 kg/m^2 of dry stem per season [33] Due to its impressive stiffness and strength, hemp fibre has a long history of applications dating back as far as 6,000 years. Earlier applications of hemp fibre took advantage of its long fibres to manufacture robust rope and textiles. Modern day applications have been hindered due the plants similarities between marijuana, an illegal plant from the same species used as a recreational drug. However, extensive research into the plants potential has helped to reform laws and make it to easier to access. The fibre is still used in the textile industry, but the inclusion of hemp fibre into modern composites is a more wide spread industrial application. Automotive companies such as Ford, Audi and BMW all have components such as door panels, boot linings and parcel trays made from hemp fibre composites [34].

2.4 Harakeke Fibre

Harakeke, otherwise known as Phormium tenax, is a plant native to New Zealand consisting of strong fibre harvested from the leaf. In the early 1920s it was a significant export for the country and used to produce rope, clothing and sacks [35]. The use of synthetic fibres have since replaced harakeke and the plant is mainly used for crafts. Although the plant it is similar in appearance, it is not biologically related to flax and has not been as extensively studied for use in composite materials [36]. The time it takes to grow a harakeke plant to full maturity is 7 years and it has been documented that the mechanical properties are highly dependent on the environment [37]. Whilst hemp fibre has been more extensively studied for applications into composite materials, harakeke has demonstrated similar mechanical properties and is a much finer fibre. A comparison of fibre content between each species can be seen in Table 2.1 below.

Table 2.1, Comparison of fibre content between hemp and harakeke [38]

Fibre	Cellulose (%)	Hemicellulose (%)	Lignin (%)	Pectin (%)
Hemp	55 – 78.3	10.7 – 22.4	2.9 - 13	0.8 – 1.6
Harakeke	45.1 - 55	27.3 – 30.1	7.8 – 11.2	0.7

2.5 Gypsum Powder

Gypsum is an abundant mineral which is otherwise known as calcium sulfate dihydrate. By weight, unprocessed gypsum contains approximately 21% water which is in crystalline form so the material appears to be dry. When heated to temperatures exceeding 100°C, crystalline water turns gaseous and evaporates. Pulverised gypsum that has had 75% of its moisture removed is known as plaster of paris or stucco in the construction industry. This can then be combined with liquid water and moulded into shapes and upon drying the reconstituted gypsum will regain its solid form in the shape of the mould [39]. The versatility of gypsum has seen it used extensively for decoration and construction in applications as far back as ancient Egypt to its most common modern application in wallboard materials [40]. The wide spread application of gypsum in the building industry comes as a result of the minerals good fire resistance, thermal and sound isolation properties.

The microstructure of gypsum powder consists of needle like crystals in cluster form as shown in (Figure 2.5). Mechanical size reduction of gypsum powder results in the brittle fracture of crystals and separation into smaller clusters [41].

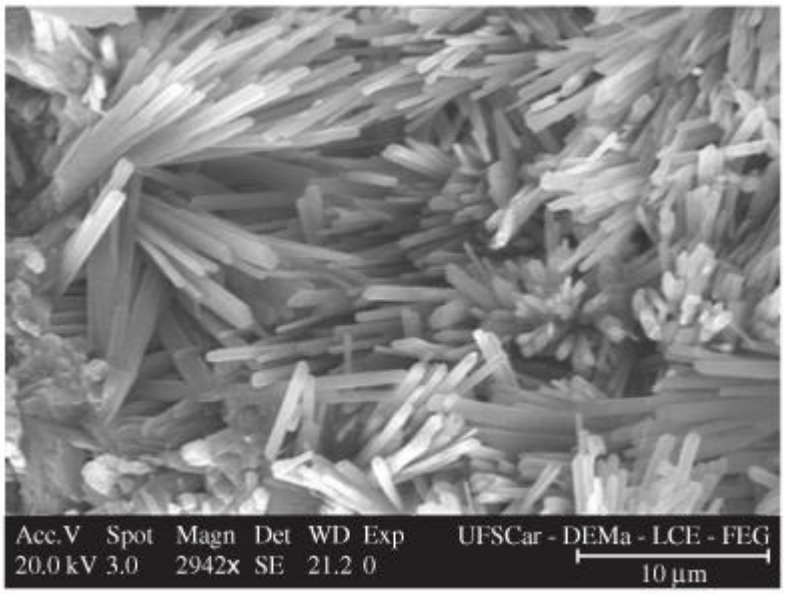

Figure 2.5, SEM image of needle shaped gypsum microstructure [41]

2.6 Thermoplastic Matrices

When it comes to matrix material selection, thermoplastics are becoming an increasingly compelling choice. Benefits of thermoplastic matrices can include infinite shelf life, low moisture absorption and mechanical properties specific to the application [10]. Generally, processing natural fibre composites at temperatures exceeding 200°C will result in lignocellulose degradation which could have adverse effects on mechanical properties [42]. Thermoplastic matrix materials selected for fabricating natural fibre composites must therefore be selected with processing temperature as the primary concern. A comparison of different commodity thermoplastics and their melting temperatures can be seen in Table 2.2 below. The relatively low melting temperature of polypropylene for example, would make it a more favourable choice as a matrix material than polyethylene terephthalate or polystyrene.

To successfully fabricate a light weight composite material it is advantageous to choose a matrix with a low density. Comparing the density values in Table 2.2 it can be seen that either polypropylene or low density polyethylene would make a good choice in this regard. The contributions of the polymer matrix to the overall mechanical properties are found to be increasingly less significant in fibre composites with fibre content in excess of 50 wt% [43]. Therefore, for strong light weight applications, low density is of higher significance than mechanical properties in terms of matrix material selection.

Table 2.2, Melting temperatures and densities for different thermoplastics [44-48]

Type of thermoplastic	Melting temperature (°C)	Density (g/cm^3)
Polypropylene	150 - 160	0.935
High density polyethylene	120 -180	0.956
Low density polyethylene	105 - 115	0.923
Polyethylene terephthalate	235 - 260	1.38
Polystyrene	210 - 245	1.05

2.6.1 Polypropylene

Polypropylene (PP) is a semi-crystalline polymer that is produced through the polymerisation of propylene monomers in the presence of a Ziegler-Natta catalyst [49]. PP is derived from propene, which is a by-product of the oil refining process. Much like polyethylene (PE), PP is a linear hydrocarbon polymer (Figure 2.6), and shares several similarities with the former. Factors such as molecular weight and distribution, along with the variety and quantity of copolymerising monomer, will influence the final physical and processing characteristics of PP [49-51]

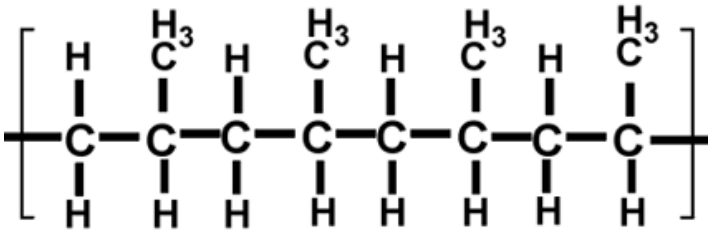

Figure 2.6, Molecular composition of polypropylene [52].

The versatility of polypropylene has allowed it to be adopted for a wide range of industrial applications. Low cost, reasonable thermal stability and simplicity of reprocessing are several of the attributes that are gradually increasing the global demand for PP [50; 53; 54] . PP typically has a density of 90 g/cm^3, a glass transition temperature of -10 ^{o}C, and a melting point of 165 ^{o}C [51]. These properties demonstrate that PP is compatible with natural fibre reinforcement, although chemical treatment of fibres, and the addition of coupling agents are required to improve interfacial adhesion [49] . The low moisture absorption properties of PP are beneficial for minimising the effects of water absorption, since water can have an adverse effect on the fibre/matrix interface of composites [51] . The mechanical characteristics of PP closely resemble some engineering thermoplastics, and are essentially identical with the addition of reinforcement. With a number of favourable attributes, along with being an existing material for additive manufacturing filament, PP is a suitable candidate for further investigation with natural fibre reinforcement.

2.6.2 Polymer Shrinkage

Unlike pure amorphous plastics, during solidification the molecular chains of some thermoplastic materials arrange in periodic patterns producing crystalline regions. This crystallinity occurs in the form of folding chains known as lamellae as shown schematically in Figure 2.7below. Factors such as entanglement within polymer chains and differences in molecular weight within the polymer are known to limit the degree of crystallisation that will occur within a semi-crystalline polymer [55] . The regions of the polymer that cannot crystallise remain amorphous and have different physical properties than crystalline regions [56]. As a polymer melt is allowed to cool and solidify, the contracting forces caused by crystallisation can result in polymer shrinkage and warping. This is the reason why polymers with higher crystallinity experience a higher degree of shrinkage when compared to amorphous polymers [18; 57]. Although polymer shrinkage can be attributed to several factors such as non-uniform cooling rates, density changes and temperature, the degree of crystallinity is an important factor to consider when it comes to shrinkage in semi-crystalline polymers.

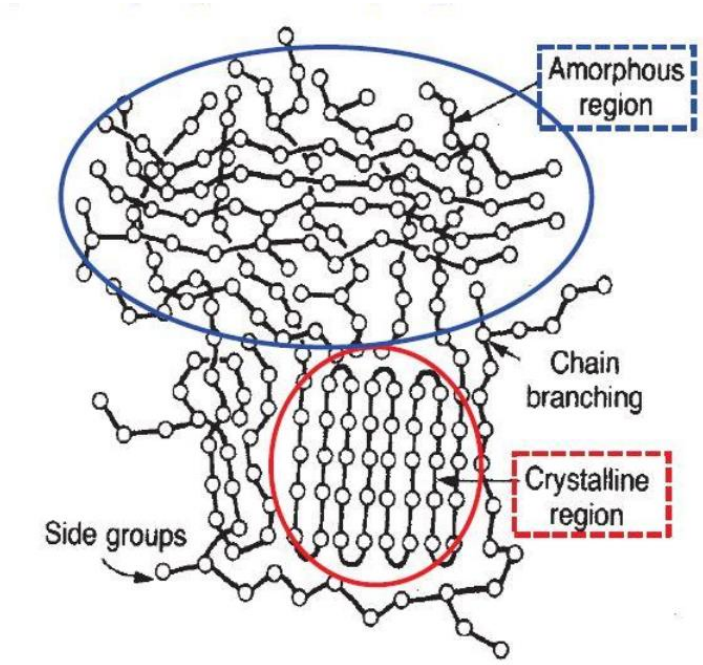

Figure 2.7, Structure of monomer chains for semi-crystalline polymers [55]

Another factor that has considerable influence on polymer shrinkage and is particularly relevant to this research is the content of filler material. Generally, the addition of particulate or fibre fillers will reduce the shrinkage effects within the polymer [18-20]. This can be understood intuitively by considering that if the filler material is dimensionally stable, then including it within the polymer will reduce the amount of less dimensionally stable polymer and therefore the overall shrinkage. Filler material may also interfere with the crystallisation process by creating physical barriers between lamellae regions [58].

Tan et al. [20] studied the effects on volumetric shrinkage reduction with the addition of short coir fibres in a polypropylene matrix. The inclusion of 40 wt% fibre corresponded to a reduction in volumetric shrinkage from 1.3 to 0.6%. Hakimain *et al* studied the influence of glass fibre reinforcement on shrinkage and achieved a 29% reduction with the addition of 30 wt% fibre glass. The study also showed that the shrinkage was lower when the fibre orientation was high.

2.6.3 Polymer Rheology

The most important flow property of a polymer or polymer composite is viscosity which describes the resistance to shearing. As the molten material is forced to move through a cavity there is a large amount of shearing occurring, much like a deck of cards sliding over one another, referred to as laminar flow. This results in the outer walls of the polymer moving much slower than the interior as indicated in **Error! Reference source not found.** [59].

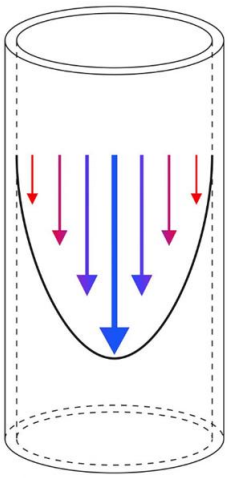

Figure 2.8, Laminar flow of polymer through cylindrical die [59]

These shear forces cause the polymer to orientate itself in the flow direction and internal strains will build up. These strains recover as it exits the die which can potentially result in a swelling effect known as die swell. The extent of die swell is largely dependent on the materials ability to store deformation energy. When a polymer is extruded through a short capillary, the internal stresses resulting from elongation at the die entrance will have the greatest effect on die swell. When the polymer is extruded through a long die (L/D > 30) the stresses caused by entrance effects have time to relax out and die swell is predominantly caused by shear forces generated in the die itself [60; 61].

Sharkskin is a term used to describe surface undulations which are thought to originate near the exit of the die and result from a stick-slip phenomena (Figure 2.9). When the shear stress between the polymer and the walls of the die reaches a critical level, the skin of the extrudate will begin to rupture in a quasi-periodical manor [62; 63]. Methods of reducing sharksnin include heating the die and slightly modifying the die to decrease wall shear or modifying exit angle to avoid stick [61; 62].

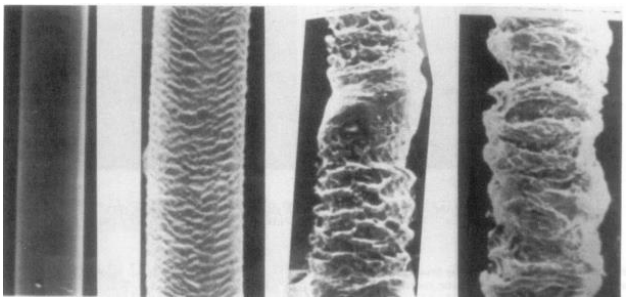

Figure 2.9, Development of sharkskin in LLDPE extrudates [49]

The addition of filler materials such as fibre or particles can change the rheology significantly depending on a number of factors. These factors include filler shape, size, concentration and the extent of any interactions between the constituents. In general, increased filler content will result in an increased viscosity and a decrease in die swell. [64]. A study conducted by Khalina *et al* [65] investigated melt flow and viscosity behaviour of 42 wt% kenaf/polypropylene composites fabricated with varying fibre sizes of 250, 450 and 850 micron. The results show a sharp decrease in melt viscosity for all materials with an increasing shear rate. The increased fibre length gave rise to an increase in viscosity which complimented the theory that higher specific area of additives tend to increase viscosity.

2.7 Natural Fibre Composites and the Factors Influencing Effective Fabrication

Composite materials consist of multiple phases in which the phase distribution and geometry have been deliberately tailored to optimise one or more properties [66]. The use of natural fibres to reinforce materials dates back for thousands of years with the ancient Egyptians using straw to enhance the properties of clay[67]. What are considered to be modern composites only started emerging and gaining momentum during World War 2. This was when glass fibre was combined with thermoset plastics for various military applications such as aircraft and communications equipment [68]. The two phases that make up a natural fibre composite are either a cellulose, protein or mineral based fibre and the matrix. The main purpose of the matrix is to transfer the force experienced on the component to the fibre reinforcement which is generally stronger than the matrix [69]. There are a number of factors outlined in this section that influence the overall properties of a natural fibre composite material.

2.7.1 Fibre Orientation

The orientation of fibres is an important factor that influences strength and other properties in fibre-reinforced composites. The most effective reinforcement is generally achieved when the fibres are oriented longitudinally to the direction of the applied load [70]. Figure 2.10 represents (a) continuous and aligned, (b) discontinuous and aligned, and (c) randomly orientated modes of fibre arrangement.

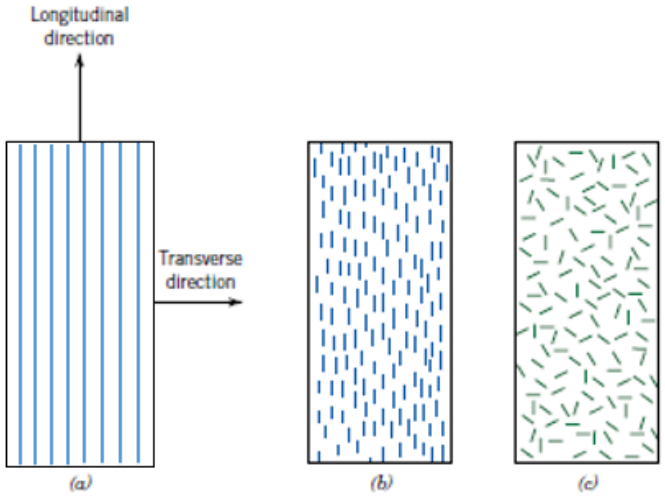

Figure 2.10, Representation of different modes of fibre orientation [70]

In practice, it is very difficult to achieve universal short fibre alignment in a single direction. Many natural fibre composite materials will display largely isotropic properties, due to dispersed and randomly orientated fibres. Several processing techniques, such as injection moulding and extrusion, allow for moderate improvement of fibre alignment in the flow direction. This can be attributed to the shear forces from die walls forcing fibres to align in the flow direction [71].

2.7.2 Fibre Aspect Ratio

The length to diameter ratio of a fibre is known as the fibre aspect ratio and is of critical importance when trying to optimise composite properties. The mechanical properties of a fibre reinforced composite are heavily influenced by the extent of applied load transfer from the matrix phase to the fibres [70] . This load transference is dependent on the degree of interfacial bonding between the fibre and matrix phases. When a tensile load is applied to a fibre composite, the load is transferred to the reinforcing fibres via shear forces at the fibre matrix interface. Increasing the fibre surface area that is in contact with the matrix increases the shear forces resulting in better reinforcement of the composite. The critical fibre aspect ratio is the minimum fibre aspect ratio in which the maximum allowable fibre stress can be achieved for a given load. The critical fibre aspect ratio can be calculated using equation 2.1 below.

$$\frac{l_c}{d} = \frac{\sigma_f}{2\tau} \tag{2.1}$$

Where l_c is the critical fibre length, σ_f is the tensile strength of the fibres, d is the fibre diameter and τ is the interfacial shear stress [70; 72]. Increasing the fibre length will generally lead to an increase in mechanical properties of the composite. The advantages gained with increasing length will eventually plateau once a threshold is passed, offering no further improvement in mechanical properties [72] .

2.7.3 Moisture Absorption

In general, as the volume of natural fibre in the composite increases, the rate of moisture absorption as well as the total moisture the material can retain will also increase. The grey squares shown in Figure 2.11 represent fibres distributed within a white matrix. With lower fibre content shown in Figure 2.11a, the fibres on the outer layer of the composite will absorb moisture up until they reach saturation point at which point no more water will be absorbed. In the case of a higher fibre content (Figure 2.11b) it is more likely that the fibres will be in contact with one another in the form of bundles [73]. This will allow water to be absorbed through neighbouring fibres further into the composite material and the composite will therefore retain more water.

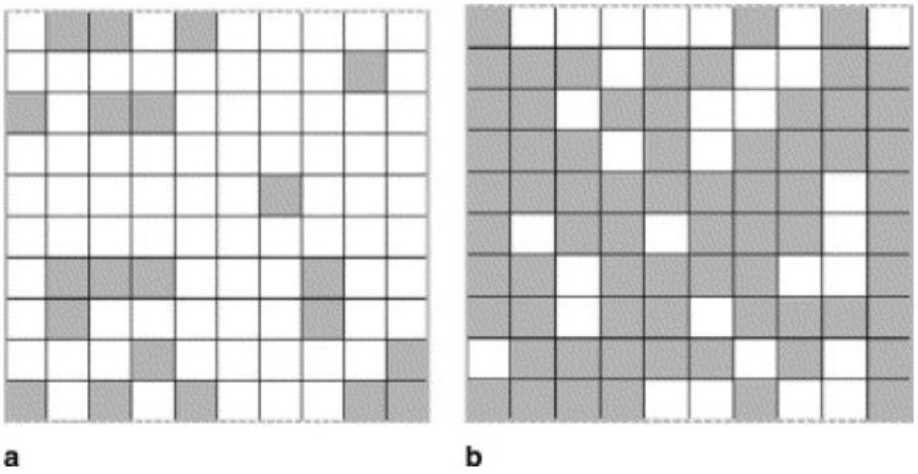

Figure 2.11, Low and high fibre volumes distributed in matrix material [73]

Fortunately, moisture absorption can be controlled to an extent through chemical treatment of the natural fibre prior to processing. The incorporation of a coupling agent will also increase the interaction of the fibre and matrix phases, improving the moisture resistance of a composite [74; 75] .

2.7.4 Thermal Stability

Cellulose based fibres are generally known to thermally degrade at temperatures exceeding 200 ^{o}C, although there have been cases where degradation onset takes place as low as 160 - 190 ^{o}C [76; 77]. This restricts the addition of natural fibre reinforcement to matrix materials with low melting temperatures. Chemical modification such as alkalai treatment has been found to increase the fibres resistance to thermal degradation by removing lignocellulose and increasing the interfacial bond between fibre and matrix [78]

A study conducted by Talla *et al [79]* investigated the extent of thermal degradation of alkilai treated hemp fibre in a PET matrix subjected to a range of temperatures and heating rates. It was found that the heating rate 10 ^{o}C could be used to minimise the effects of fibre degredation.

2.7.5 Methods of Improving Interfacial Adhesion between fibre and matrix

The mechanical properties of natural fibre composite materials are often limited due to poor adhesion between the fibre and matrix [66]. However, the interfacial adhesion can be improved by making modifications to the fibres, the matrix or both the fibres and the matrix. Two common methods used in natural fibre composites are the addition of chemical coupling agents to matrix materials and chemical surface treatments of the fibre. A coupling agent can be defined as a compound which provides a chemical bond between two dissimilar materials, usually inorganic and organic materials [80]. Generally coupling agents yield two primary functions: The first is to react with the surface of the fibre and the second is to react with functional groups of the polymer matrix [66].

2.7.5.1 Alkali Fibre Treatment

Improvements in fibre strength can be achieved by using alkali treatment to remove amorphous non-cellulosic substances while also increasing the percentage crystallinity and molecular alignment of cellulose [81]. The main variables concerning the success of the alkali treatment are: chemical concentration, temperature and time spent in the digestion process [82]. Research conducted by Islam [81] investigated the effects of alkalai treatment of hemp fibre by testing 16 different combinations of NaOH and Na_2SO_3 concentration, temperature and treatment time. It was concluded that 5 wt% NaOH, 2 wt% Na_2SO_3 and 120^{o}C for 60 minutes was the most favourable combination producing the best fibre qualities of the study. These include the removal of non-cellulosic constituents, fibre separation from bundles, increased surface roughness and increased crystalline cellulose.

2.7.5.2 MAPP Coupling Agent

Maleic anhydride grafted polypropylene (MAPP), or maleated polypropylene, is among the most popular coupling agents considered specifically for natural fibre polypropylene composites. The use of MAPP has encountered notable success in optimising the mechanical performance of composites [83] . A study conducted by Mutjet *et al* [80] used MAPP coupling agent, at 4% wt/wt with respect to varying hemp fibre volume fraction for an injected moulded hemp fibre polypropylene composite. At 40 wt% fibre and 1.6 wt% MAPP, the ultimate tensile strength (σ_t) and flexural strength (σ_f) increased by 49% and 38% respectively, relative to the composite without coupling agent. A similar investigation carried out by El-Sabbagh [83] , where MAPP content was varied with respect to fibre volume fraction. The experiment was not restricted to just hemp fibres, as flax and sisal reinforced polypropylene composites were also evaluated. The optimum MAPP to fibre ratio was determined to be within 10% and 13.3% for all three fibre species, as the maximum increase in stiffness, strength and impact properties were observed at those compositions. As shown in Figure 2.12, improvements of 66.1% and 60.1% for 50 wt% flax, and 28.5% and 39.5% wt% hemp, were observed for strength and impact properties respectively with optimum MAPP: NF ratios. Both scenarios clearly demonstrated significant increases in mechanical properties with ideal MAPP concentration [83] .

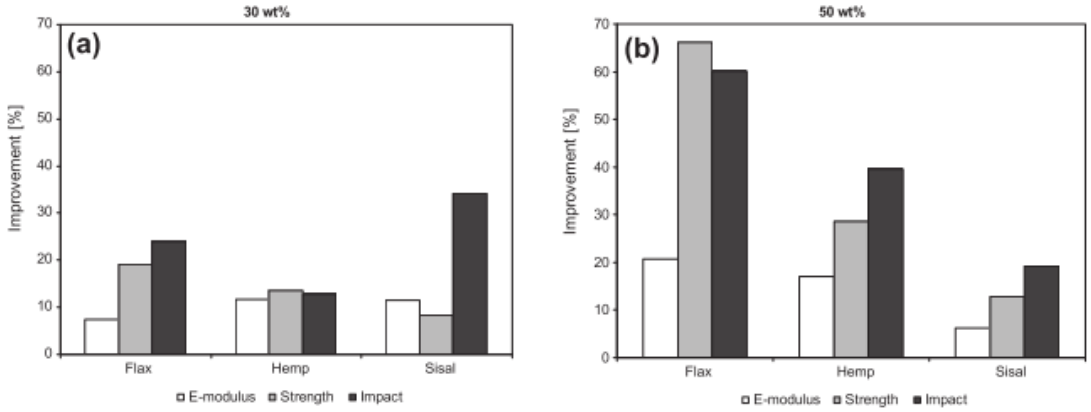

Figure 2.12, Improvement in mechanical properties with 30 wt% fibre (left) and 50 wt% fibre (right) when combined with MAPP coupling agent

2.7.6 Fibre Volume Fraction

A critical factor necessary for determining optimal composite properties is the amount of reinforcing fibre contained within the material. Many studies have shown that increasing fibre content corresponds to an increase in mechanical properties, particularly stiffness and tensile strength [10; 84-86]. However, there is a point where the benefits gained from additional fibre peak and begin to decline. Experiments conducted by Ku *et al* with varying content of kenaf fibre in polypropylene showed increased tensile strength with fibre loadings up to 40wt% before a decline was observed [87]. Nishino *et al* showed similar results when using kenaf fibre in a PLA matrix, the relationship between fibre content, Young's modulus and tensile strength can be seen in Figure 2.13 below. The decline in tensile strength with excessive fibre loading could be attributed to increased fibre-fibre and fibre-equipment contact leading a reduction in fibre length and fibre efficiency. These increased solid-liquid interactions generally increase the viscosity of molten/liquid composites which can effect various processing parameters such as extrusion speed and injection mould complexity.

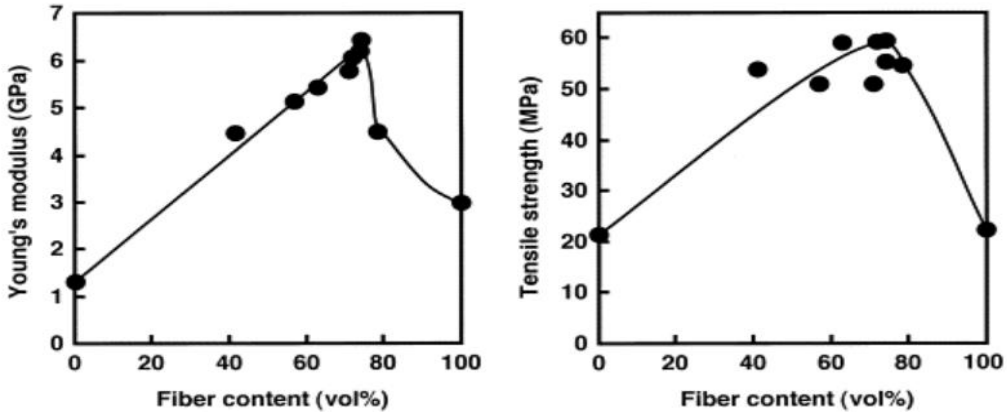

Figure 2.13, Effect of increased fibre loading on Young's modulus and tensile strength of kenaf/PLA composites [88]

2.8 Particle Reinforced Thermoplastic Composites

Particle reinforced composites are a broad range of materials which offer enhanced material properties and relative ease of processing. Advantages of particle composites include increased hardness, thermal stability, shrinkage resistance and lower cost. Some filler materials are also known to enhance mechanical properties such as tensile strength and stiffness, however, these enhancements are small relative to fibre reinforcment [89]. Factors such as moisture absorption, interfacial adhesion and filler volume fraction are applicable to both particle and fibre composites.

Kim *et al [90]* investigated the effects of shrinkage in the injection moulding process with increasing talc particle content with talc/PET composites. Experimental results show a clear correlation between talc content reductions in shrinkage as shown in Figure 2.14 below. It was also observed that talc particles of a smaller size were found to be more effective in terms of shrinkage reduction. This was attributed to the increased interfacial area between polymer and talc particles. Particle reinforcement could offer a low cost method of achieving shrinkage reduction in 3d printed components.

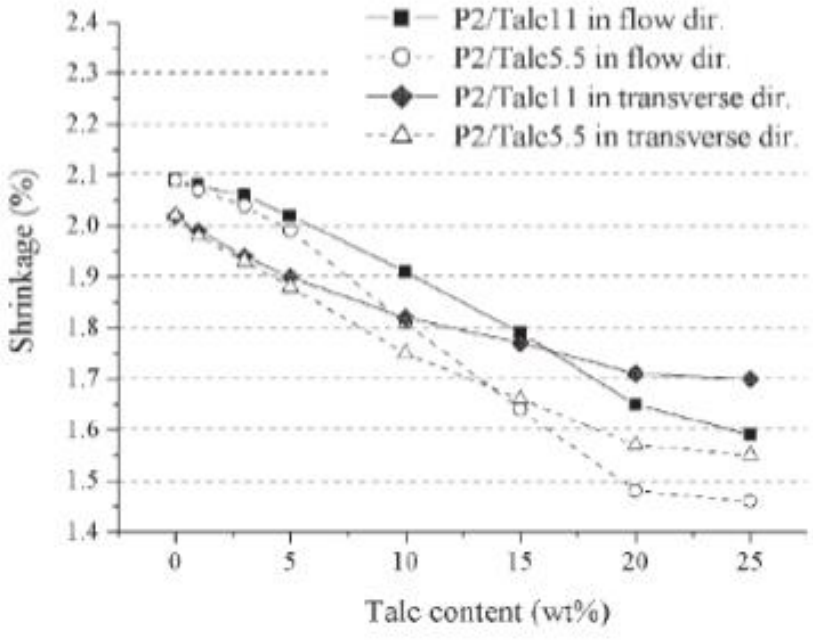

Figure 2.14, Correlation between talc content and shrinkage for talc/PET composites [90]

2.9 Processing of Short-Fibre Reinforced Composites

2.9.1 Extrusion

Polymer composite extrusion is the process of heating and melting the polymer/fibre blend to a workable temperature and forcing the mixture through a small hole or die of the desired shape. The two main types of extruder are twin screw extruders and single screw extruders [91]. The single screw extruder uses screw shaped rod which is concealed inside a heated chamber to force the material through the chamber and out through the die. The twin screw extruder uses the exact same principle but uses two screws in various configurations and rotation directions customised for improved feeding, melting, mixing and material flow [92].

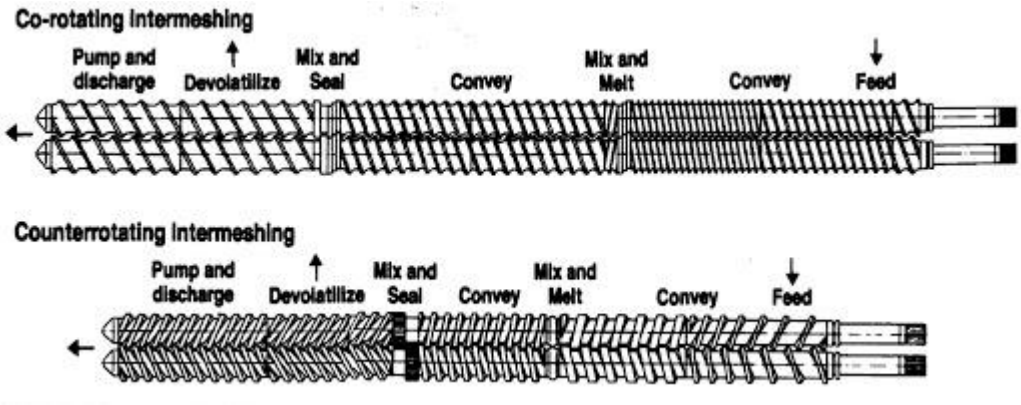

Figure 2.15, Twin extrusion screw set up including mixing and feeding regions [93].

Some example screw configurations for counter and co-rotating twin screw extruders are shown in Figure 2.15.Generally the twin screw extruder is better for achieving homogenous fibre distribution and improved fibre wetting compared with single screw extruders [91]. However, the different sections for mixing and the shear forces caused between the two screws can cause damage or decrease the length of the fibres and therefore reduce the reinforcement effect.

Differences in the densities between the fibres and polymer can result in uneven feeding into the extruder when using traditional feeding mechanisms. This affects the weight percentage of fibre and the fibre distribution though the finished extrusion. To achieve effective fibre-matrix compounding Peltola [84] and Keller

[94] use the common technique of extrusion mixing where the fibre and polymer is combined and extruded through a small circular die then processed through a granulator. These granules were then used as feedstock to produce the final test pieces with close to homogenous fibre distribution.

To increase the fibre distribution and the fibre wetting in the initial extrusion, Keller [94] used an additional fibre preparation processing step. The fibres were spun into a thread with a specific mass of 2 g/m (BIA) or transferred into fleeces (1.7 g/m). This meant that once the fibre had begun to be pulled into the extruder it would continue at a constant rate and therefore increasing the homogeneity of the sample.

An additional advantage of extrusion as a form of composite formation is that in the process of forcing the polymer/fibre mix through the small hole, there is a degree of alignment occurring. A study conducted by Peltola *et al* [84] investigated the effect combining hemp and flax fibre with triethyl citrate plasticized starch. The micrograph shown in Figure 2.16 below is taken of the polished perpendicular cross sections of extruded samples consisting of 20wt% flax fibre. The figure shows that most of the fibres appear to be aligned in the flow direction which is thought to be caused by the normal force of the extrusion die on the composite [84] and [95].

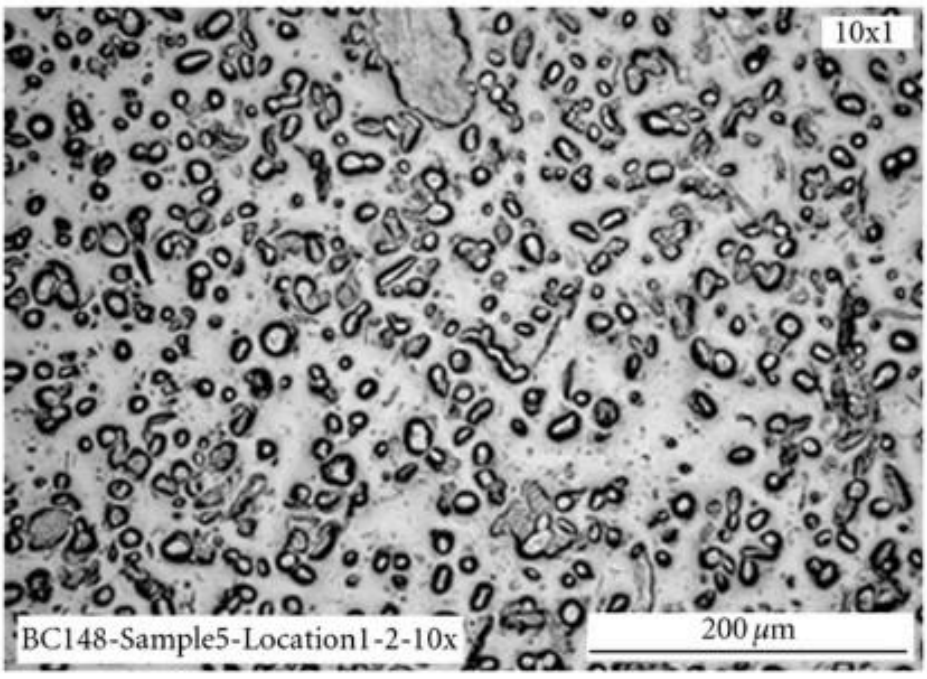

Figure 2.16, Cross section of extrusion [84]

2.10 3d Printing Technologies and Their Potential Implications for Composite Fabrication.

2.10.1 Stereolithograghy

Stereolithography (SL) was one of the first commercial methods of additive manufacturing and is currently producing some of the most dimensionally accurate results [97]. Traditional SL uses a moving ultra violet laser to precisely solidify ultra violet curable photopolymer (Figure 2.17). The laser traces out and solidifies the liquid polymer to form each layer of the component then the build platform is lowered a distance equal to the layer height. The process is then repeated for each layer until the shape is complete.

The accuracy of the laser and the fact that the polymer particles are on the nano scale mean that a high degree of dimensional precision can be achieved. To achieve a high resolution finish on the object it is necessary to keep the layer of liquid polymer as shallow as possible. This will increase the resolution of the whole shape by adding solidifying shallower layers in each cycle [98]. Once the parts are finished the parts are often cleaned of any excess partially solidified polymer and the part is subsequently cured in an ultraviolet oven. SL is a relatively expensive additive manufacturing technique with the machines ranging from $4000 to upwards of $350,000 NZD and the liquid polymer ranging from $400 - $1100 NZD [12; 96].

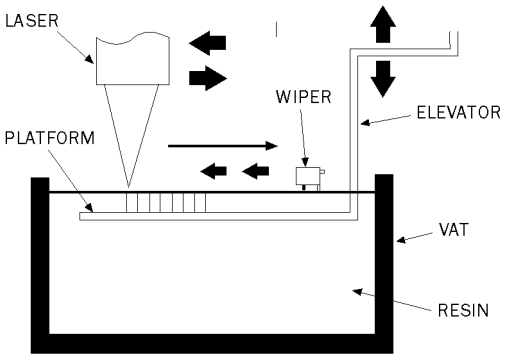

Figure 2.17, Schematic view of a SL machine [96].

2.10.2 Micro Stereolithography (MSL).

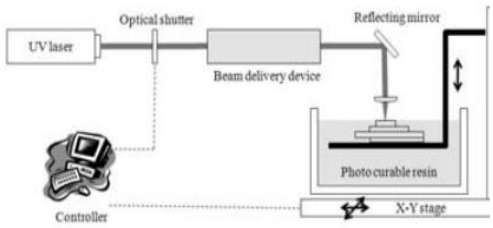

Figure 2.18, Scanning microstereolithography [99].

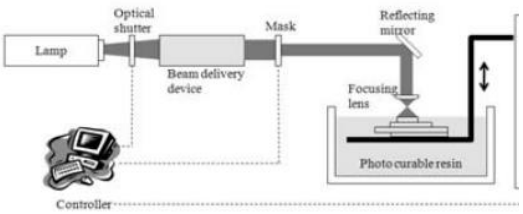

Figure 2.19, Projection microstereolithography.[99]

This form of additive manufacturing was derived from conventional SL and is capable of producing complex 3D microstructures with resolution of approximately 5µm [100]. MSL technology can be divided into scanning or projection methods (Figure 2.18 and Figure 2.19) each with different levels of accuracy and fabrication speeds [99]. The key difference between these two methods is that scanning MSL uses the point of the laser to fabricate fine microstructures while projection MSL quickly creates each layer with one exposure by using a mask [99] and [101].

The first scanning method was reported by Ikuta and Kirowatari in 1993 and was known as the integrated Heyden Polymer process [102]. Over the past two decades researchers have developed the technology to the point where many different microstructures can be fabricated at resolutions far exceeding those reported in 1993.

The projection method uses a liquid crystal display (LCD) to generate each of the projected layers to be solidified. Projection MSL systems using LCD's have developed to the point where complex microstructures can be fabricated to the tolerance of several microns [99]. This process has been described as a dynamic pattern generator. As the projection method projects entire layers at a time in a very predictable and identical manor this method is preferred for both speed and accuracy in repetitive patterns such as lattice structures [99] and [100]. The scanning method is generally more preferred in applications of complicated and dynamically variable dimensions such as in tissue or organ engineering [103].

Researchers from MIT and the Lawrance Livermore National Laboratory [100] have recently created what is being called a new class of materials or metamaterials through the use of projection microstereolithography. This technique allows the microstructure of a material to be assembled into highly ordered, nearly isotropic and have high structural connectivity within varying architectures shown in Figure 2.20 [100]. These micro lattices shown in can be manufactured with critical features ranging from 20µm – 40nm and specifically designed to withstand different types of loading.

The densities of the samples produced were measured to be within a range from 0.87kg/m^3 – 468kg/m^3 while one of the lowest density materials currently available (aerogel) has a density ranging from 5kg/m^3 - 200kg/m^3 [100; 104]. Although the material has a similar weight and density as Aerogel the Young's modulus of this new material was determined to be 530MPa, 10,000 times greater than aerogel. Theoretically the Young's modulus and yield strength of these materials can be scaled linearly i.e $E/E_S \approx (\rho/\rho_S)$ and $\sigma/\sigma_s \approx (\rho/\rho_S)$ as opposed to the quadratic or greater relationships between strength and density of natural materials of random porosity [100].

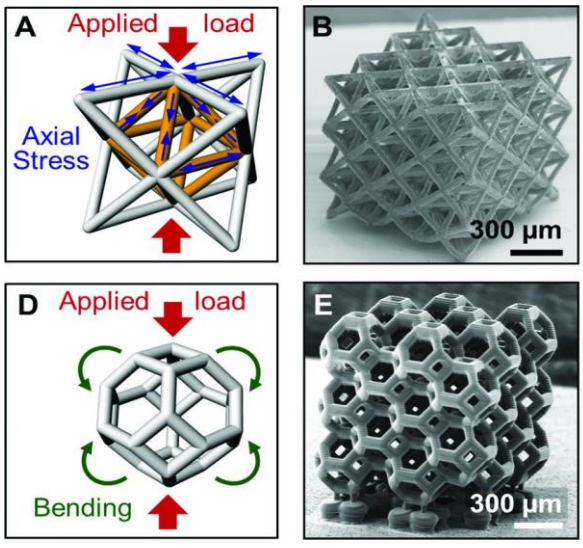

Figure 2.20, Micro lattices produced with microstereolithograpgy [100]

2.10.3 Stereolithography and Microstereolithography Composites

[105; 106]. UV curable resin impregnated with 10-15wt% carbon fibre has been used to manufacture sections of turbine blades shown in Figure 2.21 and 2.22 below [105]. Printed blades were then tested to find the maximum bending strength and fracture toughness of 350MPa and 4.49MPa/$m^{1/2}$ were reached.

Figure 2.21, Carbon fibre turbine blade section produced through stereolithography [105]

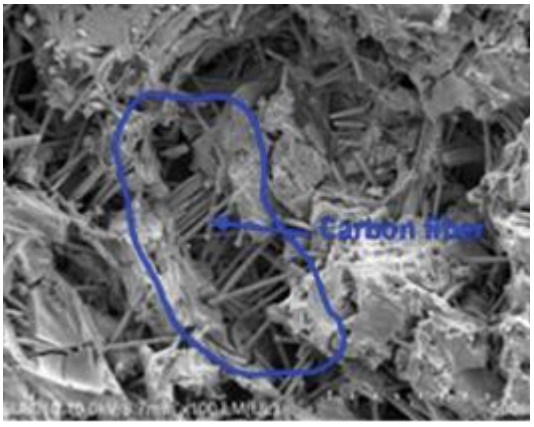

Figure 2.22, SEM image of interface between carbon fibre and polymer matrix [105]

Sakly *et al* [107] investigated the incorporation of Al-based quasicrystalline alloy particles into a UV curable resin. Increased hardness, reduced wear and lower friction coefficients were reported from the successfully manufactured composites. Lower than expected mechanical properties were thought to be due to the high reflectivity of intermetalics in the UV visible range.

Nickel plating was applied to already formed 1,6-hexanediol diacrylate (HDDA) lattices producing a metallic/polymer composite [100]. This composite could be left as it is or using thermal decomposition the polymer could be removed, leaving the hollow-tube nickel-phosohorus microlattice. Photosensitive PEGDA liquid pre polymer was combined with ≈150nm alumina nanoparticles underwent the same microsteriolithogropgy process to produce a ceramic/polymer composite. The formation of these composites shows the diversity and structural potential of microsteriolithography as a composite forming technique.

2.10.4 Selective Laser Sintering (SLS).

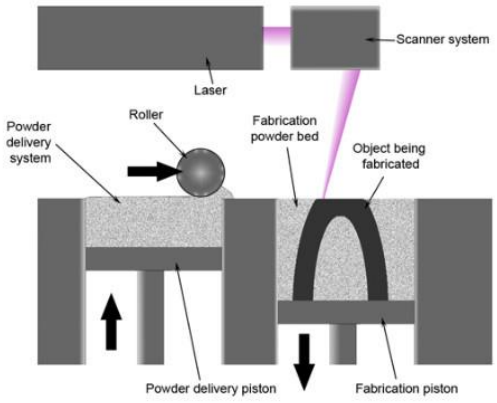

Figure 2.23, Selective laser sintering process [97].

This form of additive manufacturing is similar to SL in that SLS uses a directed laser and a moving platform to control the dimensions of the component. The difference is that instead of ultraviolet curable resin and a UV laser SLS uses very fine powder and a thermal laser to effectively melt the powder particles together (Figure 2.23). Each layer of powder is spread out over the top of the last by a roller as the support platform lowers. The laser will then sinter the powder and fuse the new layer to the existing shape. The resolution of the end shape is controlled by the temperature and speed of the laser as well as the depth of the powder layer being sintered [97]. As the laser will only sinter the powder included in the geometry of the component the remaining powder acts as a support structure eliminating the need to incorporate them into the design.

2.10.5 Selective Laser Sintering Composites

SLS can be used to fabricate a range of composite materials using ceramics, metals natural and synthetic fibres [108-111]. Zeng.W *et al* [112] combined hot melt adhesive powder (co-polyester) with birch wood powder, a viscosity reducer and a light stabilizer. The SLS system uses a CO_2 laser with varying laser energy density distribution levels to investigate the extent of the wood powder damage in the process. The addition of viscosity reducer (graphite, white carbon black, calcium carbonate, talcum or glass powder) resulted in more even dispersion of wood powder/co-polyester layers. The finished parts were infused with wax to which resulted in reduced porosity and improved surface finish this is shown in Figure 2.24.

Figure 2.24, Wax infused SLS produced wood Powder composite

The optimal laser energy density distribution factor that produced the best impact, bending and tensile strengths was found to be 340W/mm^2. At this intensity the impact of the initial and wax infused samples were 5.9 and 7MPa respectively. The initial sample showed negligible tensile properties and the wax infused composite had a tensile strength of 1.3MPa. The poor tensile properties were largely attributed to porosity and poor interfacial bonding between the powder and the matrix and shown in Figure 2.25.

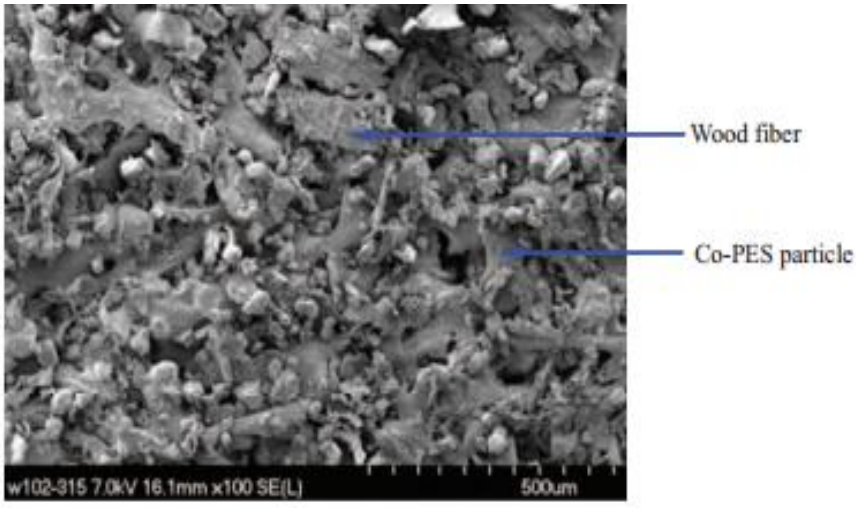

Figure 2.25, SEM image of wax infused wood powder composite interface.

Zeng.W *et al* [110] also produced similar composites using powdered rice husks in a co-polyester matrix with the same viscosity reducers and stabilizers. The surface of the rice husk composite was less porous than the wood fibre on both the initial and wax infused test pieces. The tensile strength of the rice husk composites were 13% higher than the wood but the impact strength was 47% lower.

2.10.6 Fused Deposition Modelling (FDM)

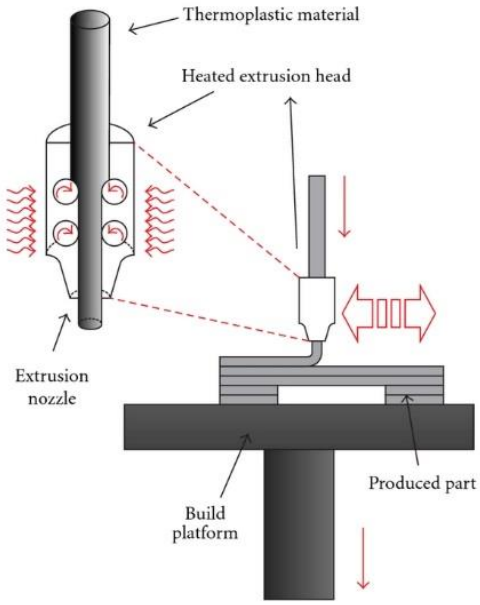

Figure 2.26, Fused deposition modelling system [97]

FDM uses a miniature extruder capable of moving in three dimensions to extrude material and build components in layers (Figure 2.26). Each of the layers fuses together due to the high temperature and forms a solid structure. The resolution of the finished component is dependent on the size of the extrusion hole which dictates the thickness of each layer. FDM is one of the simplest and most affordable systems available with machines retailing as low as $200 US [54]. Currently the majority of materials available are different thermoplastics primarily PLA and ABS, but there has been success using metallic and ceramic materials such as eutectic Bi58Sn42 alloy [113] and concrete [114].

The mechanical properties of components produced by FDM are determined by the adhesion between layers, width of the extrusion, presence of voids within the component and the orientation of the filament [115]. Effects of filament alignment and orientation on the bending and tensile strength have been investigated by printing ABS polymer filament with an extrusion temperature of 270^{o}C into three layer samples of 5 configurations. It was found that samples extruded in the longitudinal direction had higher values of tensile strength and stiffness values relative to samples of predominately transverse orientation. It was concluded that the function of the product should be considered before determining the orientation.

As most FDM 3d printers are programed under the assumption that the dimensions of the filament remain constant, they will only extrude materials at a constant rate. Therefore, variations in filament diameter, the presence of surface irregularities or internal voids can have an adverse effect on the final print surface quality and mechanical properties.

2.10.7 Fused Deposition Modelling Composites.

As with traditional extrusion of composite materials, the viscosity and size of the extrusion die largely dictate the flow and quality of the composite material. It is well documented [84; 92; 116] that with increasing fibre content, there is an increase in viscosity and complications in extrusion including blockages. However, mechanical properties generally increase with increasing fibre content [24; 28]. This means that to design an effective short fibre composite for use in FDM an optimal fibre content must be found.

Compton.B *et al* [95] of Harvard university have recently developed a short carbon fibre/ epoxy composite for use in a modified FDM system. The base epoxy was made from Epon 826 epoxy resin, nano-clay platelets, and dimethyl methyl phosphonate. Short fibres of silicone carbide carbon were added and the mixture was put into a syringe. The syringe was mounted on a three axis system and the flow was controlled. What is most notable from this research is the visible alignment of the short fibres in the direction of extrusion (see Figure 2.27).

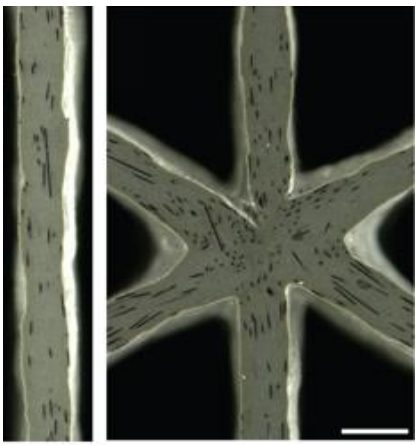

Figure 2.27, Fibre alignment of sample [95].

To investigate the effects of alignment on the mechanical properties, tensile test samples were fabricated with fibres aligned in both longitudinal and transverse directions. The samples were tensile tested and the results are displayed in Figure 2.28. The graph clearly shows a dramatic increase in engineering stress and decreased failure strain values with the incorporation of fibre. Longitudinally orientated samples show significantly increased properties. However, these results will be less susceptible to the effects of bond strength between extrusions.

.

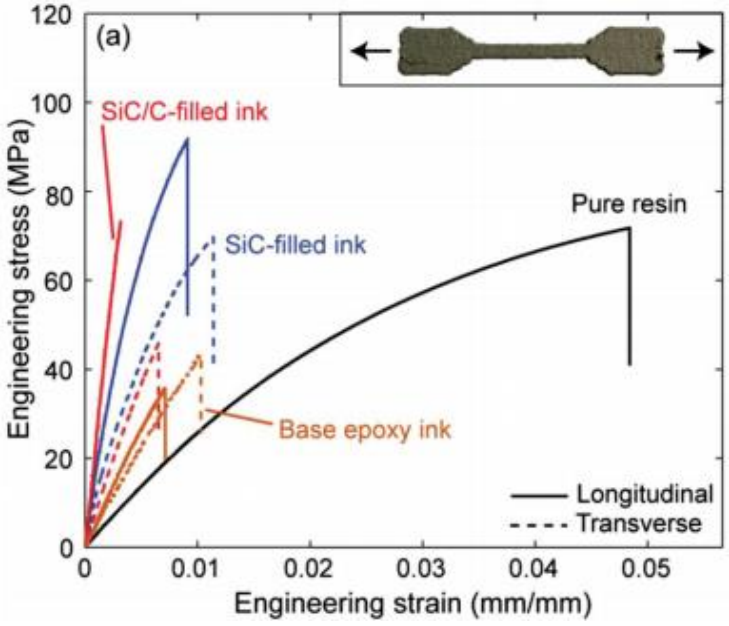

Figure 2.28, Stress vs strain graph for longnitudal and transverse aligned fibres [95].

Zhong.W *et al* [17] investigated the effects of impregnating short glass fibre, plasticizer, and compatibilizer in an ABS matrix for use in FDM. Glass fibres were mixed through a twin screw extruder then pelletized and extruded into 1.5-1.9mm filament by means of single screw extruder. The cross section of the filament was controlled by the tension and winding speed of an electric roller that collected the extrusion. The material was then used to produce test samples of longitudinal and transverse orientation (type 1 and type 2 respectively) and the mechanical properties were tested. Tensile tests of type two samples revealed an increase in adhesion between the layers for glass fibre reinforced ABS (GFR-ABS) compared to plain ABS. The adhesion continued to increase with increasing fibre content and was speculated to be because of increased chance of fibres bridging the between layers. Figure 2.29 shows the cross section perpendicular to the flow direction of GFR-ABS filament. Fibre ends can be seen protruding from the matrix which suggests a reasonably high degree of alignment.

A

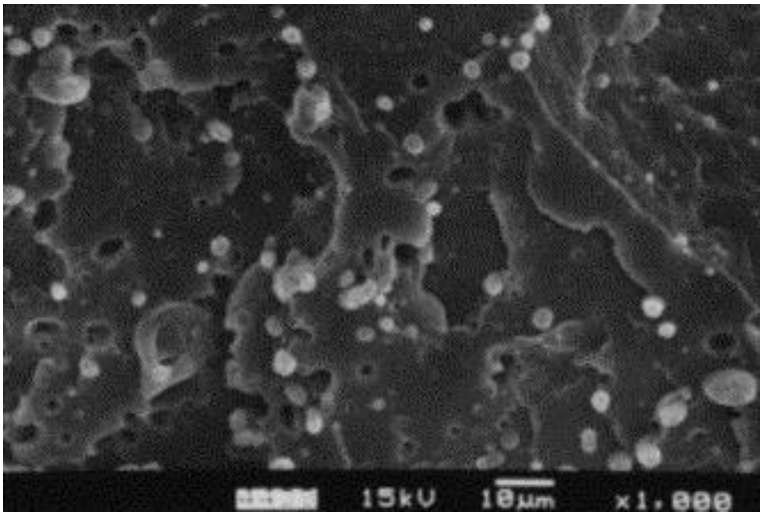

Figure 2.29, SEM image of filament cross section [17].

similar effect was observed by Compton. B *et al* [95] regarding the fibre alignment through the extrusion process. This was thought to contribute to the increase in tensile strength of 49% relative to plain ABS.

To utilise the further reinforcement benefits of continuous fibre, Matsuzaki *et al* [117] have recently developed a modified FDM printer to embed continuous carbon and jute fibres inside a PLA matrix. PLA filament is melted and extruded through a nozzle while continuous fibre strands are mechanically fed through the same nozzle by a side inlet shown in Figure 2.30. PLA/fibre composite is then extruded through a small nozzle to form layers much like conventional FDM. To avoid tangling of the continuous fibre, a cutting mechanism will cut the fibre according to the geometry of the print.

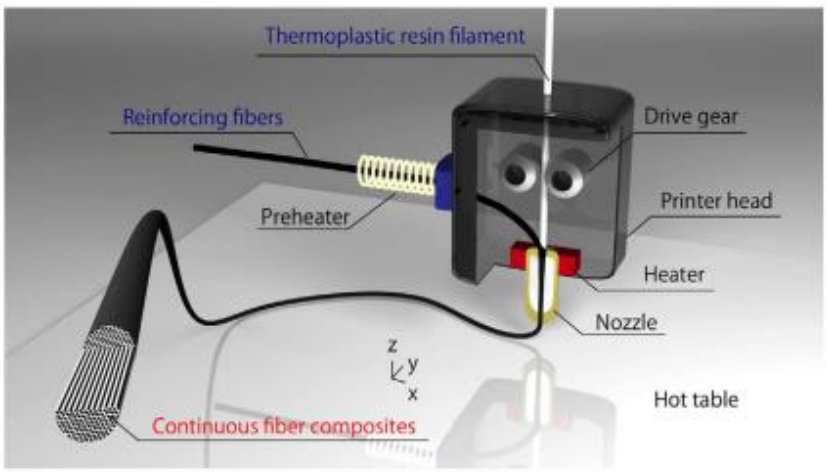

Figure 2.30, Continuos fibre FDM printer configuration

Tensile test samples were printed and the tensile strengths of carbon and jute reinforced composite were measured to be 185.2 and 57.1MPa respectively. This corresponds to an increase of 435 and 134% relative to unreinforced PLA samples. Improving the interfacial adhesion and fibre distribution were identified as methods for possible improvements in future work.

A similar method for fabricating continuous fibre composites has been successfully commercialised by MarkFrorged Inc in 2014 [118]. The difference between this method and that researched by Matsuzaki *et al*, is that the Markforged printer lays down a layer of nylon matrix material then the fibre which has already been combined with a small amount of polymer is deposited on top of it in a separate step. Repeating the process creates a laminating effect between the fibre and the matrix until the final part is formed.

The four types of fibre reinforcement currently offered by the company are carbon, high strength high temperature fibreglass (HSHT), fibre glass and kevlar. Of these materials, carbon fibre reinforced composites show the best tensile strength and stiffness measured to be 700MPa and 470GPa respectively [119]. The printing software developed by the company can calculate the placement of the fibre based on where the stresses will be applied to achieve effective reinforcement. This is illustrated in Figure 2.31 where the black carbon fibre can be seen in the high stress areas.

Figure 2.31, Bicycle crank arm showing strategically placed carbon fibre reinforcement [118]

Chapter 3:
Materials and Methods

Chapter 3

Materials and Methods

3.1 Experimental Overview

This chapter describes how hemp and harakeke fibres as well as gypsum particles were used in varying weight percentages in recycled polypropylene to fabricate 3d printing filament composites. The purpose of doing so was to improve properties applicable to 3d printing, namely tensile strength, stiffness, shrinkage and surface finish.

Pre and post-consumer recycled polypropylene were selected as matrix materials based on availability, contamination level and pre-established markets. Hemp and harakeke fibres underwent alkali treatment to remove lignin, improve fibre separation and roughen the fibre surface in an effort to improve adhesion with the matrix. Maleated polypropylene (MAPP) was used as a coupling agent in a MAPP: particle or fibre ratio of 1: 10.

Composites were produced by compounding the particles or fibres with polypropylene in a co-rotating twin screw extruder. A method of fabricating accurate 3mm filament was created and used to determine improved processing parameters before using those parameters on all subsequent filaments. All composites were then 3d printed into test samples, used to determine their tensile strength, stiffness, surface roughness and shrinkage.

3.2 Composite Material Constituents.

3.2.1 Pre-Consumer Recycled Polypropylene

Pre-consumer recycled polymers are derived from an industrial waste which are produced insignificant quantities by large plastics manufacturers as a result of their high volume production methods. For example, in injection moulding, waste from 3 to 5% of the total plastic used is produced as a result of rejects and the waste in inlet cavities which allow the plastic to fill the mould. Generally speaking this form of waste polymer usually contains fewer contaminants, which can often limit the recyclability of the polymers from post-consumer products.

Pre-consumer recycled polypropylene was supplied for the current research in granule form by Astron Plastics Group, Auckland. Prior to processing, polymer samples were dried in a convection oven at 80^{o} C or 105^{o} C for a minimum of 24 hours. Samples were removed from the oven immediately prior to extrusion to reduce moisture absorption from the environment.

3.2.2 Post-Consumer Recycled Polypropylene Woven Bags

When sourcing the post-consumer polypropylene for experimentation, the premise was that the polymer cannot already have an end market but instead would otherwise be disposed of at a refuse centre.

Large woven polypropylene bags, as shown in Figure 3.1, were supplied by Transpacific Recycling Centre located in Tauranga. The bags are a post-consumer product resulting from a large local salt importer. Although there are relatively small local markets that reuse some of these bags, contamination issues restrict their use in many markets.Although the bags are predominantly made from woven polypropylene, they are stitched together using polyester thread. There was no practical way to remove all traces of this thread, so the two materials were processed in a combined form. In addition to the impracticality of separation, the literature suggests possible mechanical property enhancements when combining polyester fibres in a polypropylene matrix [46; 120; 121] and so their presence could have potential benefits.

Bags were manually cut into pieces approximately 200mm x 200mm and then granulated using a Castin laboratory scale granulator. The resulting plastic strands (Figure 3.2) were then washed with dishwashing liquid in hot water before being rinsed thoroughly and oven dried at 105 ^{o}C for a minimum of 24 hours. The fibres were then compounded in a ThermoPrism TSE-16-TC 16mm screw diameter co-rotating twin screw extruder (later referred to as the 16mm extruder) before being granulated and dried at 105 ^{o}C for a minimum of 24 hours.

Figure 3.1, Post consumer polypropylene woven bags.

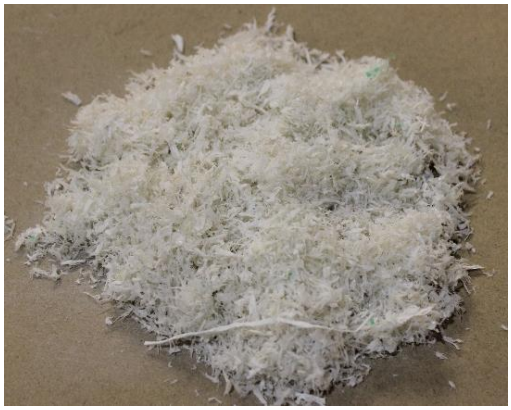

Figure 3.2, Shredded polypropylene bags

3.2.3 Hemp Fibre

Hemp fibre was locally grown from October 2013, harvested in February 2014 after a 120 day cycle, and subsequently donated by the Hemp Farm NZ Ltd. Green hemp stalks were air dried before the bast fibre was separated from the stalks by hand. The bast fibre was thoroughly inspected to ensure it was free of visible defects before being chopped into shorter lengths using a laboratory scale Castin granulator. An 8 mm sieve was used to regulate the size of the resultant fibre which produced an average fibre length of 10mm.

3.2.4 Harakeke Fibre

Mechanically separated harakeke was air dried and supplied to the University in bundle form by the Templeton Flax Mill in 2014. Fibre bundles were manually cut with scissors into 200mm lengths to avoid entanglement in the granulator blades. The chopped fibres were then fed into a Castin laboratory scale granulator using the same 8mm sieve as used with the hemp fibre giving a similar average material length.

3.2.5 Alkali Treatment

Sodium hydroxide (NaOH) treatment is commonly used in the pulp and paper industry in order to remove lignin and separate cellulose fibres. For natural fibre composites the mechanical properties can potentially be enhanced with an optimised treatment cycle. To achieve effective results the process must remove the right amount of lignin, avoid fibre degradation and achieve a high degree of separation. The digestion of hemp and harakeke fibre was performed at high temperatures and pressures within a lab scale digester (Figure 3.3). The digester consisted of a 15 litre pressure vessel which could be mechanically rotated in a pendulum motion to a maximum angle of 55° either side of the vertical axis. The temperature was controlled by heating elements positioned within the walls of the vessel with an upper limit of 200°C.

Figure 3.3, Lab scale digester

For added safety and the ability to treat small batches of fibre, four stainless steel 1L capacity digestion canisters were used to contain the fibre/solution mixtures. These canisters were housed inside the larger pressure vessel of the digester which was then filled with water and sealed before the cycle began.

Sodium hydroxide (NaOH) powder and sodium sulphite ($NaSO_3$) pellets, with a purity level of 98% were acquired from Scharlau Chemie S.A. Oven dried hemp or harakeke fibres were weighed into 90g samples and carefully placed into each of the steel canisters. For hemp fibres, a solution containing 36 g of NaOH and 684 ml of water was mixed in a conical flask. Four batches of this solution were prepared and combined with the fibres inside the canisters immediately prior to treatment. For harakeke fibres, the solution containing 36 g of NaOH, 14.4 g $NaSO_3$ and 670 ml of water was prepared for use in a similar way.

Figure 3.4 shows the temperature profiles used for both harakeke and hemp fibre treatment. For hemp fibre, the temperature was set to rise at a uniform rate from room temperature to 160°C within the first 90 minutes where it was maintained for 30 minutes before cooling. Similarly, for harakeke fibre the temperature was set to rise to 170°C in the first 90 minutes and was held there for 40 minutes before cooling. An investigation conducted by Efendy *et al* [122] had previously determined that these treatments provided the optimal thermal parameters for the aforementioned fibre species.

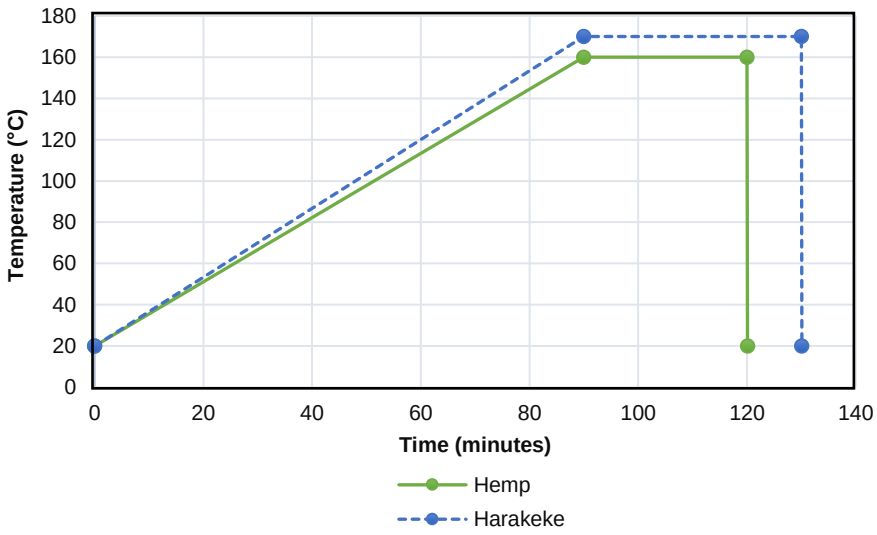

Figure 3.4, Digester cooking cycles for hemp and harakeke

Once the treatment cycle was completed, the fibres were removed from the canisters and thoroughly washed until all remnants of the alkali solution had been removed. The washed fibre pulp was then separated into smaller pieces by hand before being placed in an oven to be dried for a minimum of 24 hours. Dried fibre clusters were then put through the granulator for separation prior to composite fabrication.

3.2.6 Recycled Gypsum Powder

Recycled gypsum board was obtained from local building developments underway within the Hamilton area. All gypsum board used in experiments was manufactured by Gib Plasterboards. The constituents for Gib plasterboard are detailed in Table 3.1 below.

Table 3.1, Gib Plasterboard gypsum board constituents

Component	Typical %
Gypsum	93.0%
Paper	6.0%
Acid Modified Wheat or Corn Starch	0.5%
Sugar	> 0.5%
Calcium Naphthalene Sulphonate	> 0.5%
Boric Acid	> 0.5%
Fibreglass	> 0.5%
Vermiculite	> 0.5%
Fly Ash	> 0.5%

To separate the gypsum powder from the paper, boards were cut into 100 x 300 mm sheets and fed into a Filamaker lab scale shredder. The resulting mixture was then put through a 2mm sieve which effectively removed the majority of the paper. The sieved powder was then processed to a smaller size in a Nutribullet food blender for 5 minutes and placed in an oven at 105^{o} C for 24 hours. The resulting particles were measured using a Malvern Mastersizer 2000 and the results are shown in Table 3.2. The instrument was set to analyse with a refractive index of 1.525 which is the recorded standard for measuring gypsum powder.

Table 3.2, Particle size for recycled gypsum powder

Lower 10% (µm)	Surface weighted mean (µm)	Volume weighted mean (µm)	Upper 10% (µm)
> 3.766	8.429	95.775	< 236.466

3.3 Composite Fabrication

3.3.1 Pre-Consumer PP Composite Compounding

Differences in densities between the polymer granules, fibre and mineral additives resulted in poor fibre distribution prior to compounding leading to blockages within the extruder and poor fibre adhesion within the matrix. To avoid this, oven dried constituents were weighed and spread in even layers in a square plastic container. A flat scoop was then used to pick up portions of the mixture and force feed it into the 16mm extruder to ensure all fibre was included. The five heating elements on the extruder were held at 150, 170, 170, 170 and 180 ^{o} C from entrance to exit respectively

3.3.2 Post-Consumer PP Composite Compounding

Once the PP bags had been shredded, the polymer was in the form of fibrous strands varying in length from 2-10mm. Composite constituents were weighed and placed in a sealed plastic bag where they were shaken until relatively even distribution was achieved. The similar uncompressed densities of the hemp, harakeke and PP strands (0.0618, 0.0589 and 0.0686 g/cm^3 respectively) lead to better mixing than obtained with polymer granules. The premixed materials were then force fed into the 16mm extruder in a similar way to pre-consumer PP using the same temperature profile.

3.3.3 Filament Fabrication

Prior to processing different filaments, the auto feed hopper was cleaned with compressed air removing any traces of contaminants. Polyolefin purge material was then used to clean the barrel of the extruder before removing and cleaning any remaining purge from the die.

Polymer or composite granules of each different combination were stave fed at a rate of 12 rpm into a Labtech 1201-LTE20-44 20mm screw diameter twin screw extruder shown in Figure 3.5 (later referred to as the 20mm extruder). The screw speed was maintained at 50 rpm for composites up to 30wt% fibre, but decreased with increasing fibre content to maintain a pressure near the end of the barrel below 70% of the allowed maximum pressure. Tests were conducted on 3mm diameter dies with capillary lengths of 0, 23, 40 and 50mm. Analysis of the results showed that the capillary length of 40mm produced the highest accuracy and therefore this was used for the fabrication of all filaments. The 11 heating elements on the extruder barrel were held at 150, 160, 170, 170, 170, 170, 175, 185, 190, and 190^{o} C from entrance to exit respectively.

Figure 3.5, Labtech 1201-LTE20-44 extruder used for filament fabrication

With a screw speed of 50 rpm, the filament exited the die at approximately 0.05 m/s and was still in a semi molten form. To increase dimensional consistency, a filament spooling machine was designed and built (Figure 3.7)This consisted of a machined cylinder which was belt driven by a small low geared electric motor. The speed of the motor was governed by a variable power supply which was located underneath the cylinder.

By matching the rotational speed with the exit velocity of the filament and controlling the vertical height (labelled x in Figure 3.6) the filament diameter could be controlled. As the filament wound onto the cylinder, the machine was slowly moved sideways to avoid filament being spooled onto itself. To limit contamination resulting from purge material remaining in the barrel, the beginning of every filament was marked with tape and test samples were taken from the opposite end of the roll.

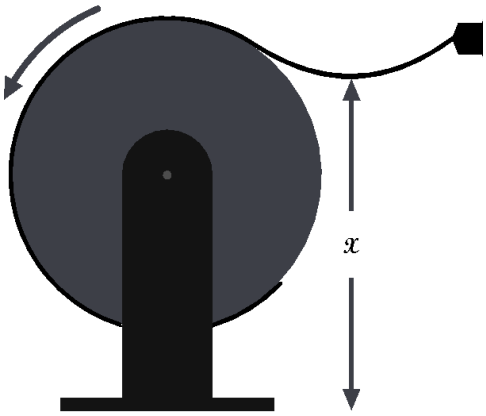

Figure 3.6, Filament dimension control

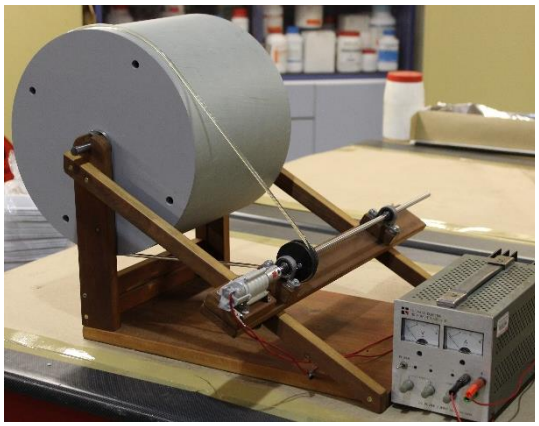

Figure 3.7, Filament spooling machine

Four variations of the initial filaments were fabricated from 20wt% harakeke fibre and pre-consumer PP as the matrix (Table 3.3). These filaments were used to confirm the best constituent drying temperature, compounding extruder and physical form of MAPP. The tensile strength, stiffness and surface finish of the resulting filaments were compared and used to determine the processing method for future composites.

Table 3.3, Initial filament processing parameters

Screening experiment	Drying temperature	MAPP	Compounding extruder
S1	80	Powder	16mm
S2	105	Powder	16mm
S3	105	Granules	16mm
S4	105	Powder	20mm
S5	105	Powder	None

The compositions of the filaments that were produced following the initial screening can be seen in Table 3.4 below.

Table 3.4, Filament constituent compositions

Test Filament	Pre-consumer PP (%)	Post-consumer PP (%)	Hemp (%)	Harakeke (%)	Gypsum (%)
F1	100				
F2	89		10		
F3	78		20		
F4	67		30		
F5	56		40		
F6	45		50		
F7	89			10	
F8	78			20	
F9	67			30	
F10	56			40	
F11	45			50	
F12		100			
F13		89	10		
F14		78	20		
F15		67	30		
F16		56	40		
F17		45	50		
F18		89		10	
F19		78		20	
F20		67		30	
F21		55		40	
F22		44		50	
F23	89				10
F24	78				20
F25	67				30
F26	56				40
F27	45				50

3.4 3d Printing

The conventional method of printing onto a heated print bed did not work for polypropylene due to lack of adhesion. A 5mm thick polypropylene sheet was retrofitted into the print bed and used for all 3d printing.

Inherent variations in diameter, shrinkage and viscosity between filaments necessitated the calibration of the 3d printing software parameters for each individual filament. Prior to printing, the filament diameter was measured with digital callipers and input into the software. A rectangular calibration sample measuring 15 x 5 x 1mm was then printed through a 1mm die. As the sample was printed, the width of the extruded bead labelled 'b' in Figure 3.8 was carefully measured using markings on the print bed and a magnifying glass. The filament diameter parameter in the software was altered until the value of b was measured to be 1.1mm. The software would then print each bead such that distance 'a' was equal to 2mm making the overlapping distance 'c' approximately equal 0.2mm.

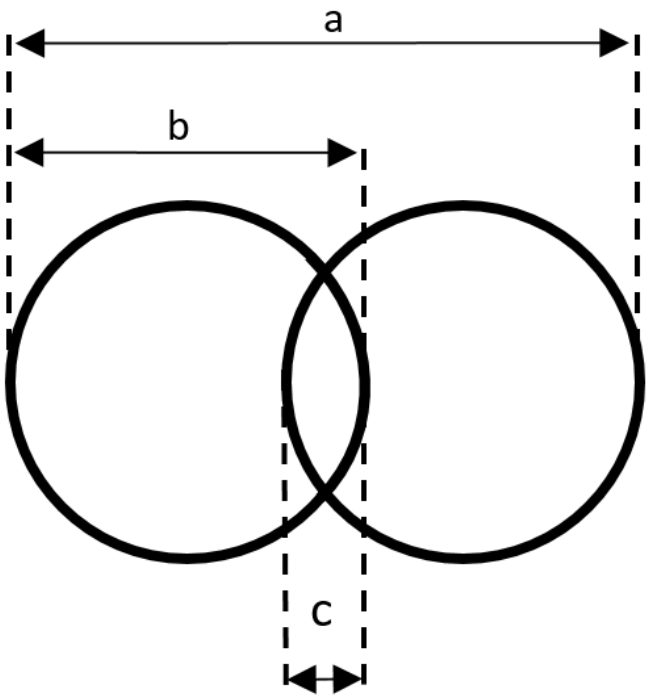

Figure 3.8, Cross section of 3d printed intersecting beads

3.4.1 Composite Tensile Testing

Tensile tests were performed according to ASTM D638: Standard Test Method for Tensile Properties of Plastics. The ultimate tensile strength and Young's modulus of the dog bone and filament specimens were determined using an Instron 33R4204 universal testing machine equipped with a 5 kN load cell. A standard cross-head speed of 1 mm/min was applied to both dog bone and filament specimens. Strain was measured using an Intron 2630-112 extensometer fitted to the samples. The gauge length of the dog bone specimens was 4.88 mm, whilst a 50 mm gauge length was assigned to each of the filament samples. All composite specimens were tested until failure, whereas unfilled polypropylene specimens were only tested to a point of maximum stress due to excessive necking.

To investigate fibre-matrix adhesion and fibre alignment, the fracture surfaces of selected tensile test specimens were observed using a Hitachi S-4100 Field Emission Scanning Electron Microscope (SEM)

3.4.2 Shrinkage Testing of 3d Printed Parts

To measure the effects of shrinkage specific to fused deposition modelling, a novel method was developed and introduced simulating a problem found in early testing where printed samples would peel upwards from the bed and eventually become dislodged. This was found to significantly reduce the accuracy of the resulting print. Test samples with dimensions indicated in Figure 3.9 were printed in a single layer 0.8mm thick. Because the sample solidified while adhering to the print bed the warping effects of shrinkage were minimised. Once the sample had been printed digital callipers were used to measure the length of each arm. A razor blade was then used to dislodge the arms from the bed while leaving the centre in attached. A second layer was then printed on top of the first sample using a Z offset of 0.8mm.

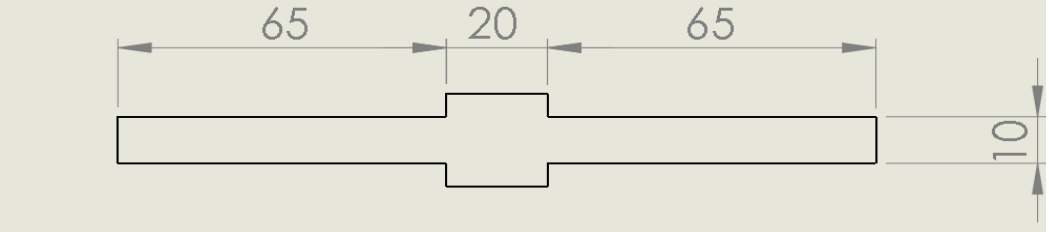

Figure 3.9, Shrinkage test dimensions (mm)

Figure 3.10, , 3d printed sample showing exaggerated shrinkage effect

As the second layer solidified the shrinkage caused each end to distort in a controlled direction shown in Figure 3.10. The radius of curvature was used to establish a relative shrinkage value useful for comparing shrinkage properties inherent in each material. Full details of test sample geometry and formulas used are shown in Appendix 1.

3.4.3 Density Measurements

The density measurements of composite samples were carried out using the ASTM 792-00 (Standard Test Methods for Density and Specific Gravity (Relative Density) of Plastics by displacement). Distilled water was used to in an Archimedes test apparatus. Density measurements were calculated by taking the average of five separate specimens for each of the polymer and composite samples.

Chapter 4:
Results and Discussion

Chapter 4

Results and Discussion

4.1 Tensile Strength and Stiffness of Initial Screening Composites

The tensile strength and Young's modulus results for the initial parameter screening experiments are shown in Figure 4.1 and Figure 4.2 with the error bars representing ± 1 standard deviation. Comparing the properties of S1 and S2 it can be seen that the increased drying temperature corresponds to increased composite tensile strength and Young's modulus of 10 and 37.2% respectively. This indicates that there could have been a small amount of moisture remaining inside the harakeke fibre which was removed by increasing the drying temperature; the removal of such moisture would be expected to affect the interfacial bond strength and could account for the increase in properties.

The lower results observed in S4 may have been caused by a reduction in fibre length due to longer and more severe mixing zones in the 20mm screws as opposed to those of the 16mm extruder. Avoiding the compounding step altogether as shown with S5 samples yielded lower tensile results than compounding on the 16mm extruder. This is thought to be primarily caused by poor fibre distribution throughout the matrix leading to poor fibre wetting.

Comparing the properties obtained for S2 and S3 the effect of MAPP in powder and granule form was investigated. Using MAPP in powdered form increased the tensile strength and Young's modulus of 17.7% and 18.5% relative to granule form thought to come as a result of better MAPP distribution throughout the matrix.

Overall, the S2 samples were shown to give the highest tensile strength and Young's modulus results of all screening samples with an increase of 38% and 162% respectively when compared to plain PP.

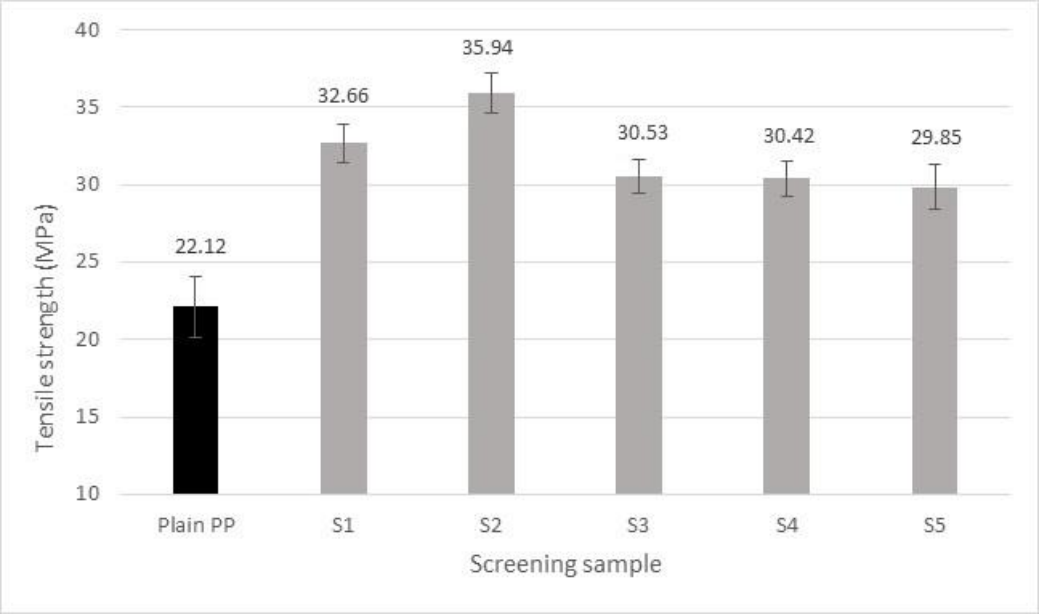

Figure 4.1, Tensile strength of 20wt% harakeke filament under different processing parameters.

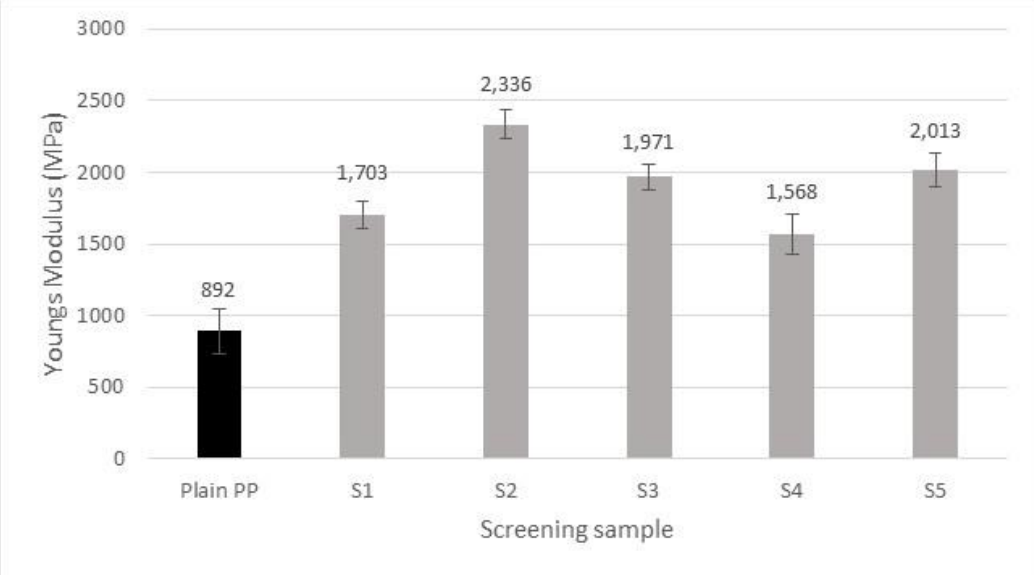

Figure 4.2, Young's modulus of 20wt% harakeke filament under different processing parameters.

4.1.1 Microscopic Evaluation

The fracture surfaces of all samples were observed using a scanning electron microscope (SEM). The SEM micrographs in Figure 4.3 to Figure 4.6 show the effects of varying compounding parameters on void formation and interfacial bonding. Comparing the fracture surface of S5 with that of S2 (Figure 4.3 and Figure 4.4) S3 showed a noticeable reduction in pore size. This implies that the additional compounding step helps with pore size reduction contributing to higher mechanical properties. The fracture surface of sample S3 in Figure 4.6 supports poor interfacial adhesion between the fibre and matrix as indicated by voids surrounding the reinforcing fibres. Closer inspection of the S2 fracture surface supports there to be regions of good interfacial adhesion between fibre and matrix as a result of using MAPP in powdered form (Figure 4.5). However, the fibre pull-out indicates that the fibre length of the protruding fibres could be below the critical length and/or that the interface was not strong enough to prevent pull-out.

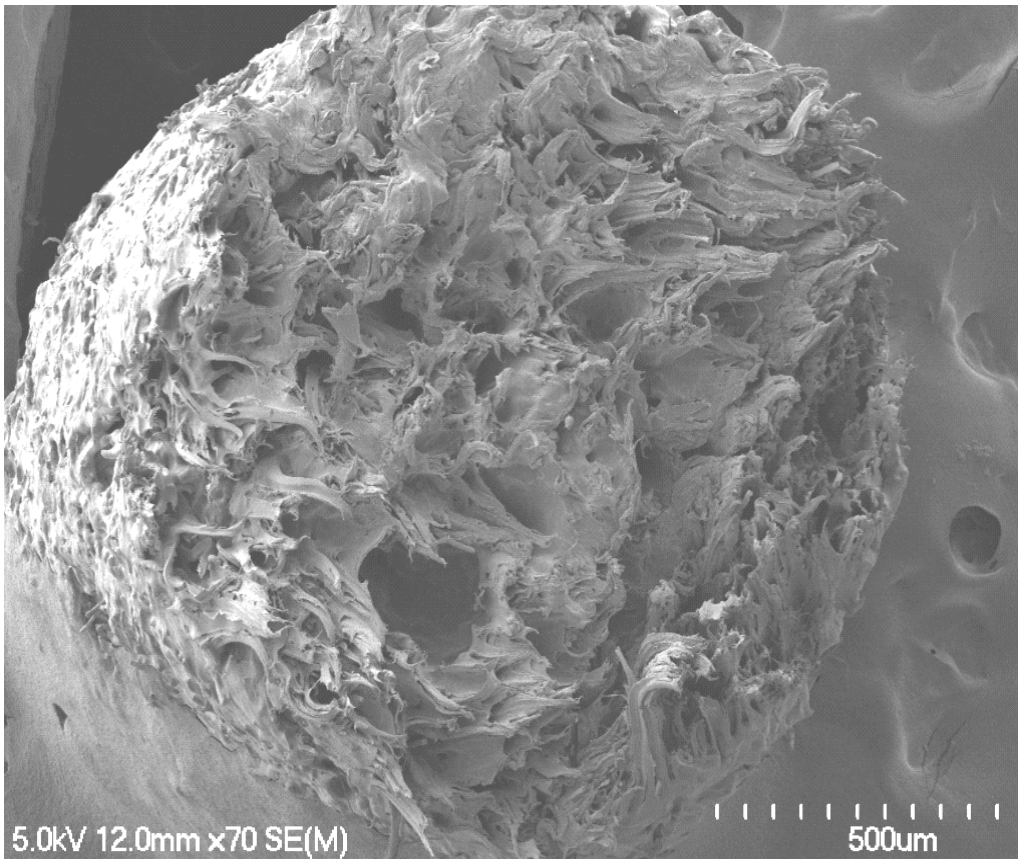

Figure 4.3, Sample S5 showing large pores and fibre pull-out

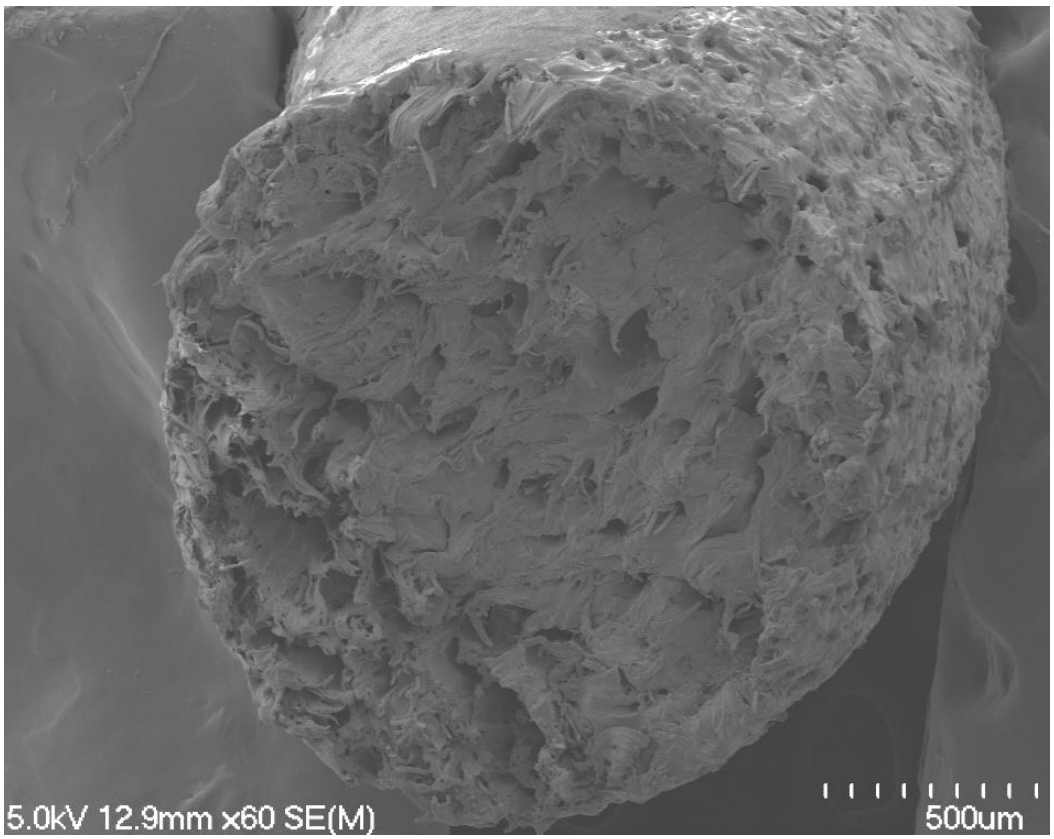

Figure 4.4, Sample S2 showing reductions in pore size

Figure 4.5, S2 sample showing fibre pull out and fibre fracture near the surface

Figure 4.6, S3 sample showing fibre pull out and poor interfacial bonding

4.2 Pre-consumer Polypropylene Composites

4.2.1 Tensile Strength and Stiffness of Hemp and Harakeke Fibre 3d Printing Filament

The tensile strength and Young's modulus of 3mm diameter composite filaments are compared to plain polypropylene filaments in Figure 4.7 and Figure 4.8 respectively. The results clearly show an increase in strength and stiffness as a result of a higher fibre weight fraction. This is supported by highly significant R^2 values and positive gradients of regression lines fitted to both graphs. Hemp and harakeke fibres show similar reinforcing qualities with any variation being well within the standard deviation error. The greatest improvement was for 30 wt% harakeke which had a tensile strength and Young's modulus 52% and 147% higher than plain polypropylene. Increasing the fibre content from 10% to 20 wt% raised the tensile strength and Young's modulus by around 8 and 720 MPa respectively. However, increasing the fibre content from 20% to 30 wt% gave lower increases of 2.5 and 430 MPa. This could possibly be due to reduced fibre wetting with the increased fibre content resulting in underutilised reinforcing fibre.

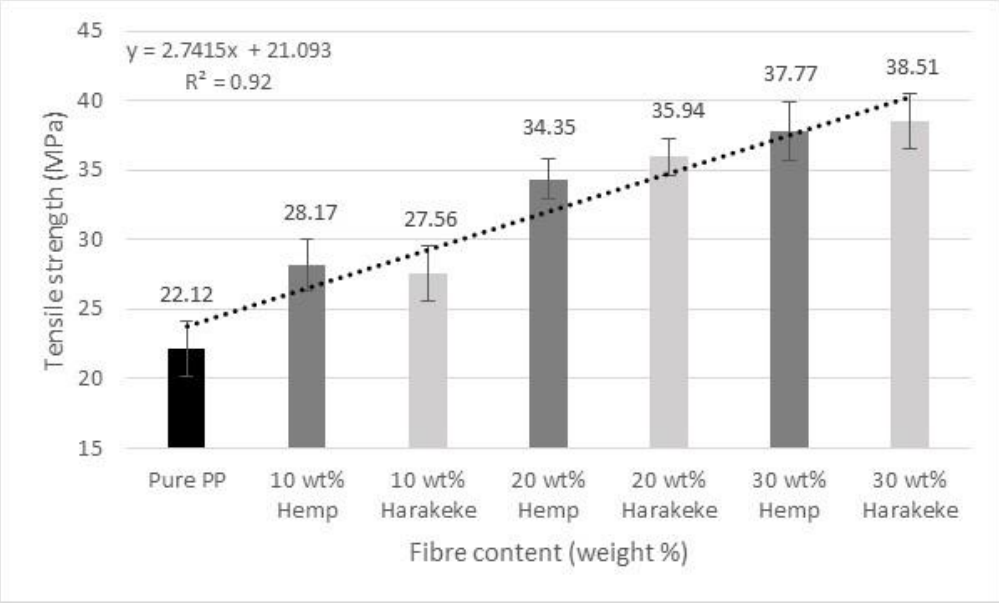

Figure 4.7, Tensile strengths of the 3mm composite filaments produced using pre-consumer PP as a matrix (MPa).

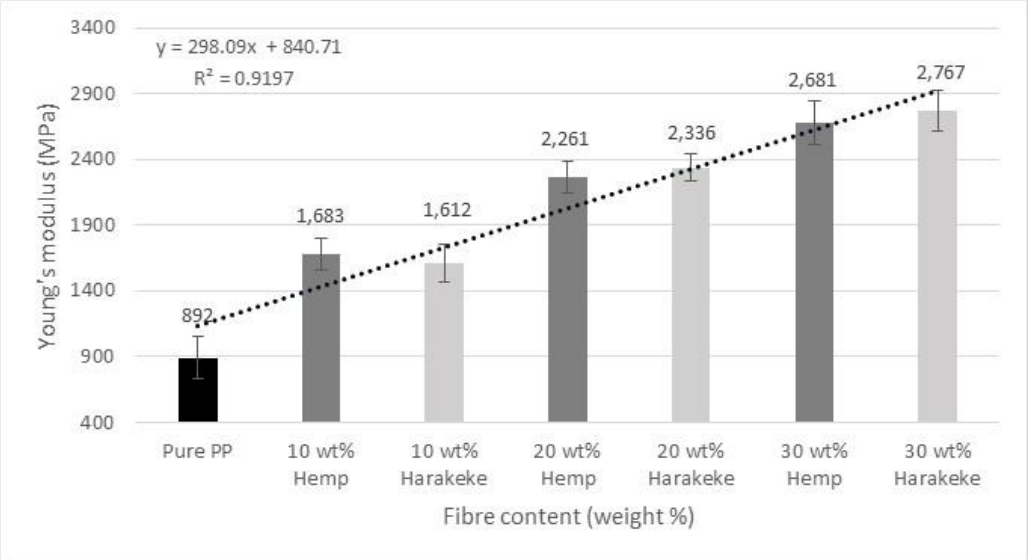

Figure 4.8, Young's modulus of composites produced using pre-consumer PP as a matrix (MPa).

Research conducted alongside with this research at the University of Waikato investigated the effects of E-glass fibre reinforcement in the same pre-consumer polypropylene; glass fibre/polypropylene 3d printing filament was fabricated using similar temperature profiles and processing machinery [123]. However, the fibre and polypropylene matrix were compounded using a twin screw compound mixer instead of a twin screw extruder. The tensile strength and Young's modulus results for glass fibre/polypropylene 3mm filaments are shown in Table 4.1 below. Glass fibre can be seen to result in tensile strength enhancements lower than those of natural fibre composites. However, the Young's modulus values of glass fibre composites are between 18 and 21% higher than those reinforced with harakeke fibre. The study attributed poor mechanical performance to severe fibre length reductions caused by the brittle failure of glass fibres.

Table 4.1, Mechanical properties of natural fibre compared to glass fibre reinforced 3d printing filament

Sample	Tensile strength (MPa)	Net increase (%)	Young's modulus (MPa)	Net increase (%)
Plain PP	22		892	
10 wt% Glass	29	33	1995	124
20 wt% Glass	32	39	2016	126
30 wt% Glass	36	62	3386	280
10 wt% Harakeke	28	25	1612	81
20 wt% Harakeke	36	62	2336	162
30 wt% Harakeke	39	74	2767	210
10 wt% Hemp	28	27	1683	89
20 wt% Hemp	34	55	2261	153
30 wt% Hemp	38	71	2681	201

4.2.2 Influence of Fibre Content on Filament Fabrication

Originally it was planned to examine composite filament ranging from 10 to 50 wt% fibre content. Fabrication of 10, 20 and 30 wt% filament proved relatively simple with little variation of die pressure and extrudate exit velocity. Increasing the fibre content from 30 to 40 wt% gave rise to a sharp increase in die pressure and screw torque which forced a reduction in screw speed from 50rpm to 30 rpm to avoid damage to the machine. Reducing the screw speed corresponded to a considerable reduction in exit velocity allowing the composite more time to solidify prior to spooling. This rendered the spooling machine ineffective as it relies on the filament being malleable enough to wrap around the cylinder. Given the ineffectiveness of the spooling machine, filament with fibre content in excess of 40 wt% was not dimensionally consistent enough for application in 3d printing.

Figure 4.9 shows the increasingly coarse surface finish resulting from increased fibre content. Filaments containing 10 wt% fibre content gave a semi-gloss type smooth finish which dulled as the fibre content increased. A 'sharkskin' effect began to develop with the 40 wt% samples and was very severe when fibre content was increased to 50 wt%. This effect could possibly be reduced by increasing the die temperature or modifying the die to reduce shear stress from die walls [61].

Figure 4.9, Influence of fibre content on surface finish

4.2.3 3D Printed Samples

4.2.3.1 Tensile Strength and Stiffness

Contrary to the steady increase of tensile properties observed for 3mm filament, the results shown in Figure 4.10 and Figure 4.11 display a less predictable relationship between fibre content and mechanical properties. The largest increase in tensile properties was obtained for the 20wt% harakeke fibre 3d printed dog bone specimen, with an ultimate tensile strength almost 49% higher than unfilled polypropylene whilst the 20 wt% hemp composite dog bone possessed a tensile strength of approximately only 13 MPa, which is 21% lower than the unfilled polypropylene specimen. The favourable data from filament testing suggests that the concern would lie with the subsequent FDM processing.

Generally, most samples had relatively large standard deviation values compared to 3mm filament, particularly with Young's modulus. The Young's modulus also reduced more substantially than tensile strength with reductions of up to 950% for 30 wt% harakeke. The reduction in Young's modulus suggests that dog bone samples are experiencing more strain during tensile testing than 3mm filament making it more likely to be caused by shape geometry or layer delamination.

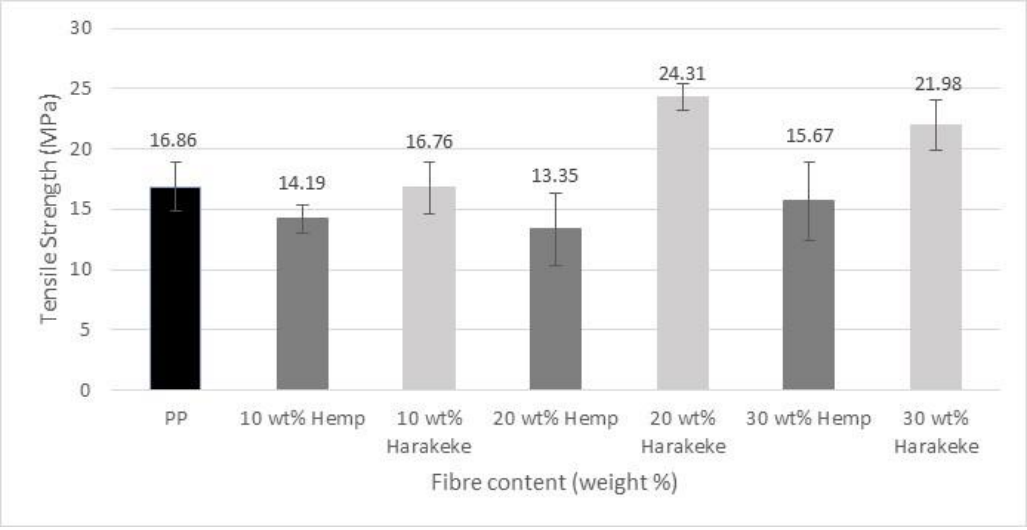

Figure 4.10, Tensile strength of 3d printed dog bone composite samples

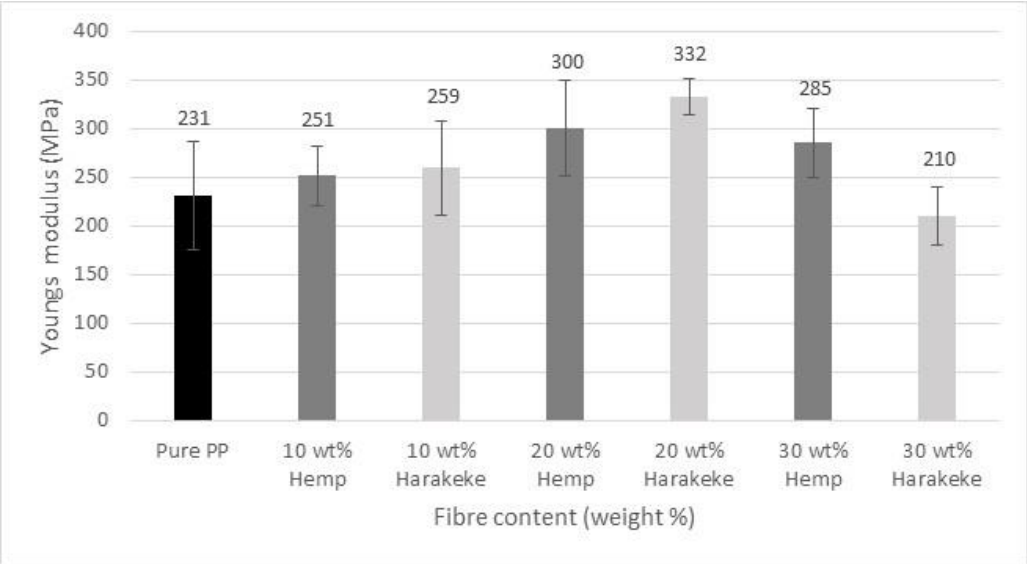

Figure 4.11, Young's modulus of 3d printed dog bone composite samples

Analysis of the 3d printed dog bone samples showed the concentric fill pattern that the 3d printer followed caused voids on either side of the sample as indicated in Figure 4.12 below. In addition to the void created by the printing process, this was a region where the alignment of the printed bead was not parallel to the tensile force. The fact that every sample would break in this region suggests that the tensile results were not only less than their potential but also that alignment of the printed polymer could influence the overall strength of the component. This outlines the importance of properly customising 3d printing settings and carefully choosing the geometry if mechanical performance is of particular interest.

Figure 4.12, FDM printed dog bone sample showing stress concentration point

To examine mechanical performance regardless of print geometry and layer delamination, tensile tests were repeated using 1mm filament extruded through the 3d printer. To 3d print 1mm tensile samples, the filament feed speed was kept constant at 50mm per minute and the temperature was maintained at 230 ^{o}C. The trend observed in 3d printed 1mm filament (Figure 4.13 Figure 4.14) is very similar to that seen in the 3mm filament providing evidence for the theory that geometry has a significant influence on 3d printed components. However, the results show a significant decrease in tensile properties when compared to the 3mm filament (the only difference being the 3d printing extrusion process). Contrary to predictions of increased mechanical properties as a result of increased fibre alignment. The fact that the plain polypropylene filament showed a drop in strength and Young's modulus similar to that of composite samples indicates that the cause is largely related to issues with the polypropylene. This is investigated more thoroughly by measuring density and moisture absorption in section **Error! Reference source not found.** on post-consumer polypropylene composites.

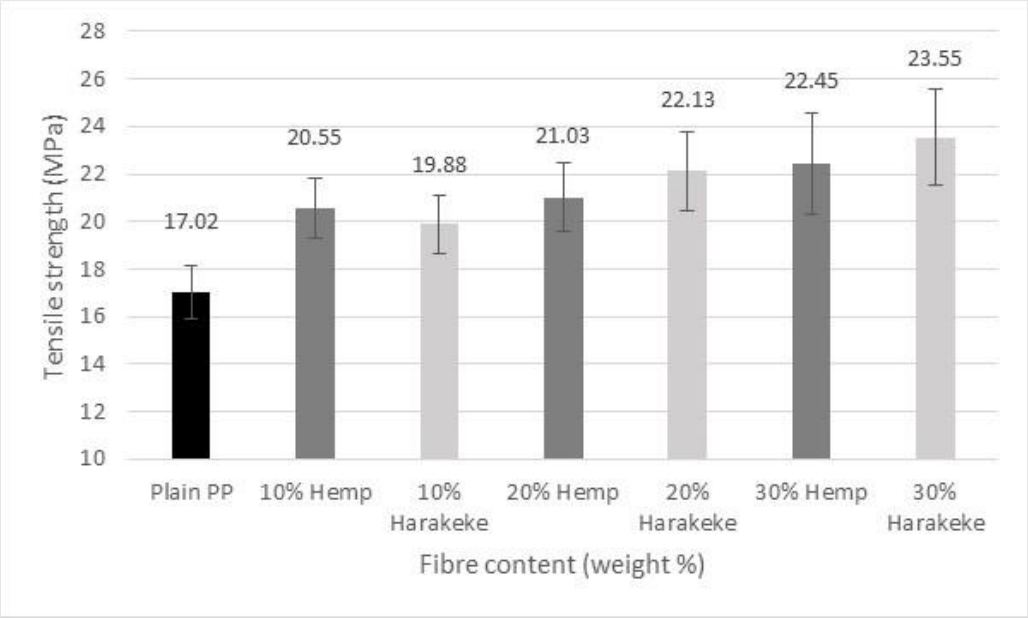

Figure 4.13, Tensile strength of 3d printed 1mm pre-consumer filament

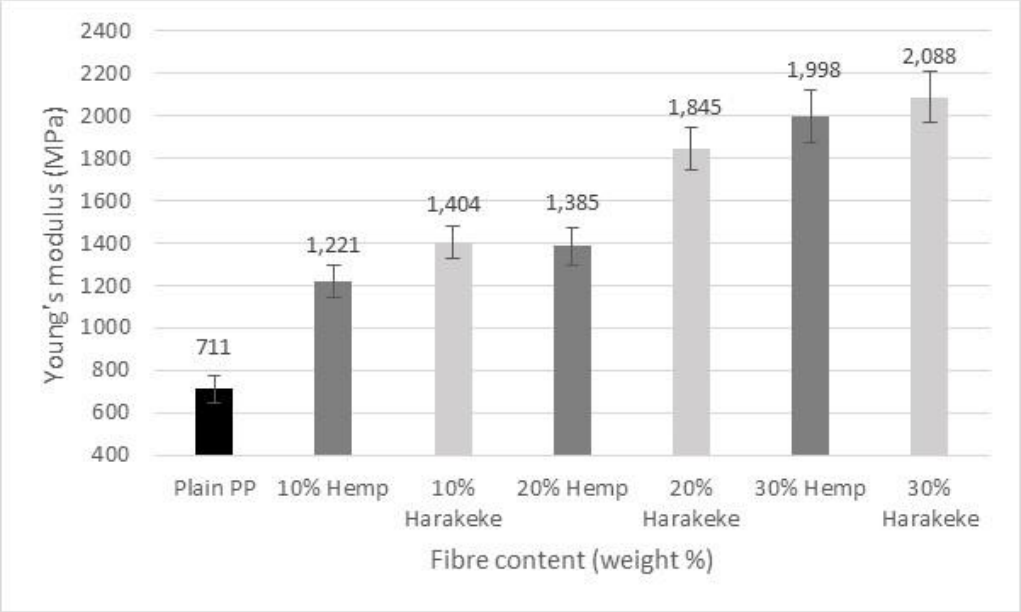

Figure 4.14, Young's modulus of 3d printed 1mm pre-consumer filament

4.2.3.2 Surface finish of FDM composite specimens

According to the literature, surface finish of fibre reinforced polymer composites become progressively more abrasive and dull with increasing fibre content [28; 124] . This relationship was largely observed in harakeke, and to a lesser degree in hemp composites during this investigation. All 10 wt% natural fibre dog bone specimens maintained identical geometrical accuracy to the unfilled polypropylene specimens, although with a lower gloss texture. A small proportion of the 20 wt% samples, along with most of the 30 wt% samples, possessed an irregular surface finish with a ribbon like texture, as shown in Figure 4.15

Figure 4.15, Asymmetrical surface finish of a 30 wt% harakeke dog bone specimen

The cause of this unusual surface finish was attributed to partial blockages in the 1mm extrusion nozzle. The intermittent obstructions affected the exit velocity of the filament, having an adverse effect on print accuracy. These blockages did not appear to have any influence on layer adhesion of the specimens. Investigations were also carried out with regard to altering the diameter of the extrusion nozzle. Using a smaller 0.5 mm extrusion nozzle resulted in irregular obstructions that disrupted the flow of molten filament, leading to noticeable gaps in test specimens. However, increasing the diameter of the extrusion nozzle to 2 mm virtually eliminated this effect, at a cost of lower print resolution.

4.2.4 Tensile Strength and Stiffness of Recycled Gypsum 3d Printing Filament

Gypsum particle reinforced pre-consumer polypropylene composites were fabricated using the same processing temperatures as fibre reinforced composites. Unlike composites containing 40 and 50 wt% fibre, there was no significant increase in torque or pressure when extruding with 40 and 50 wt% gypsum.

The tensile strength and Young's modulus of pre-consumer polypropylene/ gypsum powder composites containing 10 to 50 wt% gypsum are shown in Figure 4.16 and 4.17. A small increase in tensile strength of 9% relative to plain PP was observed for samples containing 10 wt% gypsum. As the gypsum content increased further there was a gradual decline in tensile strength to reach a reduction of 2% for the 50 wt% gypsum. The Young's modulus, however, showed a reasonably linear increase with 50 wt% gypsum composites having a maximum improvement of 88%. The decrease in tensile strength could have been caused by the agglomeration of the gypsum particles with increasing gypsum content. Agglomerated particles have the effect of decreasing interfacial adhesion and act as stress concentration points [125]. The gradual increase in stiffness with increased particle content can be explained by a reduction in polymer chain mobility.

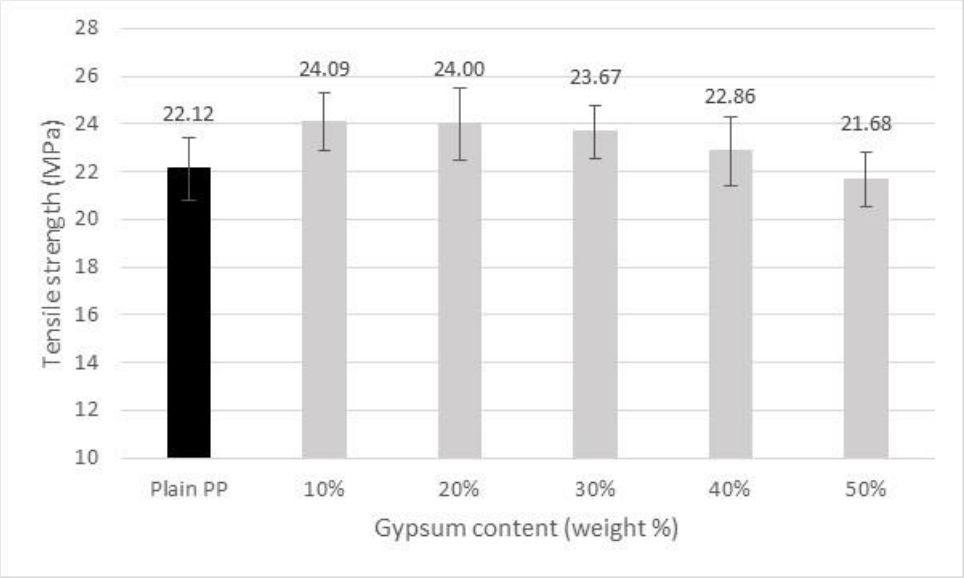

Figure 4.16, Tensile strength of composites containing gypsum compared to plain PP

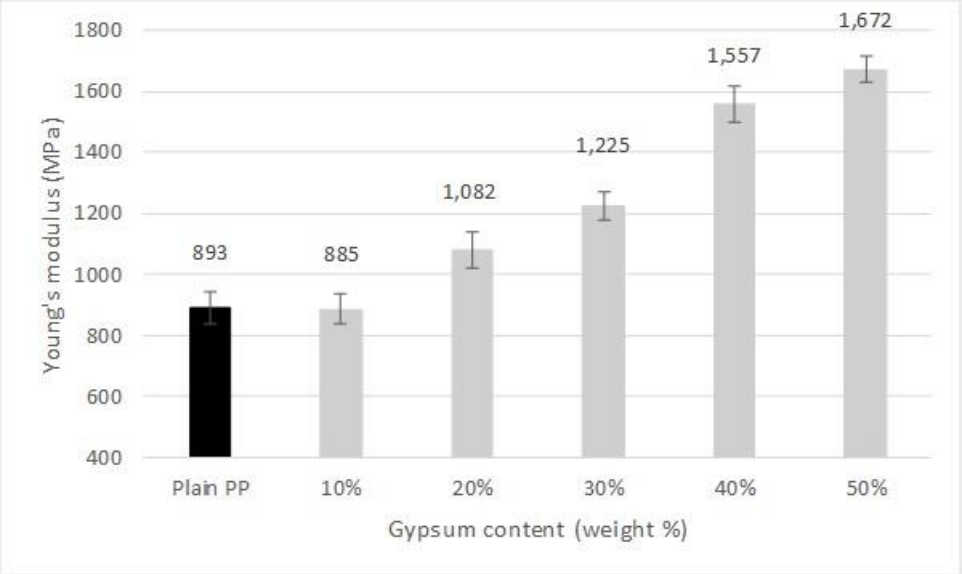

Figure 4.17, Young's modulus of composites containing gypsum compared to PP

4.2.5 Microscopic Evaluation

Brittle fracture surfaces were prepared with the aid of liquid nitrogen for examination of gypsum composites with the scanning electron microscope. At reinforcement content < 30 wt% the gypsum appeared to be broken down and dispersed throughout the matrix, with a mixture of small particles and crystal clusters (Figure 4.18 and 4.19). As the gypsum content increased, the crystals grouped together to form larger conglomerates of gypsum shown in Figure 4.20 and 4.21.

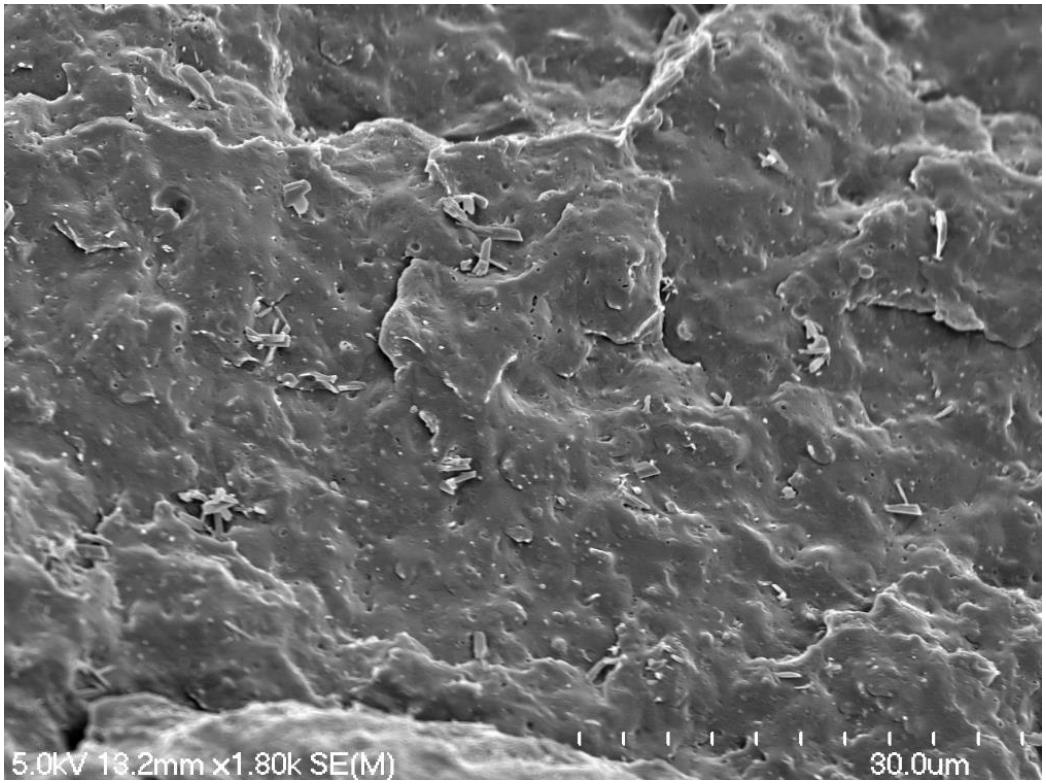

Figure 4.18, 20 wt% gypsum filament showing particles distributed with gypsum crystal clusters

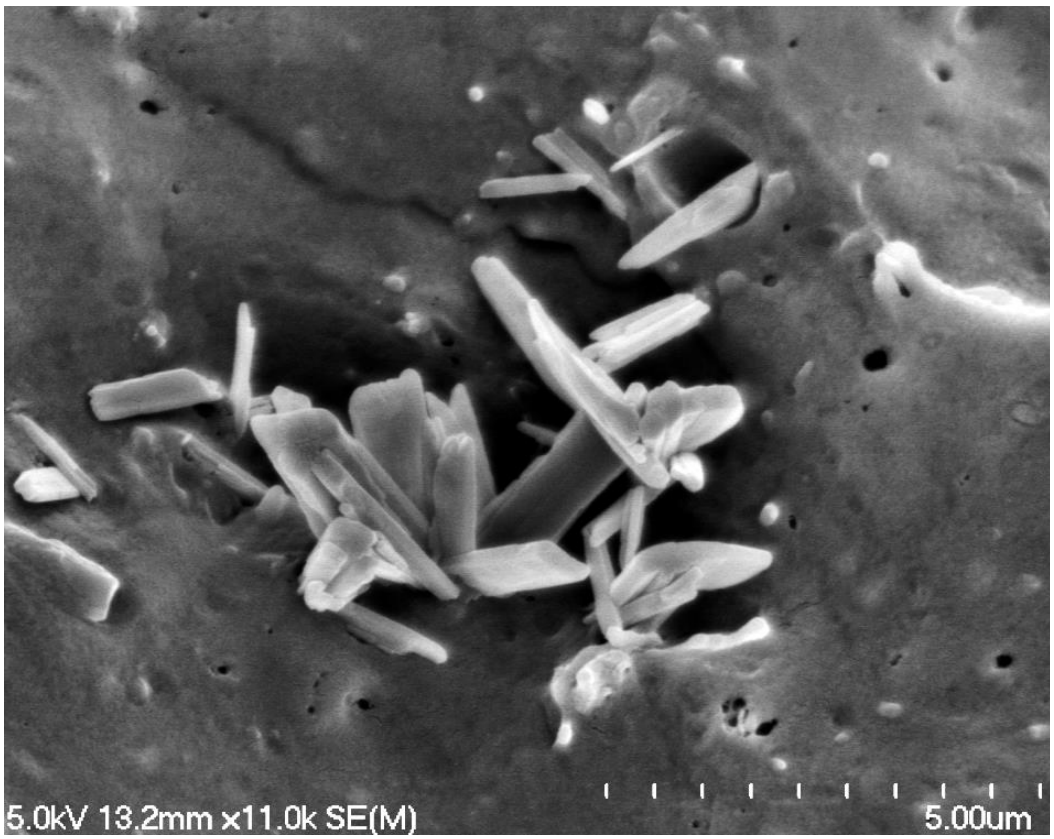

Figure 4.19, Small gypsum cluster within 20 wt% gypsum filament

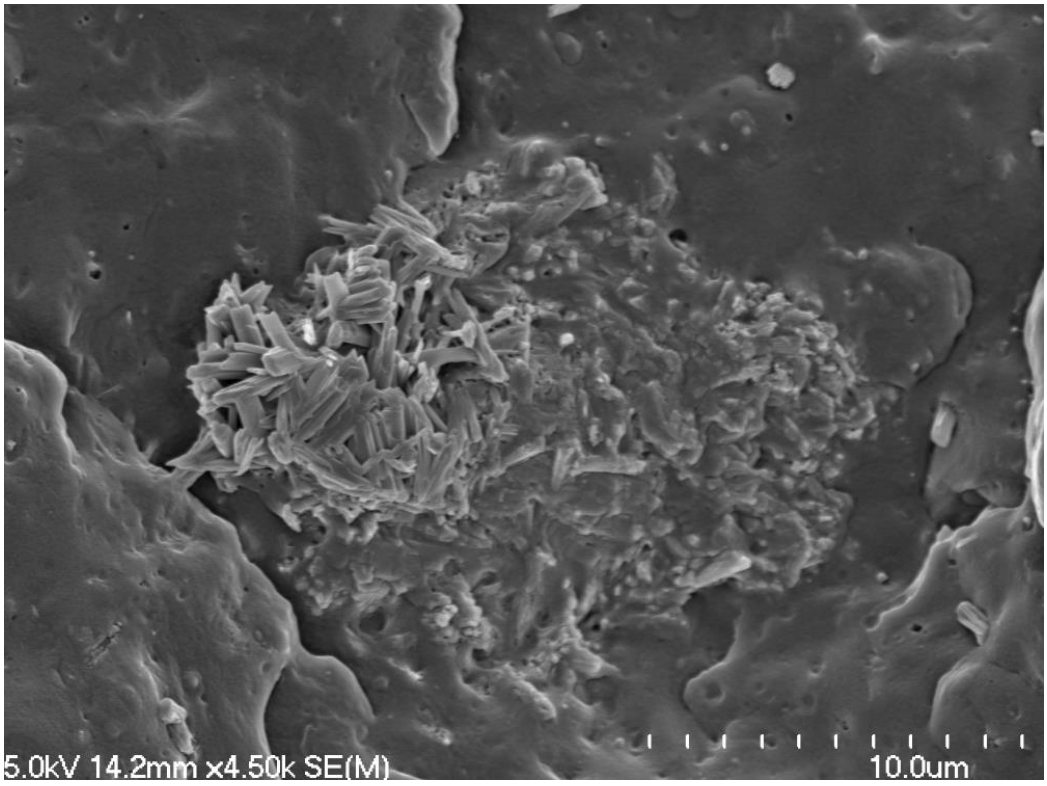

Figure 4.20, 40 wt% gypsum fracture surface showing partially covered crystal cluster

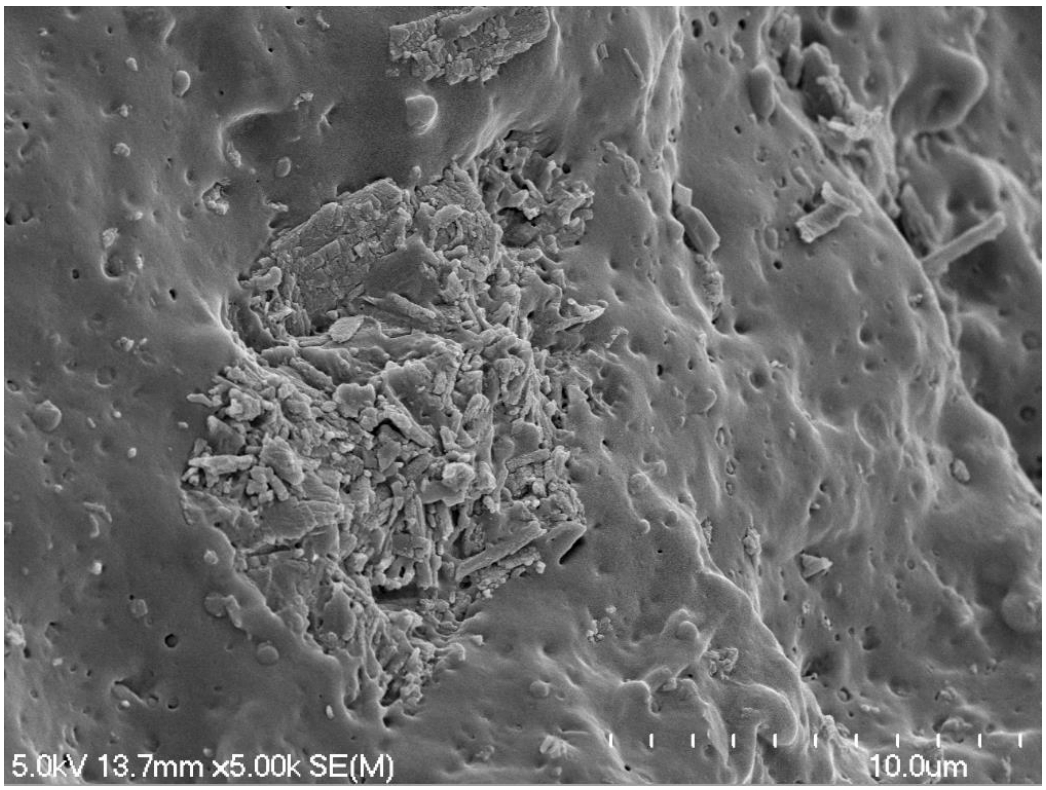

Figure 4.21, 50 wt% gypsum fracture surface showing crystal cluster.

4.2.6 Shrinkage

The shrinkage results for hemp, harakeke and gypsum composites are shown in Table 4.2 below. Natural fibre additives appeared more effective than gypsum in terms of shrinkage reduction. The greatest reduction was that of 30 wt% harakeke filament with a shrinkage of 0.34% corresponding to a 84% reduction compared to plain polypropylene.

Table 4.2, Shrinkage values for pre-consumer polypropylene composites

Sample	Shrinkage (%)	Net reduction (%)
Pre-consumer PP,	2.13	-
10% Hemp	1.17	45
20% Hemp	0.65	69
30% Hemp	0.47	78
10% Harakeke	1.18	45
20% Harakeke	1.2	44
30% Harakeke	0.34	84
10% Gypsum	1.53	28
20% Gypsum	1.51	29
30% Gypsum	1.39	35
40% Gypsum	1.26	41
50% Gypsum	1.15	46

Figure 4.22, Plain polypropylene shrinkage sample

Figure 4.23, 10 wt% hemp shrinkage sample

Figure 4.24, 20 wt% hemp shrinkage sample

Figure 4.25, 30 wt% hemp shrinkage sample

The shrinkage experienced in all composites generally decreased with increased additive content. This can be seen by following the reductions in hemp composites shown in Figure 4.22 to Figure 4.25. It also implies that if the fibre content is increased beyond 30 wt% further reductions in shrinkage could be achieved; the difficulties in processing higher fibre contents were not present when processing gypsum composites. This shows that potentially more effective shrinkage reductions could be achieved by fabricating a gypsum/fibre hybrid composite without encountering similar processing difficulties.

4.3 Post-Consumer Polypropylene Composite Results

4.3.1 Tensile Strength and Stiffness of Hemp and Harakeke Reinforced 3d Printing Filament

The tensile strength and Young's modulus results for post-consumer PP/ fibre composites are shown in Figure 4.26 and 4.27 below. The 30 wt% harakeke samples showed the most significant improvements in strength and Young's modulus of 76.8% and 274.9% respectively compared to plain post-consumer PP. The post-consumer PP filament performed better than the pre-consumer with higher strength and Young's modulus values of 6% and 14% respectively. This is believed to be a result of either the polymer being a superior grade and/or the polyester fibre content within the post-consumer PP. The increased performance of all post-consumer composites relative to those fabricated using pre-consumer PP also justify this observation.

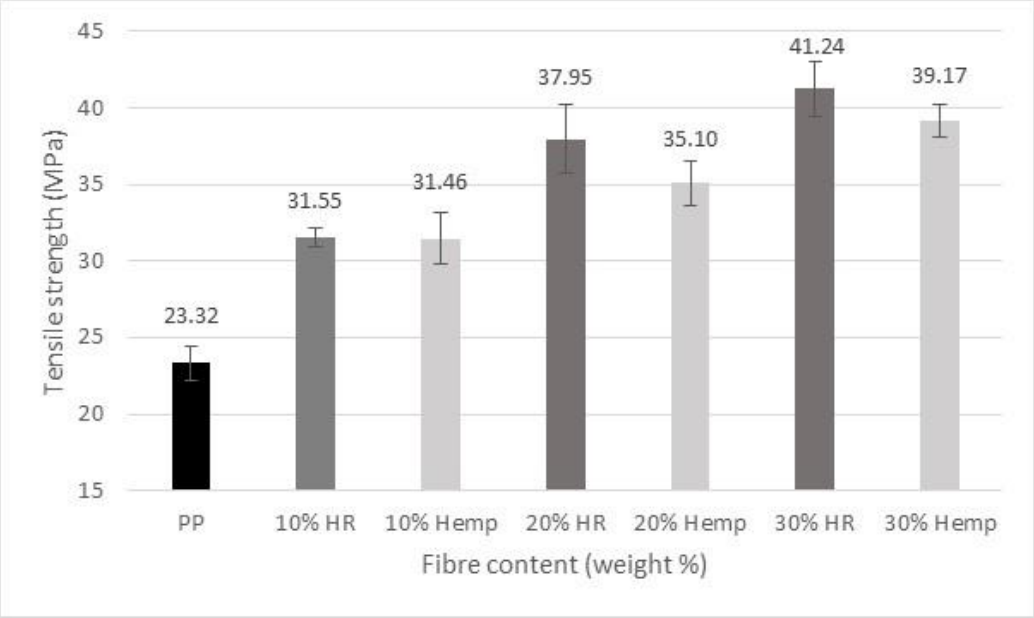

Figure 4.26, Tensile strength of post-consumer PP/Harakeke and PP/hemp fibre composites (MPa)

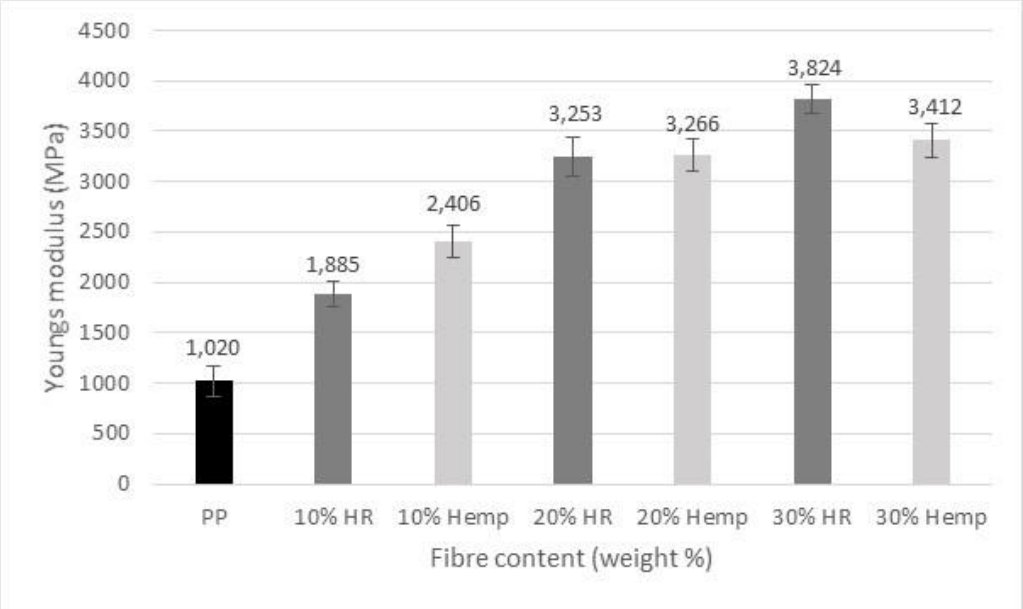

Figure 4.27, Young's modulus of post-consumer PP/Harakeke composite filament (MPa)

When compared to glass fibre/pre-consumer PP composites in the parallel study mentioned previously, post-consumer PP reinforced with natural fibre showed greater improvements in both strength and Young's modulus as shown in Table 4.3 below. The 30 wt% harakeke composite had a tensile strength and Young's modulus 15% and 13% higher than composites fabricated using 30 wt% glass fibre

Table 4.3, Comparison of pre-consumer PP/ glass fibre composites with post-consumer PP natural fibre composites

Sample	Tensile strength (MPa)	Net increase (%)	Young's modulus (MPa)	Net increase (%)
Plain PP	23.32	-	1020	-
10 wt% Glass	29.33	26	1995	96
20 wt% Glass	30.64	31	2016	98
30 wt% Glass	35.78	53	3386	232
10 wt% Harakeke	31.55	35	1885	85
20 wt% Harakeke	37.95	63	3253	219
30 wt% Harakeke	41.24	77	3824	275
10 wt% Hemp	31.46	35	2406	136
20 wt% Hemp	35.1	51	3266	220
30 wt% Hemp	39.17	68	3412	235

4.3.2 Microscopic Evaluation

The SEM micrographs shown in Figure 4.28 and 4.29 clearly show polyester fibres protruding from the fracture surface of 30 wt% harakeke/post-consumer PP samples. The length of the protruding fibres is indicative of poor interfacial matrix adhesion between polyester and polypropylene. Poor interfacial adhesion is also evident by examining the interface in Figure 4.32. In addition to interfacial adhesion implications, protruding fibres also indicate a degree of fibre alignment parallel to flow direction. Further evidence of fibre alignment beneath the surface is also apparent in Figure 4.30.

The fracture surface shown in Figure 4.31 shows evidence of harakeke fibre fracture close to the surface but also evidence of fibre pull out. This could suggest that although there was good interfacial adhesion, a proportion of the harakeke fibres used were below the critical reinforcement length. The same figure shows a large void that previously housed a polyester fibre providing a relative size comparison to harakeke fibres.

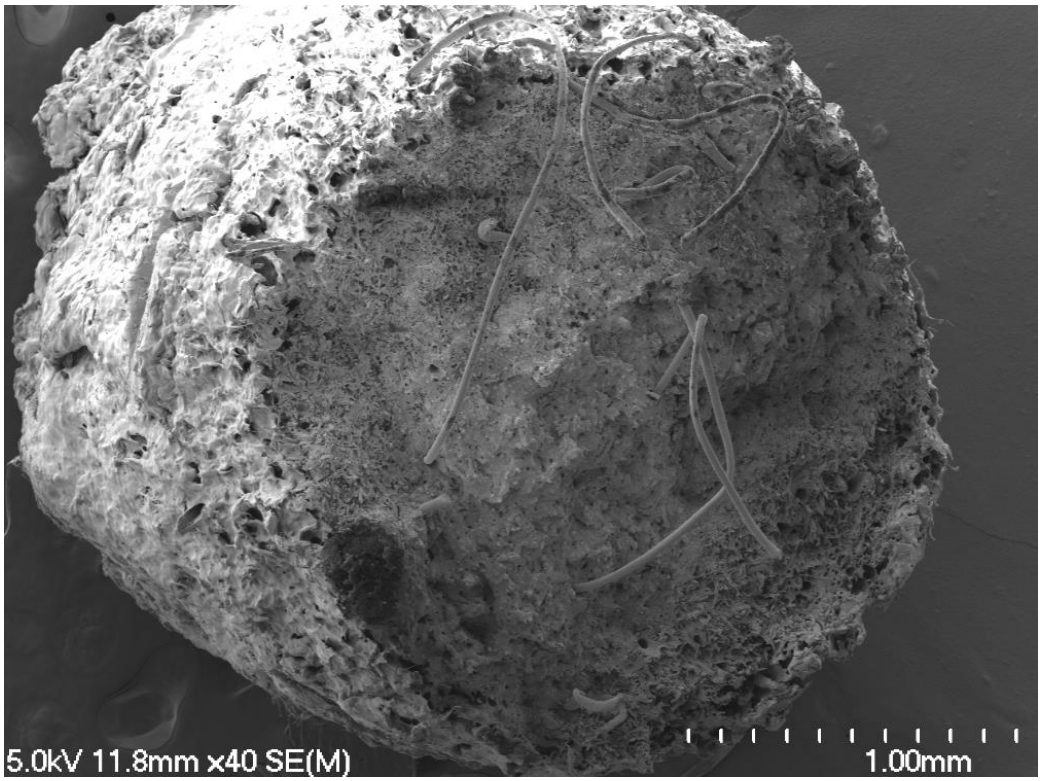

Figure 4.28, 30 wt% harakeke filament fracture surface showing polyester fibres

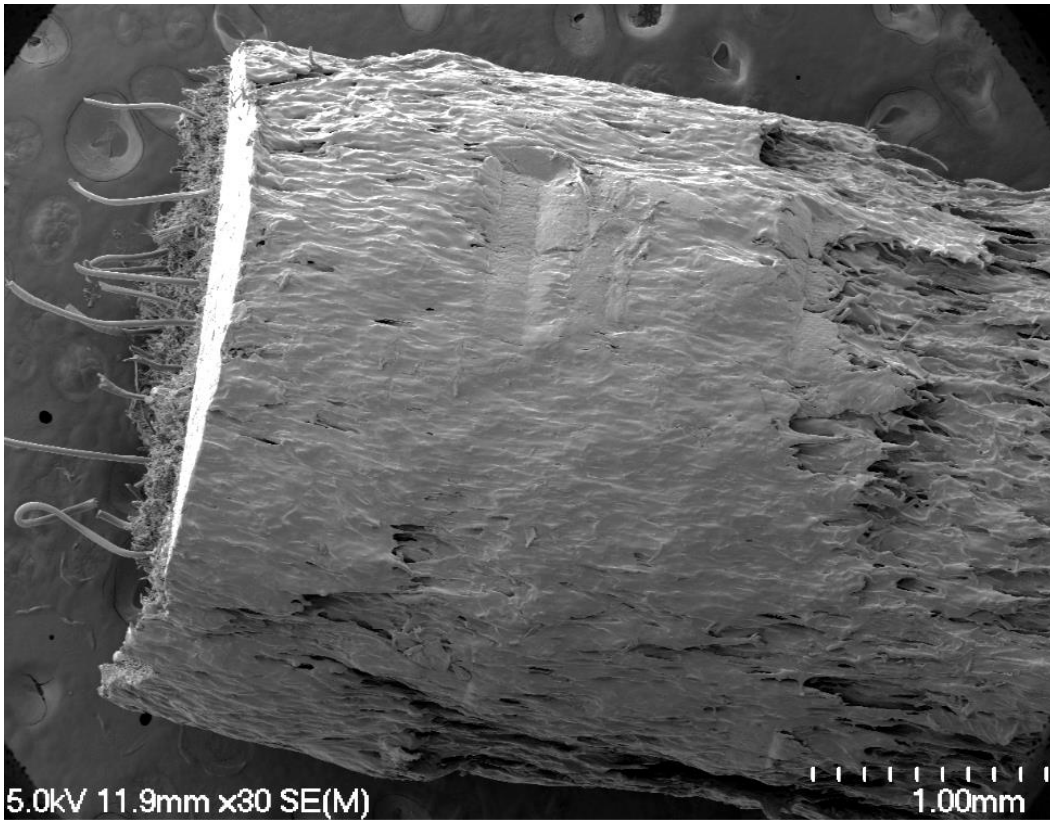

Figure 4.29, 30 wt% harakeke filament showing surface finish and fibre alignment

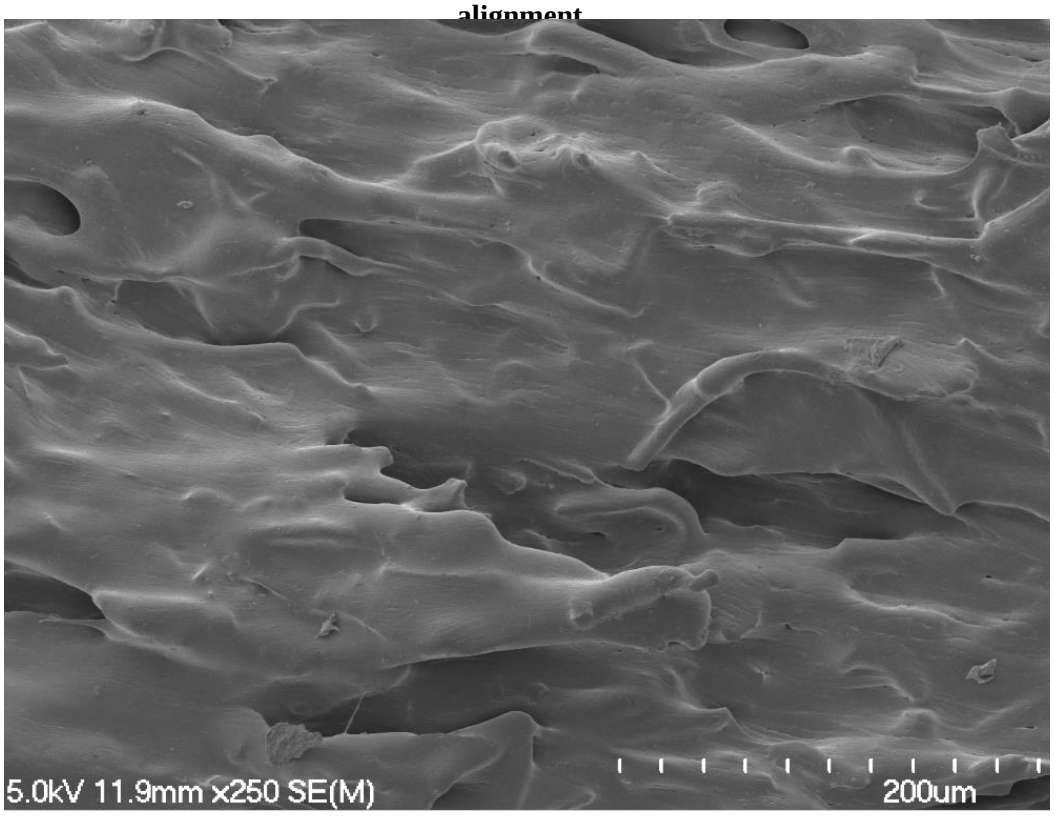

Figure 4.30, 30 wt% harakeke filament aligned fibre beneath the surface

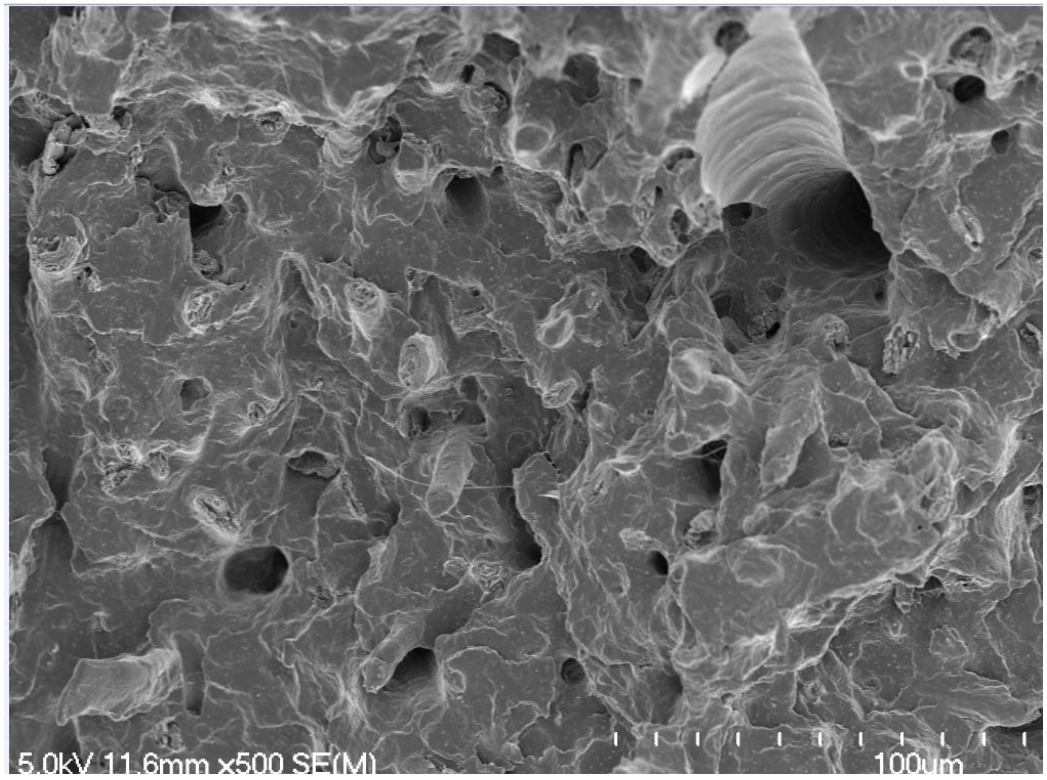

Figure 4.31, 30 wt% harakeke filament fracture surface showing fibre alignment and fibre pull out

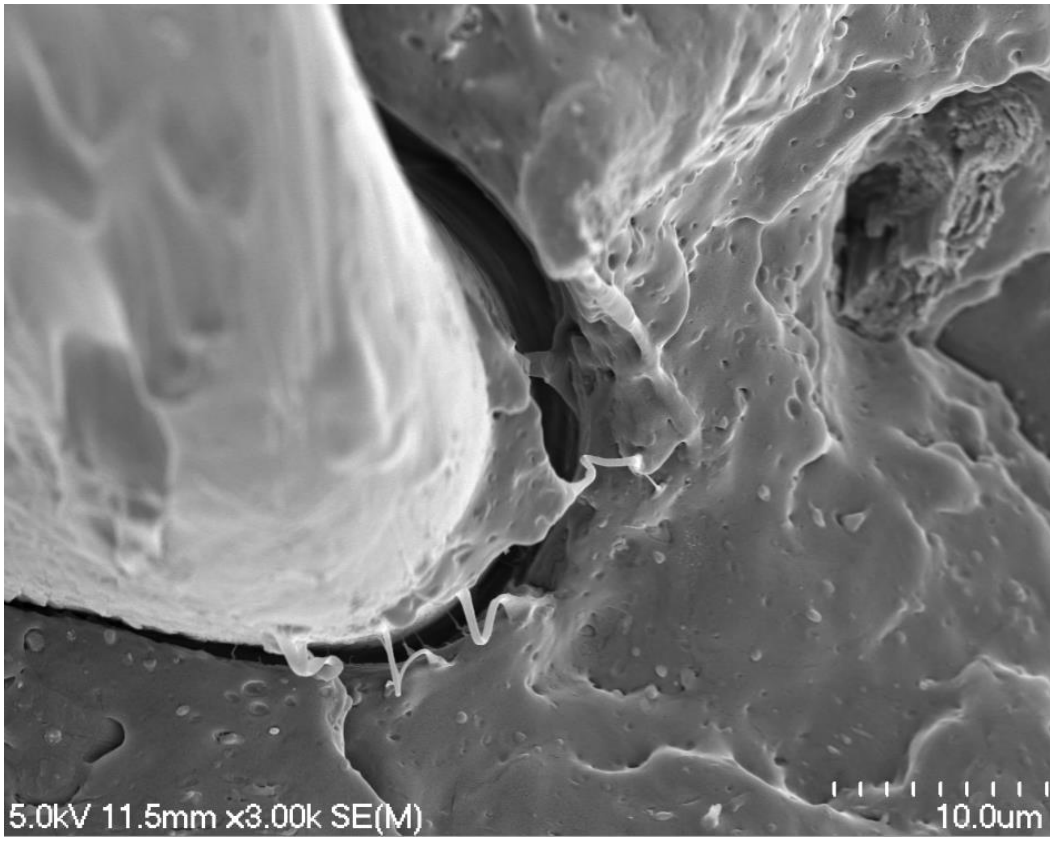

Figure 4.32, Polyester fibre adhesion within 30 wt% harakeke filament

4.3.3 3d Printed Samples

4.3.3.1 Tensile Properties and Moisture Absorption of 1mm 3d Printed Filament

One of the factors thought to be possibly contributing towards the drop in tensile properties of 3d printed samples was the moisture absorbed from the air into the 3mm filament prior to printing. To investigate this further one set of 3d printed tensile samples were printed with filament after being exposed to room humidity (wet) and one set were printed after the filament was dried at 105 ^{o}C for 24 hours (dried). A mass balance was used to measure the dry and wet weights of filament samples prior to printing, the results for which are summarised in Table 4.4. The tensile strength and Young's modulus results are plotted in Figure 4.33 to Figure 4.36, alongside the 3mm filament for reference.

Analysis of tensile results show a significant increase in both strength and Young's modulus resulting from the pre-drying process. Although the effects of drying the plain polypropylene are observed to be insignificant (due to hydrophobic nature of the polymer). The hydrophilic hemp and harakeke fibres however, are believed o be the primary cause of moisture absorption. During the 3d printing process, temperatures exceeded 100^{o}C causing any moisture within the filament to evaporate. The evaporated steam could have affected the interfacial adhesion between fibre and matrix materials and or created voids within the composite, both of which would have an adverse effect on the mechanical properties.

Table 4.4, Mechanical property comparison for dry and wet printed 1mm filament

Sample	Tensile strength (MPa)			Young's modulus (MPa)		
	Wet	Dry	Net increase (%)	Wet	Dry	Net increase (%)
30 wt% Hemp	23.1	29.2	21	2063	2969	31
20 wt% Hemp	20.9	27.6	24	1401	2502	44
10 wt% Hemp	21.2	25.0	15	1244	2025	39
30 wt% Harakeke	24.5	32.9	26	1544	2806	45
20 wt% Harakeke	20.9	28.1	26	1197	2556	53
10 wt% Harakeke	20.0	26.3	24	1031	1999	48

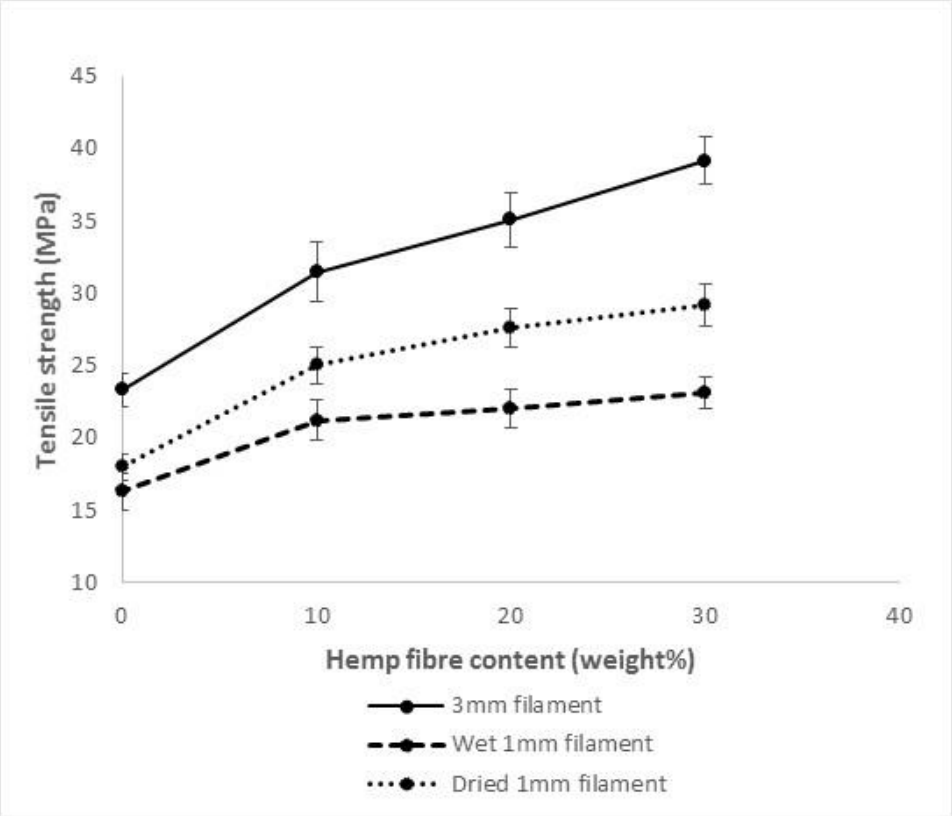

Figure 4.33, Tensile strength comparison between 3mm, dry 1mm and wet 1mm printed hemp filaments

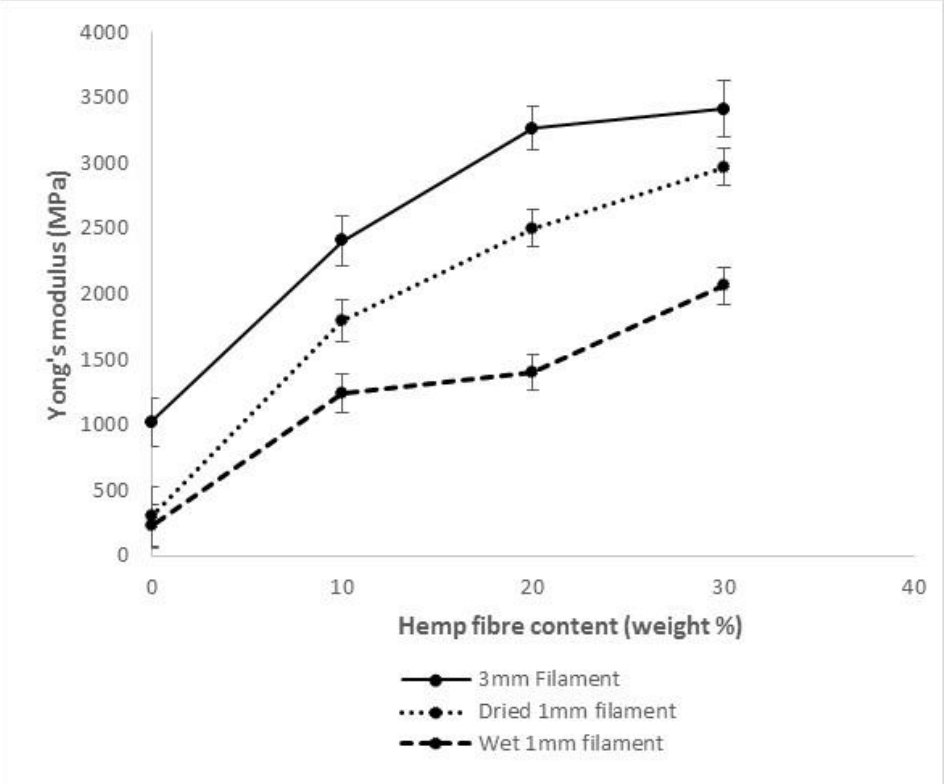

Figure 4.34, Young's modulus comparison between 3mm, dry 1mm and wet 1mm printed hemp filaments

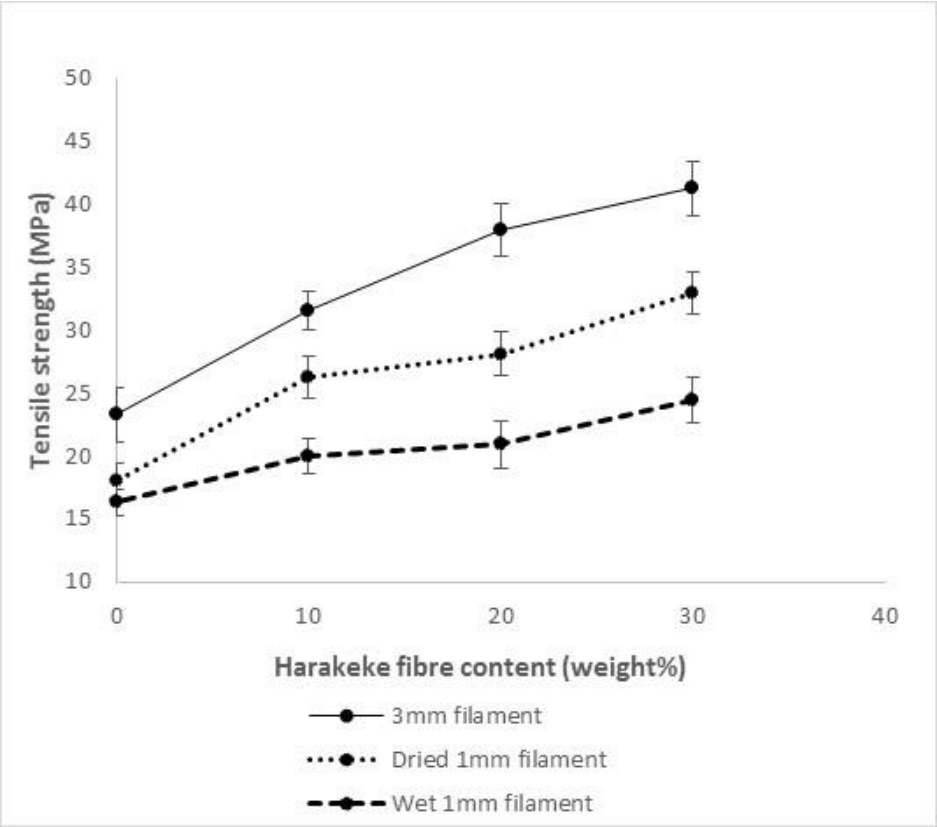

Figure 4.35, Tensile strength comparison between 3mm, dry 1mm and wet 1mm printed harakeke filaments

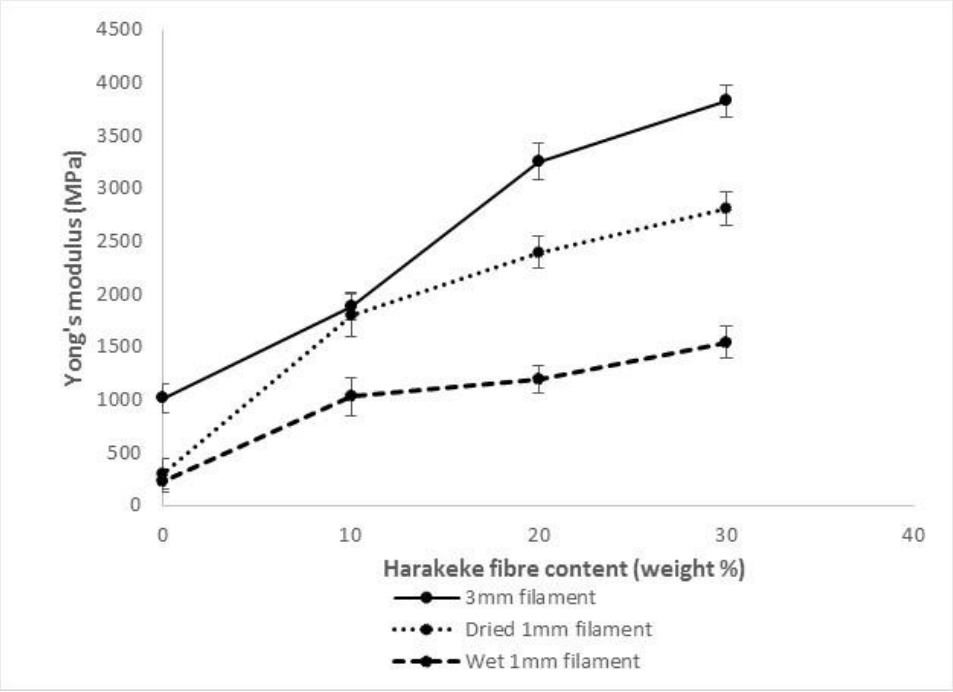

Figure 4.36, Tensile strength comparison between 1mm printed filaments produced from dried and undried filament

4.3.3.2 3D Printed Filament Density

Although the properties increased as a result of pre-drying feedstock material, 3d printed samples still showed tensile strength and Young's modulus values lower than those of the 3mm filament. The comparisons between density values of 3mm and 1mm dried filaments can be seen in Table 4.5 below.

Results show that extruding the 3mm filament through the 3d printer causes composite density reductions ranging from 11.12 to 16.49%. Increasing the fibre content does not appear to influence this reduction in filament density. The plain polypropylene filament however, showed significantly lower reductions than composite filaments. This implies that the presence of fibre is likely to be contributing to the variations in density.

Comparing the theoretical density with the density measurement of the 3mm filament, there is a reduction ranging from 3.3% to 9.1%. This is likely to be caused by trapped air within the composite as a result of the extrusion process. The 3mm filament was extruded through a 40mm capillary which induced a reasonable amount of pressure on the filament as it solidified. This pre-stress may have compressed the polymer and air inside the composite filament. The 3d printer however, uses a very short capillary (≈ 0.2mm). The shorter die means that the 3d printed polymer experiences very little pressure allowing the polymer to relax and the air to expand. If this is occurring, it is possible that polymer relaxation may also be contributing to reductions in properties.

Table 4.5, Density of 3mm filament compared to 1mm printed filament

Sample	Theoretical density (gm/cm^3)	3mm Filament Density (gm/cm^3)	3d printed Filament Density (gm/cm^3)	Net decrease (%)
Plain PP	-	0.947	0.915	3.38
30 wt% Hemp	1.113	1.041	0.904	13.16
20 wt% Hemp	1.054	1.005	0.853	15.19
10 wt% Hemp	0.996	0.968	0.855	11.74
30 wt% Harakeke	1.113	1.012	0.881	12.94
20 wt% Harakeke	1.054	1.019	0.851	16.49
10 wt% Harakeke	0.996	0.935	0.831	11.12

To relate the density to tensile properties, density values were used to calculate specific strength and modulus for 3mm and 1mm filaments. Tables 4.6 and 4.7 show the differences in specific strength and modulus for 3mm and 1mm dry filament. When compared to the larger net differences observed in tensile strength and Young's modulus provides evidence that the density reduction is related to the reduction in mechanical properties of 3d printed samples. The reduction in density could be attributed to void formation resulting from either moisture, trapped air or poor fibre wetting. Any air trapped in filament feedstock material that is unable to escape will maintain its volume after printing. The same volume of air in the 1mm filament will occupy a larger volume relative to the smaller diameter, therefore creating a larger relative stress concentration point which would partially explain the drop in material properties. If this is the case, it highlights the necessity of removing voids from the feedstock material.

Table 4.6, Comparison of specific strength values for 3mm and 1mm filament

Sample	Specific strength (MPa cm^3/ gm)		Net difference (%)	Tensile strength (MPa)		Net difference (%)
	3mm	1mm	-	3mm	1mm	
Plain PP	24.6	19.7	-20	41.2	33.0	-20
10 wt% Harakeke	33.8	31.6	-6	38.0	28.1	-26
20 wt% Harakeke	37.2	33.0	-11	31.6	26.3	-17
30 wt% Harakeke	40.8	37.4	-8.	39.2	29.2	-25
10 wt% Hemp	32.5	29.3	-10	35.1	27.6	-21
20 wt% Hemp	34.9	32.4	-7.	31.5	25.0	-20
30 wt% Hemp	37.6	32.3	-14	41.2	33.0	-20

Table 4.7, Comparison of specific modulus values for 3mm and 1mm filament

Sample	Specific modulus (MPa cm^3/ gm)		Net difference (%)	Young's modulus (MPa)		Net difference (%)
	3mm	1mm	-	3mm	1mm	
Plain PP	1088	327	-70	1020	300	-71
10 wt% Harakeke	2017	2407	19	3824	2806	-27
20 wt% Harakeke	3193	3005	-6	3254	2396	-26
30 wt% Harakeke	3780	3186	-16	1885	1799	-5
10 wt% Hemp	2485	2369	-5	3412	2969	-13
20 wt% Hemp	3249	2934	-10	3266	2502	-23
30 wt% Hemp	3279	3285	0.2	2406	1799	-25

4.3.3.3 Microscopic Evaluation

SEM micrographs were taken to show the effect of drying 3d printing feedstock materials prior to printing in terms of void formation. Figure 4.37 shows the fracture surface of the original 3mm filament with only small voids present. The fracture surface of pre-dried printed samples (Figure 4.37) contain much smaller voids and in a smaller quantity than wet printed filament (Figure 4.38). Although the voids size has been reduced as a result of the pre-drying process, there are still voids present that appear larger (relative to the size of the filament) than those seen in the original 3mm filament.

Figure 4.37, 20 wt% wet harakeke 3mm filament

Figure 4.38, Fracture surface of 20 wt% harakeke 1mm filament produced with pre-dried filament

Figure 4.39, Fracture surface of 20 wt% harakeke 1mm filament produced with no pre-drying

Chapter 5:
Conclusions

Chapter 5

Conclusions

5.1 Processing of 3d Printing Filament

In this research, a series of 3mm composite 3d printing filaments were successfully extruded with varying weight fractions of hemp, harakeke and recycled gypsum. The maximum fibre content that would still allow for accurate filament fabrication was 30 wt%. Exceeding this fraction resulted in a sharkshin surface effect, increased strain on extruder close to its limitations and difficulty using the current spooling machine. For gypsum composites, no such maximum content was found and composites containing up to 50 wt% gypsum were fabricated with little difficulty.

Initial processing parameter screening tests showed that the pre-drying temperature of 105 °C sustained for 24 hours, removed more moisture prior to extrusion than that of 80°C dried for the same period of time. The greater moisture reduction increased the tensile strength by 9% and the Young's modulus by 27% when compared to samples produced using the 80°C drying temperature.

SEM micrograph evaluations supported that using MAPP coupling agent in powdered form as opposed to granulated form increased the quality of interfacial adhesion between fibre and matrix materials. These observations were also supported by powdered MAPP composites yielding strength and Young's modulus values 17.7% and 18.5% higher than the granulated alternative.

Screening tests also indicated that compounding constituent materials using a 16mm twin screw extruder produced composites of superior mechanical properties than the larger 20mm extruder. This is thought to be related to the more severe mixing zones in the 20mm screws causing a reduction in fibre length. Compounding on the smaller extruder also proved effective in terms of good fibre distribution throughout the matrix as indicated by SEM analysis.

5.2 3mm Composite Filament Results

The strongest composite filament produced in this work consisted of 30 wt% harakeke fibre in a post-consumer polypropylene matrix. This composite filament had a tensile strength of 41 MPa and a Young's modulus of 3824 MPa. These values correspond to improvements of 77 % and 275% relative to unfilled polypropylene filament. Using post-consumer PP as a matrix material resulted in better mechanical performance than using pre-consumer PP. This was attributed to either a higher grade of polymer and/or additional reinforcement from polyester fibre content. Although post-consumer polypropylene produced stronger composites than pre-consumer, all composites showed significant improvements in strength and stiffness

SEM micrographs of post-consumer PP composite fracture surfaces supported very poor interfacial adhesion of polyester fibre. This was made apparent by long polyester fibres protruding from fracture surfaces. The protruding fibres were also indicative of fibre alignment along the length of the filament.

Composites containing 10% to 50 wt% recycled gypsum showed an approximately linear decrease in tensile strength while simultaneously showing a linear increase in Young's modulus. This was explained with the aid of SEM micrographs showing conglomeration of gypsum crystals as the particle content increased, creating localised stress concentration points while still restricting polymer chain mobility.

5.3 3d Printed Composite Results

Tensile testing of 3d printed dog bone samples proved to be highly variable with the tensile results bearing no resemblance to the trend observed in 3mm filament. Variation from the 3mm filament trend was attributed to the 3d printers concentric fill pattern which created a localised stress concentration point on every specimen. This observation was verified by eliminating geometric inconsistency and conducting tensile tests on 1mm filament extruded through the 3d printer. Tensile results from the 1mm filaments showed a consistent increase in tensile properties with additional filler material, similar to that observed in 3mm filaments. This supported the claim that the fill pattern was the primary cause of variation in tensile results of 3d printed dog bone samples.

All 3d printed tensile specimens showed a drop in tensile strength and Young's modulus relative to 3mm feedstock filament. Moisture absorption resulting from exposure of feedstock material to humidity in the air was found to partially contribute to this reduction by means of void formation from evaporated moisture. Tensile samples prepared from pre-dried feedstock material showed improvements of tensile strength and stiffness as high as 26% and 54% respectively for 20 wt% harakeke composites. The difference between specific strength and stiffness values of 3mm and 1mm samples was found to be 11% and 6% respectively for 20 wt% harakeke with similar results found for other composite samples. The closer relationship between specific properties reflects the effects of an observed drop in density resulting from the 3d printing process. Reductions in density were attributed to void formation and an increased void size relative to the diameter of the 3d printed filament.

A novel method of measuring shrinkage within 3d printed components was developed and used to measure the relative shrinkage of different composites. The composite that displayed the greatest reduction in shrinkage consisted of 30 wt% harakeke with shrinkage reduction of 84% relative to plain polypropylene. Natural fibre proved to be more effective in terms of shrinkage reduction than gypsum with 50 wt% gypsum content achieving approximately the same shrinkage reduction as only 10 wt% natural fibre.

Based on the results shown in this research it can be concluded that recycled polypropylene composites have potential to be used as strong, stiff, cheap and recyclable 3d printing filament. The rapid growth in the 3d printing industry coupled with increased environmental awareness, suggest that these and similar composite filaments are highly relevant in this day and age.

Chapter 6:
Recommendations

Chapter 6

Recommendations

The results and observations obtained from this research have laid a solid foundation for further enhancement of thermoplastic composite 3d printing filament. The following are some recommendations for future work in the area:

- Optimise extrusion parameters to achieve better surface finish, reduce void content and increase fibre alignment.
- Increase natural fibre content within composite materials.
- Optimise fibre treatment regime to reduce fibre moisture absorption when exposed to room humidity.
- Investigate the influence of 3d print parameters and component geometry on mechanical performance.
- Examine the influence of 3d printer die pressure on physical properties of 3d printed components. A relationship could be established by varying the capillary length of the die.
- Investigate the effects of printing die geometry on fibre alignment.
- Compare different fibre/matrix compounding methods and influence on mechanical properties. Compounding methods could include twin screw compounding mixer, solution mixing or different extrusion screw configurations.
- Investigate the effects of plasticisers on melt flow which could help with fabrication of composites containing higher fibre volume fractions.
- Experiment with gypsum/fibre hybrid composites to achieve further shrinkage reductions.
- Increase the interfacial adhesion of polyester fibres by trying different coupling agent combinations.

References

1. Aurrekoetxea, J., Sarrionandia, M. A., Urrutibeascoa, I., & Maspoch, M. L. (2001). Effects of recycling on the microstructure and the mechanical properties of isotactic polypropylene. *Journal of Materials Science, 36*(11), 2607-2613.

2. GuerricaEchevarria, G., Eguiazabal, J. I., & Nazabal, J. (1996). Effects of reprocessing conditions on the properties of unfilled and talc-filled polypropylene. *Polymer Degradation and Stability, 53*(1), 1-8.

3. Chabowski, B. R., Mena, J. A., & Gonzalez-Padron, T. L. (2011). The structure of sustainability research in marketing, 1958-2008: a basis for future research opportunities. *Journal of the Academy of Marketing Science, 39*(1), 55-70.

4. Beckermann, G. (2004). *The processing, production and improvement of hemp-fibre reinforced Polypropylene composite materials.* M.Sc (Tech) thesis, University of Waikato, Hamilton New Zealand.

5. Kozlowski, R., & Mackiewicz-Talarczyk, M. (2000). Inventory of world fibres and involvement of FAO in fibre research. *Molecular Crystals and Liquid Crystals, 353*, 133-148.

6. Lowe, B. J., Carr, D. J., McCallum, R. E., Myers, T., Ngarimu-Cameron, R., & Niven, B. E. (2010). Understanding the variability of vegetable fibres: a case study of harakeke (Phormium tenax). *Textile Research Journal, 80*(20), 2158-2166.

7. Ramnath, B. V., Manickavasagam, V. M., Elanchezhian, C., Krishna, C. V., Karthik, S., & Saravanan, K. (2014). Determination of mechanical properties of intra-layer abaca-jute-glass fiber reinforced composite. *Materials & Design, 60*, 643-652.

8. Thakur, V. K., & Thakur, M. K. (2014). Processing and characterization of natural cellulose fibers/thermoset polymer composites. *Carbohydrate Polymers, 109*, 102-117.

9. Le Duigou, A., Pillin, I., Bourmaud, A., Davies, P., & Baley, C. (2008). Effect of recycling on mechanical behaviour of biocompostable flax/poly(L-lactide) composites. *Composites Part a-Applied Science and Manufacturing, 39*(9), 1471-1478.

10. Moran, J., Alvarez, V., Petrucci, R., Kenny, J., & Vazquez, A. (2007). Mechanical properties of polypropylene composites based on natural fibers subjected to multiple extrusion cycles. *Journal of Applied Polymer Science, 103*(1), 228-237.

11. Joshi, S. V., Drzal, L. T., Mohanty, A. K., & Arora, S. (2004). Are natural fiber composites environmentally superior to glass fiber reinforced composites? *Composites Part A: Applied Science and Manufacturing, 35*(3), 371-376.

12. Huang, S. H., Liu, P., Mokasdar, A., & Hou, L. (2013). Additive manufacturing and its societal impact: a literature review. *International Journal of Advanced Manufacturing Technology, 67*(5-8), 1191-1203.

13. Zhai, Y. W., Lados, D. A., & Lagoy, J. L. (2014). Additive Manufacturing: Making Imagination the Major Limitation. *JOM Journal of the Minerals Metals and Materials Society 66*(5), 808-816.

14. Wohlers, T. T. (2014). State of the industry. In P. Bartolo (Ed.), *Virtual and Rapid Manufacturing: Advanced Research in Virtual and Rapid Prototyping* (pp. 1-6). London, U.K.: Taylor & Francis.

15. Cotteleer, M. J. (2014). *3D opportunity: Additive manufacturing paths to performance, innovation, and growth*. Presented at the Additive Manufacturing SIMT Symposium, Southeastern Institute of Manufacturing & Technology, Florence.

16. Brooks, H., Rennie, A., Abram, T., McGovern, J., & Caron, F. (2012). Variable fused deposition modelling: Analysis of benefits, concept design and tool path generation. In P. Bartolo (Ed.), *Innovative Developments in Virtual and Physical Prototyping* (pp. 511-517). London, U.K.: CRC.

17. Zhong, W. H., Li, F., Zhang, Z. G., Song, L. L., & Li, Z. M. (2001). Short fiber reinforced composites for fused deposition modeling. *Materials Science and Engineering a-Structural Materials Properties Microstructure and Processing, 301*(2), 125-130.

18. Santos, J. D., Fajardo, J. I., Cuji, A. R., Garcia, J. A., Garzon, L. E., & Lopez, L. M. (2015). Experimental evaluation and simulation of volumetric shrinkage and warpage on polymeric composite reinforced with short natural fibers. *Frontiers of Mechanical Engineering, 10*(3), 287-293.

19. Satterthwaite, J. D., Maisuria, A., Vogel, K., & Watts, D. C. (2012). Effect of resin-composite filler particle size and shape on shrinkage-stress. *Dental Materials, 28*(6), 609-614.

20. Tan, H. S., Yu, Y. Z., Xing, L. X., Zhao, L. Y., & Sun, H. Q. (2013). Density and Shrinkage of Injection Molded Impact Polypropylene Copolymer/Coir Fiber Composites. *Polymer-Plastics Technology and Engineering, 52*(3), 257-260.

21. Tekinalp, H. L., Kunc, V., Velez-Garcia, G. M., Duty, C. E., Love, L. J., Naskar, A. K., Blue, C. A., & Ozcan, S. (2014). Highly oriented carbon fiber-polymer composites via additive manufacturing. *Composites Science and Technology, 105*, 144-150.

22. Cram, D. (2016). *High Performance HTPLA - Carbon Fiber*. Retrieved May, 2016, from https://www.proto-pasta.com/products/high-temp-carbon-fiber-pla-composite.

23. *Carbon Fiber Filament*. (2016). Retrieved May, 2016, from http://www.3dxtech.com/carbon-fiber-filament/.

24. Oksman, K., Skrifvars, M., & Selin, J. F. (2003). Natural fibres as reinforcement in polylactic acid (PLA) composites. *Composites Science and Technology, 63*(9), 1317-1324.

25. Thygesen, A. (2006). *Properties of hemp fibre polymer composites -An optimisation of fibre properties using novel defibration methods and fibre characterisation.* PhD thesis, University of Denmark.

26. Everitt, N. M., Aboulkhair, N. T., & Clifford, M. J. (2013). Looking for Links between Natural Fibres’ Structures and Their Physical Properties. *Conference Papers in Materials Science, 2013*, 10.

27. R.Raghavendra, A. D., M. G. Kamath. (2004). *Cotton Fibres*. from http://www.engr.utk.edu/mse/pages/Textiles/index.html.

28. Shah, D. U. (2013). Developing plant fibre composites for structural applications by optimising composite parameters: a critical review. *Journal of Materials Science, 48*(18), 6083-6107.

29. Bledzki, A. K., & Gassan, J. (1999). Composites reinforced with cellulose based fibres. *Progress in Polymer Science, 24*(2), 221-274.

30. Hosseinihashemi, S. K., Modirzare, M., Safdari, V., & Kord, B. (2011). Decay resistance, hardness, water absorption, and thickness swelling of a bagasse fiber/plastic composite. *Bioresources, 6*(3), 3289-3299.

31. Komuraiah, A., Kumar, N. S., & Prasad, B. D. (2014). Chemical Composition of Natural Fibers and its Influence on their Mechanical Properties. *Mechanics of Composite Materials, 50*(3), 359-376.

32. Lilholt, H., & Lawther, J. (2000). Natural organic fibres. *Elsevier, 1*.

33. Mclntosh DJ, B. R., Brown T. (1998). *5 minute guide to industrial hemp in New Zealand. Compiled by New Zealand hemp industries association*. New Zealand Hemp association Inc.

34. Kenny, J. M., Fps, Fps, & Fps. (2002). *Natural fiber composites in the European automotive industry*. 6th International Conference on Woodfiber-Plastic Composites.

35. De Rosa, I. M., Iannoni, A., Kenny, J. M., Puglia, D., Santulli, C., Sarasini, F., & Terenzi, A. (2011). Poly(lactic acid)/Phormium tenax Composites: Morphology and Thermo-Mechanical Behavior. *Polymer Composites, 32*(9), 1362-1368.

36. De Rosa, I. M., Kenny, J. M., Puglia, D., Santulli, C., & Sarasini, F. (2010). Tensile behavior of New Zealand flax (Phormium tenax) fibers. *Journal of Reinforced Plastics and Composites, 29*(23), 3450-3454.

37. Carr, D. J., Cruthers, N. M., Laing, R. M., & Niven, B. E. (2005). Fibers from three cultivars of New Zealand flax (Phormium tenax). *Textile Research Journal, 75*(2), 93-98.

38. Tan, L. M. (2016). *Harakeke Fibre as Reinforcment in Epoxy Matrix Composites and Its Hybridisation with Hemp Fibre.* PhD thesis, University of Waikato.

39. H, E. (2016). *Drywall*. from http://www.madehow.com/Volume-2/Drywall.html.

40. Association, G. (2016). *What is gypsum*. Retrieved 13/5/2016, 2016, from https://www.gypsum.org/about/gypsum-101/what-is-gypsum/.

41. Carvalho, M. A., Calil, C., Savastano, H., Tubino, R., & Carvalho, M. T. (2008). Microstructure and Mechanical Properties of Gypsum Composites Reinforced with Recycled Cellulose Pulp. *Materials Research-Ibero-American Journal of Materials, 11*(4), 391-397.

42. Pickering, K. L., Efendy, M. G. A., & Le, T. M. (2016). A review of recent developments in natural fibre composites and their mechanical performance. *Composites Part a-Applied Science and Manufacturing, 83*, 98-112.

43. Van de Velde, K., & Kiekens, P. (2001). Thermoplastic polymers: overview of several properties and their consequences in flax fibre reinforced composites. *Polymer Testing, 20*(8), 885-893.

44. Tabatabaei, S. H., Carreau, P. J., & Ajji, A. (2009). Rheological and thermal properties of blends of a long-chain branched polypropylene and different linear polypropylenes. *Chemical Engineering Science, 64*(22), 4719-4731.

45. Ye, Z. B., AlObaidi, F., & Zhu, S. P. (2004). Synthesis and rheological properties of long-chain-branched isotactic polypropylenes prepared by copolymerization of propylene and nonconjugated dienes. *Industrial & Engineering Chemistry Research, 43*(11), 2860-2870.

46. Asgari, M., & Masoomi, M. (2015). Tensile and flexural properties of polypropylene/short poly(ethylene terephthalate) fibre composites compatibilized with glycidyl methacrylate and maleic anhydride. *Journal of Thermoplastic Composite Materials, 28*(3), 357-371.

47. Fernandez, C., & Puig, C. C. (2002). Changes in melting behavior and morphology on annealing of linear and branched polyethylene. *Journal of Macromolecular Science-Physics, B41*(4-6), 991-1005.

48. Vignaud, G., Chebil, M. S., Bal, J. K., Delorme, N., Beuvier, T., Grohens, Y., & Gibaud, A. (2014). Densification and Depression in Glass Transition Temperature in Polystyrene Thin Films. *Langmuir, 30*(39), 11599-11608.

49. Goulart, S. A. S., Oliveira, T. A., Teixeira, A., Mileo, P. C., & Mulinari, D. R. (2011). Mechanical behaviour of polypropylene reinforced palm fibers composites. In M. Guagliano & L. Vergani (Eds.), *11th International Conference on the Mechanical Behavior of Materials* (Vol. 10, pp. 2034-2039).

50. Karger-Kocsis, J. (1995). *Polypropylene Structure, Blends and Composites*. (Vol. 3: Composites). Dordrecht, Netherlands: Springer.

51. Tripathi, D. (2002). *Practical Guide to Polypropylene*. Shawbury, England: Smithers Rapra.

52. *A Closer Look at Polymerization of Propylene*. (2014). Retrieved August, 2016, from http://www.chemistry.wustl.edu/~edudev/Designer/session5.html.

53. Gong, Y., Niu, P., Wang, X., Long, S., & Yang, J. (2012). Influence of processing temperatures on fiber dimensions and microstructure of polypropylene/hemp fiber composites. *Journal of Reinforced Plastics and Composites, 31*(19), 1282-1290.

54. Tong, S. (2014). *MakiBox*. Retrieved September, 2014, from http://www.makibox.com/.

55. *Chapter 3, Materials Science and Engineering*. (2001). 2016.

56. Hopmann, C., Borchmann, N., Spekowius, M., Weber, M., & Schongart, M. (2015). Simulation of shrinkage and warpage of semi-crystalline thermoplastics. In S. C. Jana (Ed.), *Proceedings of Pps-30: The 30th International Conference of the Polymer Processing Society* (Vol. 1664).

57. Gershon, A. L., Gyger, L. S., Bruck, H. A., & Gupta, S. K. (2008). Thermoplastic Polymer Shrinkage in Emerging Molding Processes. *Experimental Mechanics, 48*(6), 789-798.

58. Potts, J. R., Dreyer, D. R., Bielawski, C. W., & Ruoff, R. S. (2011). Graphene-based polymer nanocomposites. *Polymer, 52*(1), 5-25.

59. Gobor, A. (2016). *Air Cooling vs Liquid Cooling*. 2016, from https://www.ekwb.com/blog/air-cooling-vs-liquid-cooling/.

60. Eggen, S., & Hinrichsen, E. L. (1996). Swell and distortions of high-density polyethylene extruded through capillary dies. *Polymer Engineering and Science, 36*(3), 410-424.

61. Moynihan, R. H., Baird, D. G., & Ramanathan, R. (1990). Additional observations on the surface melt fracture-behavior of linear low-density polyethylene. *Journal of Non-Newtonian Fluid Mechanics, 36*, 255-263.

62. Vlachopoulos, J. The Role of Reology in Polymer Extrusion. Hamilton, Ontario, Canada.

63. M.Denn. (2001). Extrusion Instabilities and Wall Slip. *Annual Reviews 33*, 265-287.

64. Franck, A. (2000). *Understanding Rheology of Thermoplastic Polymers*. 2016.

65. Khalina, A., Zainuddin, E. S., & Aji, I. S. (2011). Rheological Behaviour of Polypropylene/Kenaf Fibre Composite: Effect of Fibre Size. In S. M. Sapuan, F. Mustapha, D. L. Majid, Z. Leman, A. H. M. Ariff, M. K. A. Ariffin, M. Y. M. Zuhri, M. R. Ishak & J. Sahari (Eds.), *Composite Science and Technology, Pts 1 and 2* (Vol. 471-472, pp. 513-517).

66. R. Chollakup, W. S., P. Suwanruji. (2012). *Environmentally Friendly Coupling Agents for Natural Fibre Composites.* Natural Polymers, Composites (Vol. 1). RSC Publishing: Royal Society of Chemistry.

67. Brouwer, W. D. *Common fund for Commodities - Alternative Applications for Sisal and Henequen*. from http://www.fao.org/docrep/004/y1873e/y1873e0a.htm.

68. Johnson, T. (2014). *The Evolution of Lightweight Composite Materials*. from http://composite.about.com/od/aboutcompositesplastics/a/HistoryofComposites.htm.

69. Huber, T., Biedermann, U., & Mussig, J. (2010). Enhancing the Fibre Matrix Adhesion of Natural Fibre Reinforced Polypropylene by Electron Radiation Analyzed with the Single Fibre Fragmentation Test. *Composite Interfaces, 17*(4), 371-381.

70. Callister Jr, W. D. (2010). *Materials Science and Engineering: An Introduction*. (8th ed.). Hoboken, NJ: Wiley.

71. Fu, S.-Y., & Lauke, B. (1996). Effects of fiber length and fiber orientation distributions on the tensile strength of short-fiber-reinforced polymers. *Composites Science and Technology, 56*(10), 1179-1190.

72. Pervaiz, M., Sain, M., & Ghosh, A. (2006). Evaluation of the influence of fibre length and concentration on mechanical performance of hemp fibre reinforced polypropylene composite. *Journal of Natural Fibers, 2*(4), 67-84.

73. Wang, W., Sain, M., & Cooper, P. A. (2006). Study of moisture absorption in natural fiber plastic composites. *Composites Science and Technology*, *66*(3–4), 379-386.

74. Pan, Y., & Zhong, Z. (2014). Modeling of the mechanical degradation induced by moisture absorption in short natural fiber reinforced composites. *Composites Science and Technology*, *103*, 22-27.

75. Panthapulakkal, S., & Sain, M. (2007). Studies on the water absorption properties of short hemp—glass fiber hybrid polypropylene composites. *Journal of Composite Materials, 41*(15), 1871-1883.

76. Ho, M. P., Wang, H., Lee, J. H., Ho, C. K., Lau, K. T., Leng, J. S., & Hui, D. (2012). Critical factors on manufacturing processes of natural fibre composites. *Composites Part B-Engineering, 43*(8), 3549-3562.

77. Ouajai, S., & Shanks, R. A. (2005). Composition, structure and thermal degradation of hemp cellulose after chemical treatments. *Polymer Degradation and Stability, 89*(2), 327-335.

78. Joseph, P. V., Joseph, K., Thomas, S., Pillai, C. K. S., Prasad, V. S., Groeninckx, G., & Sarkissova, M. (2003). The thermal and crystallisation studies of short sisal fibre reinforced polypropylene composites. *Composites Part a-Applied Science and Manufacturing, 34*(3), 253-266.

79. Talla, A. S. F., Erchiqui, F., Kaddami, H., & Kocaefe, D. (2015). Investigation of the thermostability of poly(ethylene terephthalate)-hemp fiber composites: Extending natural fiber reinforcements to high-melting thermoplastics. *Journal of Applied Polymer Science, 132*(37).

80. Mutje, P., Vallejos, M. E., Girones, J., Vilaseca, F., Lopez, A., Lopez, J. P., & Mendez, J. A. (2006). Effect of maleated polypropylene as coupling agent for polypropylene composites reinforced with hemp strands. *Journal of Applied Polymer Science, 102*(1), 833-840.

81. Islam, M. S. (2008). *The Influence of Fibre Processing and Treatments on Hemp Fibre/Epoxy and Hemp Fibre/PLA Composites.* PhD thesis, University of Waikato, University of Waikato.

82. Li, X., Tabil, L. G., & Panigrahi, S. (2007). Chemical treatments of natural fiber for use in natural fiber-reinforced composites: A review. *Journal of Polymers and the Environment, 15*(1), 25-33.

83. El-Sabbagh, A. (2014). Effect of coupling agent on natural fibre in natural fibre/polypropylene composites on mechanical and thermal behaviour. *Composites Part B-Engineering, 57*, 126-135.

84. Peltola, H., Madsen, B., Joffe, R., & Nattinen, K. (2011). Experimental Study of Fiber Length and Orientation in Injection Molded Natural Fiber/Starch Acetate Composites. *Advances in Materials Science and Engineering*.

85. Riedel, U. (2003). *Applications of Natural Fiber Composites for Constructive Parts in Aerospace, Automobiles, and Other Areas.* Institut f¸r Strukturmechanik, Deutsches Zentrum f¸r Luft- und Raumfahrt,, D-38108 Braunschweig, Germany.

86. Thomason, J. L. (2008). The influence of fibre length, diameter and concentration on the modulus of glass fibre reinforced polyamide 6,6. *Composites Part a-Applied Science and Manufacturing, 39*(11), 1732-1738.

87. Ku, H., Wang, H., Pattarachaiyakoop, N., & Trada, M. (2011). A review on the tensile properties of natural fiber reinforced polymer composites. *Composites Part B-Engineering, 42*(4), 856-873.

88. Nishino, T., Hirao, K., Kotera, M., Nakamae, K., & Inagaki, H. (2003). Kenaf reinforced biodegradable composite. *Composites Science and Technology, 63*(9), 1281-1286.

89. Durowaye*, S. I., & , G. I. L., O. I. Olagbaju. (2014). Micro-structure and Mechanical Properties of Sisal Particles Reinforced Polypropylene Composite. *International Journal of Composite Materials, 4*(4), 190 - 195.

90. Kim, M. W., Lee, S. H., & Youn, J. R. (2010). Effects of Filler Size and Content on Shrinkage and Gloss of Injection Molded PBT/PET/Talc Composites. *Polymer Composites, 31*(6), 1020-1027.

91. G.M.Bohlmann. (2005). *General Characteristics, Processability, Industrial Applications and Market Evolution of Biodegradable Polymers.* Handbook

of Biodegradable Polymers. Shawbury, Shrewsbury, Shropshire, SY44NR, UK: Rapra Technology Limited.

92. Sousa, R. A., Reis, R. L., Cunha, A. M., & Bevis, M. J. (2004). Integrated compounding and injection moulding of short fibre reinforced composites. *Plastics Rubber and Composites, 33*(6), 249-259.

93. Kopeliovich, D. D. (2006). *Injection molding of polymers*. from http://www.substech.com/dokuwiki/doku.php?id=injection_molding_of_polymers.

94. Keller, A. (2003). Compounding and mechanical properties of biodegradable hemp fibre composites. *Composites Science and Technology, 63*(9), 1307-1316.

95. B.G. Compton, J. A. L. (2014). 3D-Printing of Lightweight Cellular Composites. *Advanced Materials, 26*(26).

96. Hagiwara, T. (2004). Current status and future prospects of laser stereolithography. In I. Miyamoto, H. Helvajian, K. Itoh, K. F. Kobayashi, A. Ostendorf & K. Sugioka (Eds.), *Fifth International Symposium on Laser Precision Microfabrication* (Vol. 5662, pp. 644-648).

97. G.Urbonaite. (2013) 3D Print Technologies Analysis. *18th International Conference. Mechanika 2013*. LT-51424 Kaunas, Lithuania: Mechanika.

98. Wendel, B., Rietzel, D., Kuhnlein, F., Feulner, R., Hulder, G., & Schmachtenberg, E. (2008). Additive Processing of Polymers. *Macromolecular Materials and Engineering, 293*(10), 799-809.

99. Ha, Y. M., Choi, J. W., & Lee, S. H. (2008). Mass production of 3-D microstructures using projection microstereolithography. *Journal of Mechanical Science and Technology, 22*(3), 514-521.

100. Zheng, X. Y., Lee, H., Weisgraber, T. H., Shusteff, M., DeOtte, J., Duoss, E. B., Kuntz, J. D., Biener, M. M., Ge, Q., Jackson, J. A., Kucheyev, S. O., Fang, N. X., & Spadaccini, C. M. (2014). Ultralight, Ultrastiff Mechanical Metamaterials. *Science, 344*(6190), 1373-1377.

101. Park, I. B., Ha, Y. M., & Lee, S. H. (2011). Dithering method for improving the surface quality of a microstructure in projection microstereolithography. *International Journal of Advanced Manufacturing Technology, 52*(5-8), 545-553.

102. Kirowatari, K. I. a. K. (1993) Real three dimensional micro fabrication using stereo lithography and metal molding. *IEEE MEMS'9* (pp. 42-47). Fort Lauderdale, New York, USA.

103. Skoog, S. A., Goering, P. L., & Narayan, R. J. (2014). Stereolithography in tissue engineering. *Journal of Materials Science-Materials in Medicine, 25*(3), 845-856.

104. Unit, J. P. (2008). *Aerogel, Mystifying blue smoke.*, from http://stardust.jpl.nasa.gov/aerogel_factsheet.pdf.

105. Lu, Z. L., Lu, F., Cao, J. W., & Li, D. C. (2014). Manufacturing Properties of Turbine Blades of Carbon Fiber-Reinforced SiC Composite Based on Stereolithography. *Materials and Manufacturing Processes, 29*(2), 201-209.

106. Tanodekaew, S., Channasanon, S., & Uppanan, P. (2014). Preparation and degradation study of photocurable oligolactide-HA composite: A potential resin for stereolithography application. *Journal of Biomedical Materials Research Part B-Applied Biomaterials, 102*(3), 604-611.

107. Sakly, A., Kenzari, S., Bonina, D., Corbel, S., & Fournee, V. (2014). A novel quasicrystal-resin composite for stereolithography. *Materials & Design, 56*, 280-285.

108. Yan, C. Z., Hao, L., Xu, L., & Shi, Y. S. (2011). Preparation, characterisation and processing of carbon fibre/polyamide-12 composites for selective laser sintering. *Composites Science and Technology, 71*(16), 1834-1841.

109. Czelusniak, T., Amorim, F. L., Higa, C. F., & Lohrengel, A. (2014). Development and application of new composite materials as EDM electrodes manufactured via selective laser sintering. *International Journal of Advanced Manufacturing Technology, 72*(9-12), 1503-1512.

110. Zeng, W. L., Guo, Y. L., Jiang, K. Y., Yu, Z. X., & Liu, Y. (2012). Preparation and selective laser sintering of rice husk-plastic composite powder and post processing. *Digest Journal of Nanomaterials and Biostructures, 7*(3), 1063-1070.

111. Vrancken, B., Thijs, L., Kruth, J. P., & Van Humbeeck, J. (2014). Microstructure and mechanical properties of a novel beta titanium metallic composite by selective laser melting. *Acta Materialia, 68*(15), 150-158.

112. Zeng, W. L., Guo, Y. L., Jiang, K. Y., Yu, Z. X., Liu, Y., Shen, Y. D., Deng, J. R., & Wang, P. X. (2013). Laser intensity effect on mechanical properties of wood-plastic composite parts fabricated by selective laser sintering. *Journal of Thermoplastic Composite Materials, 26*(1), 125-136.

113. Mireles, J. (2012). *Fused Deposition Modeling of Metals.* W.M. Keck Center for 3D Innovation, University of Texis at El paso. 836-845p.

114. Gosselin, C., Duballet, R., Roux, P., Gaudilliere, N., Dirrenberger, J., & Morel, P. (2016). Large-scale 3D printing of ultra-high performance concrete - a new processing route for architects and builders. *Materials & Design, 100*, 102-109.

115. Ahn, S. H., Montero, M., Odell, D., Roundy, S., & Wright, P. K. (2002). Anisotropic material properties of fused deposition modeling ABS. *Rapid Prototyping Journal, 8*(4), 248-257.

116. Pathi, S., & Jayaraman, K. (2006). Effects of extrusion on fibre length in sisal fibre-reinforced polypropylene composites. *International Journal of Modern Physics B, 20*(25-27), 4607-4612.

117. Matsuzaki, R., Ueda, M., Namiki, M., Jeong, T. K., Asahara, H., Horiguchi, K., Nakamura, T., Todoroki, A., & Hirano, Y. (2016). Three-dimensional

printing of continuous-fiber composites by in-nozzle impregnation. *Scientific Reports, 6*.

118. Mark, G. (2016). *Markforged*. Retrieved 17/5/2016, 2016, from https://markforged.com/.

119. Mark, G. (2016). *MF_Mark Two 3D Printer*. Retrieved 17/5/2016, 2016, from https://www.dropbox.com/sh/gxmxn9c00v3kayk/AACWAnFobiL9MBfUOI2g6q-Na/MF_Mark%20Two%203D%20Printer%20DS-Web.pdf?dl=0.

120. Hahm, M., Kim, C. H., & Ryu, J. (2008). A study on polypropylene and surface modified PET fiber composites. *Polymer-Korea, 32*(1), 7-12.

121. Ujhelyiova, A., Bolhova, E., Marcincin, A., & Tino, R. (2007). Blended polypropylene/polyethylene terephthalate fibres: Crystallisation behaviour of polypropylene and mechanical properties. *Fibres & Textiles in Eastern Europe, 15*(4), 26-29.

122. Efendy, M. G. A., & Pickering, K. L. (2014). Comparison of harakeke with hemp fibre as a potential reinforcement in composites. *Composites Part A-Applied Science and Manufacturing, 67*, 259-267.

123. Lang, D. (2016). *3D-Printing of Recycled Thermoplastic Composites.* thesis, École Polytechnique Fédérale de Lausanne, The University of Waikato.

124. Yan, Z. L., Zhang, J. C., Lin, G., Zhang, H., Ding, Y., & Wang, H. (2013). Fabrication process optimization of hemp fibre-reinforced polypropylene composites. *Journal of Reinforced Plastics and Composites, 32*(20), 1504-1512.

125. Deshmukh, S. P., Rao, A. C., Gaval, V. R., & Mahanwar, P. A. (2011). Mica-Filled PVC Composites: Effect of Particle Size, Filler Concentration, and Surface Treatment of the Filler, on Mechanical and Electrical Properties of the Composites. *Journal of Thermoplastic Composite Materials, 24*(5), 583-599.

Appendix

Shrinkage test calculations

Base formulas:

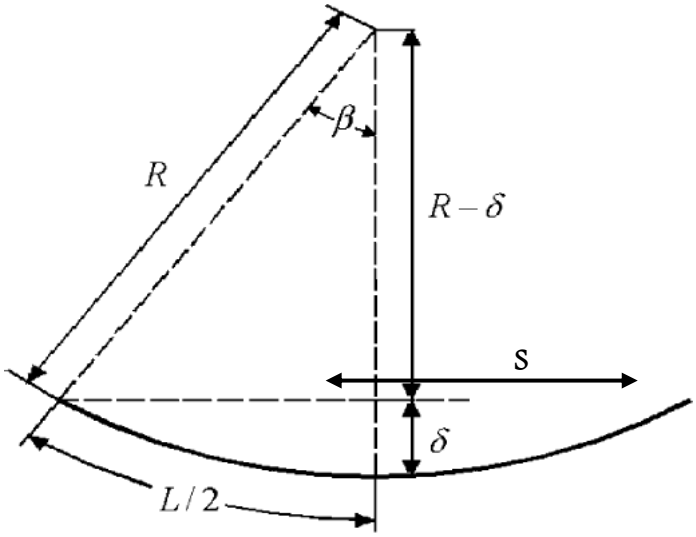

$$R(mm) = \frac{4(\delta^2 + h^2)}{8\delta} \qquad (1)$$

$$\beta(rad) = \frac{L/2}{R};\ \beta(°) = \frac{180 * L/2}{\pi * R} \qquad (2)$$

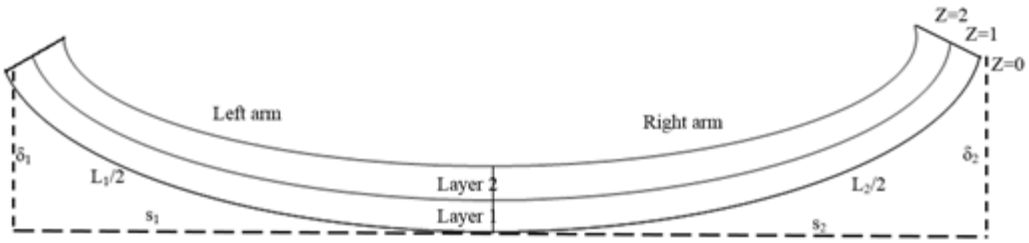

Assumptions:

1. The arm length L at height z=0 is L/2, which is the arm length without shrinkage
2. The layers have the same length at z=1
3. At z=2, the second layer has fully shrunk

On each arm, three measures are taken: the horizontal s, the vertical δ and the arm length L/2. With these, it's possible to determine the central angle β using (1) and (2).

Knowing R, β and the layer height h, it's possible to calculate the shrunk arm length at z=2:

$$L(z=2)(mm) = \frac{(R-2h) * \pi * \beta}{180} \qquad (3)$$

The shrinkage is then the difference between those two lengths

$$Shrinkage\ (\%) = 100 - \frac{100 * L(z=2)}{L(z=0)} \qquad (4)$$